Computational Lipidology

Prediction of Lipoprotein Density Profiles in Human Blood Plasma

DISSERTATION

zur Erlangung des akademischen Grades
doctor rerum naturalium
(Dr. rer. nat.)
im Fach Biologie

eingereicht an der
Mathematisch-Naturwissenschaftlichen Fakultät I
der Humboldt-Universität zu Berlin

von
Frau Dipl.-Biochem. Katrin Hübner
geboren am 09.02.1975 in Berlin

Präsident der Humboldt-Universität zu Berlin:
Prof. Dr. Christoph Markschies

Dekan der Mathematisch-Naturwissenschaftlichen Fakultät I:
Prof. Dr. Lutz-Helmut Schön

Gutachter:

1. Prof. Dr. Jens-Georg Reich
2. Prof. Dr. Hermann-Georg Holzhütter
3. Prof. Dr. Ulrike Beisiegel

eingereicht am: 17. Dezember 2007
Tag der mündlichen Prüfung: 6. Mai 2008

Abstract

Monitoring the major lipoprotein classes, particularly low-density lipoproteins ('bad' LDL) and high-density lipoproteins ('good' HDL) for characterizing risk of cardiovascular disease (CVD) is well-accepted and routine in clinical practice. However, it is only one-half of the truth as lipoprotein classes comprise non-homogeneous populations of lipoprotein particles varying significantly in their composition of lipids and apolipoproteins. Various studies have shown differing metabolic behavior and contribution to CVD of individual lipoprotein sub-populations. Nevertheless, the superiority of more detailed lipoprotein fractionation is still a matter of debate because experimental separation and analysis is an elaborate, time-consuming and expensive venture and not yet worthwhile for routine measurements.

The present work 'Computational Lipidology' aims at establishing a novel modeling approach to calculate the distribution of lipoproteins (*lipoprotein profile*) in blood plasma being the first that settles on individual lipoprotein complexes instead of common lipoprotein classes. Essential lipoprotein constituents and processes involved in the lipoprotein metabolism are taken into account. Stochastic as well as deterministic simulations yield the distribution of lipoproteins over density based on the set of individual lipoprotein complexes in the system. The model calculations successfully reproduce lipoprotein profiles measured in healthy subjects and show main characteristics of pathological situations elicited by disorder in one of the underlying molecular processes. Moreover, the model reveals the distribution of high-resolution lipoprotein sub-fractions (*hrDS*) within major density classes.

The results show satisfactory agreement with clinical observations which qualifies the work as a significant step towards analyzing inter-individual variability, patient-oriented diagnosis of lipid disorders and identifying new sub-fractions of potential clinical relevance.

Keywords:
atherosclerosis, lipoprotein metabolism, heterogeneity, lipoprotein profile, modeling, simulation

Zusammenfassung

Wichtige Marker in der klinischen Routine für die Risikoabschätzung von kardiovaskulären Erkrankungen (CVD) sind Blutcholesterinwerte auf Basis von Lipoproteinklassen wie 'schlechtes' LDL oder 'gutes' HDL. Dies vernachlässigt, dass jede Lipoproteinklasse eine nicht-homogene Population von Lipoproteinpartikeln unterschiedlicher Zusammensetzung aus Lipiden und Proteinen bildet. Studien zeigen zudem, dass solche Sub-populationen von Lipoproteinen im Stoffwechsel als auch im Beitrag zu CVD unterschiedlich sind. Mehrwert und routinemäßiger Einsatz einer detaillierteren Auftrennung von Lipoproteinen sind jedoch umstritten, da die experimentelle Fraktionierung und Analyse aufwendig, zeit- und kostenintensiv sind.

Die vorliegende Arbeit 'Computational Lipidology' präsentiert einen neuartigen Modellierungsansatz für die Berechnung von Lipoproteinverteilungen (Lipoproteinprofil) im Blutplasma, wobei erstmals individuelle Lipoproteinpartikel anstelle von Lipoproteinklassen betrachtet werden. Das Modell berücksichtigt elementare Bestandteile (Lipide, Proteine) und Prozesse des Stoffwechsel von Lipoproteinen. Stochastische wie deterministische Simulationen errechnen auf Basis aller Lipoproteinpartikel im System deren Dichteverteilung. Die Modellberechnungen reproduzieren erfolgreich klinisch gemessene Lipoproteinprofile von gesunden Patienten und zeigen Hauptmerkmale von pathologischen Situationen, die durch Störung eines der zugrundeliegenden molekularen Prozesse verursacht werden. Hochaufgelöste Lipoproteinprofile zeigen die Verteilung von sogenannten 'high-resolution density sub-fractions' (*hrDS*) innerhalb von Hauptlipoproteinklassen.

Die Ergebnisse stimmen mit klinischen Beobachtungen sehr gut überein, was die Arbeit als einen signifikanten Schritt in Richtung Analyse von individuellen Unterschieden, patienten-orientierte Diagnose von Fettstoffwechselstörungen und Identifikation neuer Sub-populationen von potentiell klinischer Relevanz qualifiziert.

Schlagwörter:
Atherosklerose, Lipoproteinstoffwechsel, Heterogenität, Lipoproteinprofil, Modellierung, Simulation

Dedication

To my parents

Contents

Table of Contents **ix**

List of Figures **xiii**

List of Tables **xv**

1 Introduction **3**

2 Biological Background **9**
2.1 Structure and metabolism of lipoproteins in blood plasma . . 9
2.1.1 Lipoprotein components 9
2.1.2 Lipoprotein metabolism 11
2.2 Hypotheses of atherogenesis 15
2.3 Clinical markers 16
2.3.1 Serum cholesterol 16
2.3.2 Small-dense LDL 17
2.3.3 Lp(a) 18
2.3.4 ApoB-100/apoA-I ratio 18
2.3.5 Lipoprotein-associated inflammatory markers 18
2.4 Medication 19
2.4.1 Statins 19
2.4.2 Fibrates, nicotinic acid and resorption inhibitors 20

3 State of the Art in the Analysis of lipoprotein metabolism **23**
3.1 Animal models 23
3.2 Pathway analysis in atherosclerosis 24
3.3 Tracer kinetic studies and compartment modeling 25
3.3.1 Methodological aspects 25
3.3.2 Studies on the VLDL, IDL and LDL metabolism . . . 26
3.3.3 Studies on HDL metabolism 28

3.3.4 Dynamics of individual lipoprotein complexes vs. compartments . . . 30
3.3.5 Summary of compartment modeling's limitations . . . 36

4 The *in silico* Model **37**
4.1 Lipoprotein components . . . 37
4.2 Kinetic processes . . . 39
4.3 Simplifications . . . 45
4.4 Model equations . . . 46

5 Methods - Experiments and Modeling Work **47**
5.1 Experiments . . . 49
5.1.1 Subjects . . . 49
5.1.2 Lipoprotein separation . . . 49
5.1.3 Lipoprotein chemistry . . . 49
5.1.4 Lipoprotein composition profile . . . 50
5.2 Modeling and simulation . . . 51
5.2.1 Stochastic simulation . . . 51
5.2.2 Deterministic simulation . . . 55
5.3 Calculation of the density profile . . . 56
5.4 Optimization . . . 58
5.4.1 Parameter estimation . . . 58
5.5 Hardware and software utilities . . . 58

6 Results **59**
6.1 Stochastic vs. deterministic simulation . . . 59
6.2 Lipoprotein profiles in healthy subjects . . . 62
6.2.1 Parameter values . . . 63
6.2.2 Calculated vs. clinically measured lipoprotein profiles . 67
6.2.3 Event frequencies . . . 69
6.2.4 Dependency on initial composition . . . 71
6.2.5 Influence of the lipid package size . . . 74
6.2.6 Sensitivity analysis . . . 75
6.3 High-resolution density sub-fractions . . . 77
6.4 Analysis of the lipoprotein composition spectrum . . . 82
6.4.1 Further macroscopic properties . . . 85
6.5 Simulated pathological profiles . . . 88
6.5.1 Hypercholesterolemia . . . 88
6.5.2 Hypertriglyceridemia . . . 91
6.5.3 Hypoalphalipoproteinemia . . . 94

7 Discussion **97**
7.1 Changing the perception of conventional experimental and modeling approaches 97
7.2 Simulated lipoprotein profiles reproduce experimental data . . 98
7.3 Lipid values in high resolution to improve risk characterization 100
7.4 Simulated pathological states correspond well to clinical observations 103
7.5 Extensions and refinements 104

8 Conclusion & Outlook **107**

Bibliography **111**

A Calculating the Number of Phospholipids **133**

B Model Parameter Values **135**

Abbreviations **141**

Contributions **143**

Acknowledgement **145**

Publications **147**

Declaration **149**

List of Figures

1.1 Schematic structure and composition of a lipoprotein. 4
1.2 Density gradient of lipoprotein classes after ultracentrifugation. 5

2.1 Crystal structure of human apolipoprotein A-I. 9
2.2 Chemical structure of lipid components. 12
2.3 Scheme of the human lipoprotein metabolism in blood plasma. 13
2.4 Scheme of a normal artery. 15
2.5 Inhibition of cholesterol biosynthesis by statins. 19

3.1 Example of a compartment model 31
3.2 Scheme of the delipidation cascade of 9 lipoprotein particles . 32
3.3 Single lipoprotein complex vs. compartment kinetics. 34

4.1 Illustration of the kinetic processes taking place on a lipoprotein complex. 39
4.2 Illustration of the kinetic processes defined in the model. . . . 43

5.1 Schematic overview of experimental and modeling methods. . 48
5.2 Steps in modeling and simulation of the lipoprotein metabolism. 51
5.3 Lipoprotein complexes in the system. 52
5.4 System development. 54
5.5 Calculation of the lipoprotein profile over common density classes 56

6.1 Stochastic vs. deterministic simulation. 61
6.2 Clinically measured lipoprotein profile 62
6.3 Simulated lipoprotein profile 62
6.4 Simulated vs. clinically measured distributions of all lipoprotein components 68
6.5 Relative frequency of events executed during simulation. . . . 70
6.6 Variation in the initial composition of B-particles 72
6.7 Dependency of simulation results on lipid package size 75

6.8 Sensitivity of the model parameters. 76
6.9 High-resolution distribution of total cholesterol within common density classes 78
6.10 High-resolution distribution of lipoprotein component concentrations within common density classes 79
6.11 Variation in the distribution of hrDS-cholesterol at moderately altered parameter values 80
6.12 Distribution of hrDS-cholesterol with different density resolutions 81
6.13 Lipoprotein compositions 82
6.14 Number of B-particle compositions 83
6.15 Number of A-particle compositions 84
6.16 Distribution of lipoprotein components between the surface and core of a lipoprotein complex. 86
6.17 Phase distribution of lipoprotein components in selected common density classes 87
6.18 Simulated distributions of lipoprotein components of pathological states: LDL receptor deficiency (50%) 89
6.19 Simulated distributions of lipoprotein components of pathological states: LPL deficiency 93
6.20 Simulated distributions of lipoprotein components of pathological states: ABCA1 deficiency 95

List of Tables

2.1 Fredrickson classification of hyperlipidemia 17

4.1 Model components. 37
4.2 Composition properties of lipoprotein complexes. 38
4.3 Description of the kinetic processes defined in the model. . . . 44
4.4 Model equations. 46

5.1 Experimental lipoprotein composition data. 50
5.2 Data for density calculation. 57

6.1 Model parameter values 64
6.2 Absolute numbers of executions for each event. 70
6.3 Initial compositions of B-particles with comparable agreement between simulation and experiment 73
6.4 Number of different lipoprotein compositions 85
6.5 Calculated phase distribution of lipoprotein components . . . 86

Preface

"Ein jegliches hat seine Zeit, und alles Vorhaben unter dem Himmel hat seine Stunde."

(Altes Testament, Prediger Salomo, 3,1)

A number of things exist both science and religion may have in common. One particular religious part of science and of life in general in my mind is to believe, to believe in something or in someone, especially in oneself in order to succeed and to achieve from the apparently impossible the possible.

The time I spent for my PhD thesis, the ups and downs, the periods of motivation and frustration, the looking for the right path like

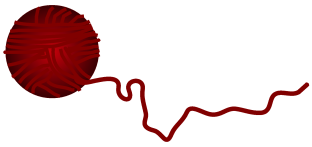

disentangling a ball of wool have not exclusively taught me that but, probably, most intensively.

Chapter 1

Introduction

"What is a scientist after all? It is a curious person looking through a keyhole, the keyhole of nature, trying to know what's going on."

(Jacques-Yves Cousteau)

Lipids, e.g. cholesterol and triglycerides, either synthesized in the body or taken up by the food are indispensable elements of cellular metabolism. Cholesterol is an essential integral component of all cellular membranes and the precursor for steroid hormones and bile acids while triglycerides (approx. 90% ingested by diet) function as major source of energy metabolism. Trigylcerides provide energy up to twice as much as the same mass of proteins or carbohydrates. Most of the triglycerides are stored in adipose tissue as energy source, for insulation from cold and heat as well as for protective padding. In case of an increased energy demand they are mobilized for degradation and energy production in another tissue, e.g. in muscle cells.

Since lipids are almost insoluble in aqueous media such as blood plasma they are transported among the various tissues by water-soluble complexes called LIPOPROTEINS. Elucidating the kinetic mechanisms involved in the formation, degradation and mutual interconversion of plasma lipoproteins is of high medical relevance as long-term perturbations of the lipoprotein distribution are considered as the major risk factor for atherosclerosis and cardiovascular diseases - the main cause of death in the western states (Murray and Lopez, 1997).

Lipoproteins are multi-component complexes of lipids and proteins (apolipoproteins) that form distinct molecular aggregates (Figure 1.1). Hereby, the apolipoproteins (apo) assure lipoprotein's water solubility and fulfill a number of regulatory functions. Each lipoprotein complex is unique with respect to its composition. An individual lipoprotein complex contains a distinct number of apolipoproteins (e.g. apoB-100) and lipid molecules (e.g. triglycerides, cholesterol), the number of which may vary between one and several hundreds or thousands, respectively. Thus, in principle, a multitude of different lipoprotein compositions results from all possible stoichiometric combinations of lipid and apolipoprotein molecules. This is commonly called *lipoprotein's heterogeneity*.

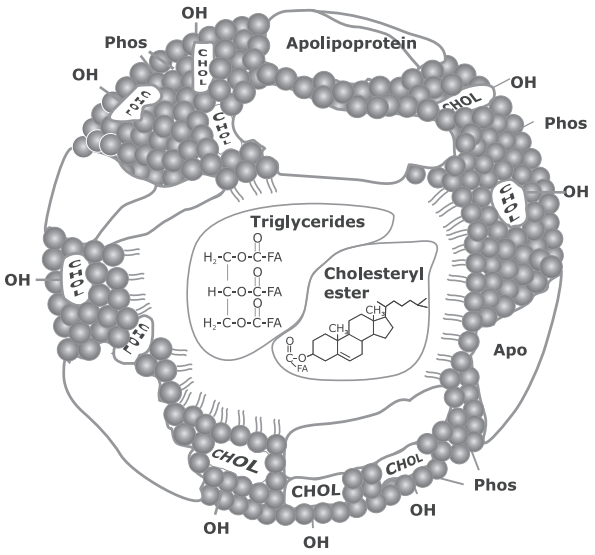

Figure 1.1: **Schematic structure and composition of a lipoprotein.** Abbreviations: Apo (apolipoproteins), Phos (phospholipids), Chol (free cholesterol)

A simple example:

In this the lipoprotein complexes are constituted of two types of components, A and B. The number of both may vary from 1 to 20 and 1 to 25, respectively. This results in $20 \cdot 25 = 500$ different lipoprotein complexes. However, a lipoprotein complex comprises more than two different components as well as the possible molecule number of each component can be much larger than it was chosen for the given example. This considerably increases the diversity up to billions (in numbers 1,000,000,000!) of individual lipoprotein complexes.

Despite this fact, for almost half a century plasma lipoproteins have been usually grouped into five main classes of lipoproteins named chylomicrons, VLDL, IDL, LDL and HDL (very low, intermediate, low and high density lipoproteins). The classification of lipoproteins originates from the work of Lindgren, Elliot and Gofmann (Lindgren et al., 1951) in which they separate lipoproteins from the other serum proteins according to their flotation characteristics (Svedberg sedimentation units [S] in reverse [S_f]).

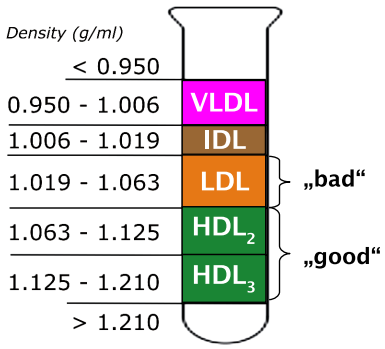

Figure 1.2: **Density gradient of lipoprotein classes after ultracentrifugation.** Abbreviations: VLDL, IDL, LDL and HDL very low, intermediate, low and high density lipoprotein, respectively.

The fractions of VLDL (d < 1.006 g/ml [S_f >20]); IDL (d = 1.006-1.019 g/ml [S_f 12-20]); LDL (d = 1.019-1.063 g/ml [S_f 0-12]) and HDL (d = 1.063-1.21 g/ml) are still in use today. HDL is commonly further subdivided into sub-fractions of HDL_2 and HDL_3. Havel et al. (Havel et al., 1955) established the method of preparative ultracentrifugation to physically separate lipoproteins according to their density from human blood plasma (Figure 1.2) and to analyze their constituents. This method has been widely used for studying lipoproteins and lipoprotein's metabolism.

However, to analyze the interrelationship between the kinetics of individual biochemical processes of the lipoprotein metabolism and the dynamics of the whole lipoprotein population in a causative and quantitative manner mathematical models are needed. Until now, even mathematical models of the lipoprotein metabolism have considered lipoprotein density classes (= compartments) as dynamic variables of the system. The phenomenological transition rates between these compartments are usually determined by radioactive or stable isotope tracer experiments. For detailed reviews the reader is referred to (Barrett et al., 2006; Parhofer and Barrett, 2006; Rashid et al., 2006).

Except for the comprehensive compartment model proposed by (Knoblauch et al., 2000) compartment models have focused on specific parts of the lipoprotein metabolism based on kinetic measurements with, e.g. labeled apoA-I (Chétiveaux et al., 2004; Frénais et al., 1999; Schaefer et al., 2000; Winkler et al., 2000), apoA-II (Ji et al., 2006) or apoB-100 (Beltz et al., 1985; Packard et al., 2000; Winkler et al., 1999).

Compartment models may provide a useful phenomenological description of the lipoprotein dynamics. However, they have some serious limitations. First, they neglect the possible heterogeneity of lipoproteins. As already mentioned above, a single density class comprises a huge number of lipoprotein complexes differing in their amount of lipids and proteins - an important fact that could be of relevance for the medical interpretation of lipoprotein density profiles. Second, the transition of a lipoprotein from one density class into another is not a single process but is accomplished in a series of successive elementary reactions in which, for example, triglycerides are removed, cholesterol is taken up from tissues and apolipoproteins are exchanged. Therefore, phenomenological inter-compartment transition rates can hardly be related to the rate of the underlying molecular processes.

Objectives

The present work provides a novel approach towards mathematical modeling of the systemic lipoprotein metabolism in blood plasma that overcomes the limitations of compartment models. This approach enables for the first time to obtain the entire spectrum of lipoprotein compositions instead of predefined lipoprotein density classes. Thus, the dynamics is described on the level of individual lipoprotein complexes as the true variables of the system. The modeling approach consists of the establishment of kinetic equations governing the temporal changes of each of them. The number of dynamic variables is, in principal, given by the number of different lipoprotein complexes that can be formed from a given number of apolipoproteins and lipids.

The established model should allow

→ to include in an adequate manner the elementary processes involved in lipoprotein metabolism

→ to calculate from the set of individual lipoprotein complexes in the system the distribution of lipoproteins over their density (=lipoprotein profile), e.g. over arbitrary density intervals.

→ to reproduce clinically measured lipoprotein distributions over predefined density classes conventionally used in the lipid diagnostics from healthy and diseased subjects

→ to assign the calculated lipoprotein complexes to narrow density classes, which are introduced as *high-resolution density sub-fractions* (hrDS). This might help to identify new sub-fractions of potential clinical relevance.

→ to simulate the impact of disorders in the lipoprotein metabolism on the distribution of lipoproteins by altering the rate constants in one of the underlying molecular processes, e.g. LDL receptor-mediated lipoprotein uptake.

In combination with clinical lipid analysis the work is assumed to be qualified for the analysis of inter-individual variability as well as for patient-oriented risk characterization and diagnosis of individual lipid disorders by a model-based analysis of high-resolution lipoprotein profiles.

Outline

Before presenting the model itself, a brief introduction will be given in related topics of this work in the following. Lipoproteins undergo a complex metabolism in blood plasma by permanent re-modeling of the content and shape catalyzed by a number of enzymes and transfer proteins. The metabolism of lipoproteins in human blood plasma will be described in more detail in section 2.1.

As already mentioned above, disorders in the metabolism of lipoproteins are a major risk factor for atherosclerosis and cardiovascular diseases. The accumulation of plasma lipoproteins, predominantly LDL, in the artery intima as the result of specific cell reactions indicate the beginning of an atherosclerotic lesion (Libby, 2002). Two hypotheses for the development of atherosclerosis are established and will be shortly introduced in section 2.2.

Lipoprotein profiles serve as important clinical indicators for the atherogenic risk state of a patient. Up to now, predominantly high LDL-cholesterol (LDL-C) values, low concentrations of HDL-cholesterol (HDL-C) and/or an increased level of triglycerides are taken as main indicators of a disturbed lipid phenotype. Besides recommendations to change life style conditions commonly anti-atherogenic drugs are applied to treat lipid disorders such as hyperlipidemia. In the past, most of the drugs, e.g. so-called statins, aim at lowering the concentration of LDL-C. State of the art clinical indicators and medications are discussed in section 2.3 and 2.4, respectively.

The application of compartment models and other approaches which have been widely used in the last decade to gain insights into the dynamics of the lipoprotein metabolism will be briefly reviewed in chapter 3.

Chapter 2

Biological Background

"To know that we know what we know, and to know that we do not know what we do not know, that is true knowledge."

(Copernicus)

2.1 Structure and metabolism of lipoproteins in blood plasma

2.1.1 Lipoprotein components

Several apolipoproteins have been identified in the past. The major of them include apoA-I, apoA-II, apoA-IV, apoB-48, apoB-100, apoC-I, apoC-II, apoC-III and apoE. They are important regulators of enzymes and ligands of receptors in the metabolism of lipoproteins. Those protein components relevant for the model definition will be shortly introduced in the following.

ApoA-I mainly synthesized by the liver and intestine is the major protein component of lipoprotein complexes within the density range of d=1.063-1.210 g/ml or greater (HDL in terms of density classes). Its prominent role in the initial event of transporting cholesterol from peripheral cells (including vascular macrophages) to the liver, a mechanism known as reverse cholesterol transport (RCT), has been comprehensively reported in the past

Figure 2.1: **Crystal structure of human apolipoprotein A-I.** (source: PDB)

(for reviews see (Barter and Rye, 2006; Curtiss et al., 2006; Frank and Marcel, 2000; Pownall and Ehnholm, 2006)). ApoA-I, as its main function, provides the structural integrity of a lipoprotein complex and mediates the uptake of peripheral cholesterol and phospholipids by interacting with receptors like ATP-binding cassette class A type 1 (ABCA1). The distinct lipid binding capacity of apoA-I enables the formation of larger, spherical lipoprotein complexes of the HDL class. Finally, apoA-I is the first described activator of the lecithin:cholesterol acyl transferase (LCAT) (Fielding et al., 1972).

ApoB-100 is the obligatory apolipoprotein of lipoprotein complexes assigned to the common density classes of VLDL, IDL and LDL. It is produced by the liver and enters the plasma as a newly secreted particle of VLDL. In general, at least four major species of apolipoprotein B have been proposed including apoB-100 (Kane, 1983). Two species, apoB-74 and apoB-26, have been identified as constituents of various LDL specimens and are assumed as truncated forms of apoB-100. The fourth species is apoB-48 as the primary component of intestine-derived chylomicrons which are rapidly formed and degraded within several hours after food intake. However, the model in its present form solely refers to apolipoprotein B-100. Beside its contribution to the integral stability of a lipoprotein complex apoB-100 acts as the ligand for the ApoB,E(LDL) receptor. The binding initiates the receptor-mediated uptake and catabolism of apoB-100 carrying lipoprotein complexes, predominantly those of the LDL class.

ApoC comprises three different apolipoproteins designated as apoC-I, apoC-II, apoC-III. Even if they fulfill diverse metabolic functions they have in common the property of redistribution among lipoprotein complexes (for reviews see (Curry et al., 1981; Mahley et al., 1984; Nestel and Fidge, 1982). In this, C apolipoproteins may play an essential role in the remodeling of lipoproteins. In addition, they are important regulators of enzyme reactions. For example, *in vitro* studies have shown that apoC-I activates LCAT (Soutar et al., 1975) which may result in normal plasma values of esterified cholesterol in face of apoA-I deficiency (see above apoA-I as main activator of LCAT). ApoC-II has been identified as an activating co-factor of lipoprotein lipase (LPL) (Fielding et al., 1970; Krauss et al., 1973; LaRosa et al., 1970; Miller and Smith, 1973), the enzyme that catalyzes the hydrolysis of triglycerides and phospholipids from triglyceride-rich lipoproteins (chylomicrons, VLDL). In contrast, apoC-III has been suggested to inhibit apoC-II activation of LPL (Breckenridge et al., 1978) and, moreover, to modulate the receptor-mediated uptake of triglyceride-rich remnants by the liver. However, over-expression of apoC-III (Batal et al., 2000) or familial deficiency in apoC-II (Breckenridge et al., 1978) yield an elevated level of triglyceride-rich lipoproteins which is

characteristic for hypertriglyceridemia in spite of a well functional lipoprotein lipase.

ApoE is probably one of the most extensively studied apolipoprotein and fulfills a number of physiological functions (for review see (Strittmatter and Hill, 2002)). Three predominant isoforms have been reported in the human population named apoE2, apoE3 and apoE4. They form six common phenotypes in which the homozygous E3/3 phenotype is the most abundant one (in about 60% of all studied subjects) (Utermann et al., 1977). As its main function in lipid transport, apoE is involved in the receptor-mediated uptake of specific apoE-containing lipoproteins (chylomicron and VLDL remnants (βVLDL), HDL_E) by interacting with the ApoB,E(LDL) receptor (LDLR) and an unique ApoE receptor (the LDLR related protein, LRP) (Mahley, 1988). ApoE binds with a much higher affinity due to multiple interaction sites as compared to the binding of, e.g. LDL. However, the removal is not uniformely effective and depends on the isoform in that apoE is present. A complete deficiency in apoE results in a defective clearance of β-VLDL and has been reported clinically with type III hyperlipoproteinemia (Ghiselli et al., 1981). ApoE has been suggested to play an important role in the environment of macrophages that produce and release substantial amounts of apoE independent of cholesterol efflux (Basu et al., 1981). Especially in human neonates, and in patients who lack apoB-containing lipoproteins (named abetalipoproteinemia), HDL with apoE is the major lipoprotein class able to deliver cholesterol to various tissues (Innerarity et al., 1984).

The **lipid** content of lipoproteins comprises triglycerides, free cholesterol, cholesteryl esters and phospholipids whose chemical structure are given in Figure 2.2.

2.1.2 Lipoprotein metabolism

A number of processes in the metabolism of lipoproteins mediated by a variety of enzymes, transfer proteins and receptors are described in the literature and have been intensively studied during the past decades. In the following, I will summarize generally accepted knowledge of the main processes. However, this overview is not intended to be exhaustive. As Figure 2.3 illustrates, the transport of lipoproteins is usually grouped into three interwoven subpaths named as the exogenous, endogenous and reverse cholesterol transport pathway.

While after a high-fat diet (exogenous lipid uptake) the intestine synthesizes chylomicrons, the body changes over to an endogenous lipid synthesis and to the formation of VLDL during fasting or after a high-carbohydrate food intake. Chylomicrons and VLDL belong to the class of triglyceride-

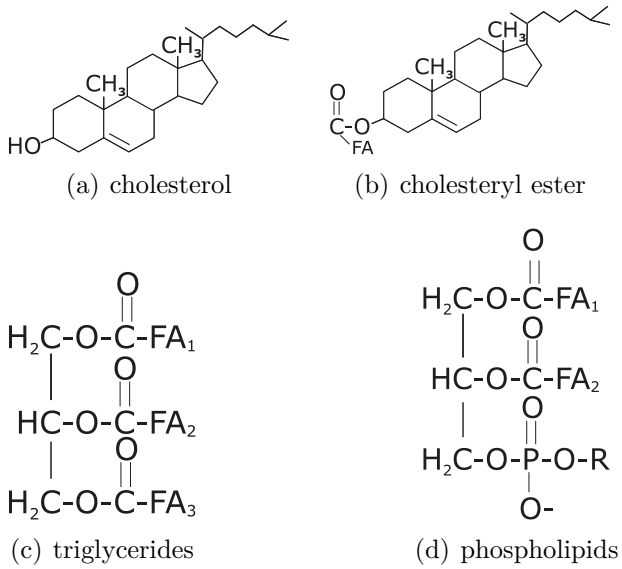

Figure 2.2: **Chemical structure of lipid components.** Abbreviations: fatty acid (FA)

rich lipoproteins. Both, when entering the blood plasma, are progressively depleted of a large amount of their triglyceride content by the action of lipoprotein lipase (LPL). Thereby, free fatty acids are released and so-called remnant particles (chylomicron remnants and IDL, respectively) are formed. Free fatty acids bound to albumin are transported to adipocytes and muscle cells to be restored as triglycerides or catabolized, respectively. Chylomicron remnants are rapidly cleared from the blood by the liver in a receptor-mediated endocytosis process most notably by the LDL receptor related protein (LRP). IDL is either taken up by the liver or further delipidated by the action of LPL and/or HL (hepatic lipase) to lipoproteins belonging to the class of LDL.

All lipoproteins of the endogenous pathway have one thing in common. They carry apolipoprotein B-100 as an integral protein constituent and ligand for the binding to the LDL receptor (LDLR). In 1985, Joseph L. Goldstein and Michael S. Brown received the Nobel Prize in physiology and medicine for the identification of the LDLR and its contribution to the cholesterol homeostasis (Brown and Goldstein, 1986; Goldstein and Brown, 1977). Mutations in the LDLR gene are described to be associated with Familial Hypercholesterolemia and lead to markedly elevated levels of LDL. Thereby, LDL has a prolonged presence in the plasma and can readily enter the artery wall by crossing the endothelial membrane. Once there, it is subject to a variety of

modifications which are assumed to cause the pro-inflammatory properties of LDL (Steinberg et al., 1989). Well known is the oxidation of both, the lipids and apoB-100. In this context, another class of receptors having a broad ligand binding specificity has been reported to act on these modified lipoproteins and is named as scavenger receptor class (SR). Most notably, modified LDL is taken up by macrophages, e.g. mediated by SRA1, which are mainly involved in the process of foam cell formation and the establishment of atherosclerotic plaques (see section 2.2).

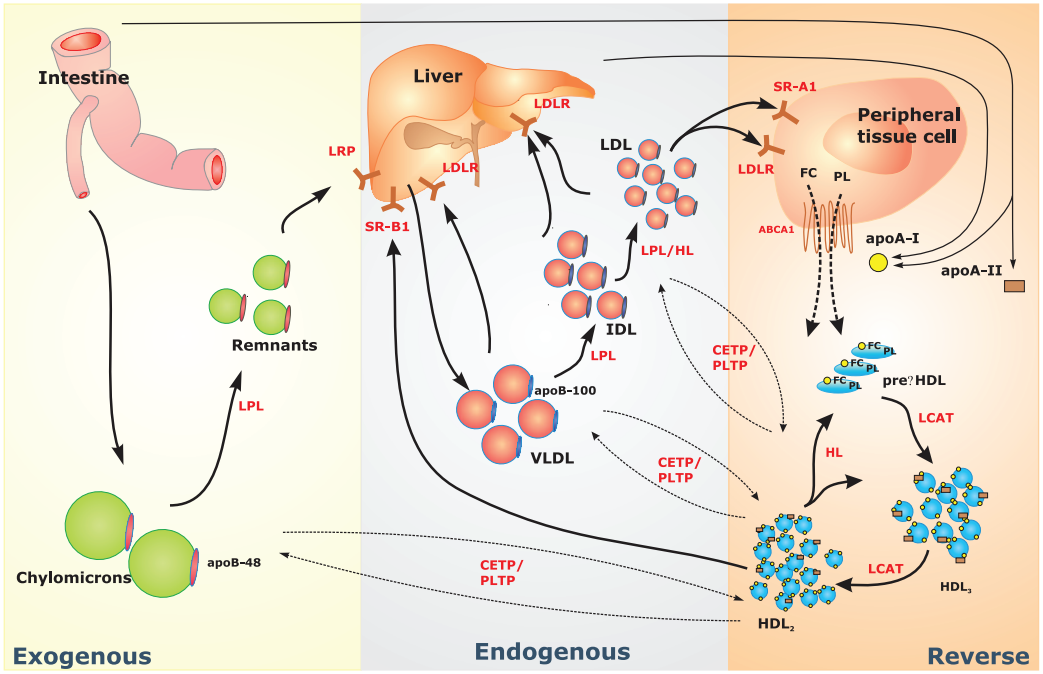

Figure 2.3: **Scheme of the human lipoprotein metabolism in blood plasma.** As lipoprotein's constituents the major apolipoproteins (apo) A-I, A-II, B-48 and B-100 are illustrated. Abbreviations: VLDL, IDL, LDL and HDL (very low, intermediate, low and high density lipoproteins, respectively); LPL (lipoprotein lipase); HL (hepatic lipase); LCAT (lecithin:cholesterol acyl transferase); CETP (cholesteryl ester transfer protein); PLTP (phospholipid transfer protein); apo (apolipoprotein); LDLR (low density lipoprotein receptor); LRP (low density lipoprotein receptor related protein); SRB1 (scavenger receptor type B1); ABCA1 (ATP-binding cassette class A type 1); FC (free cholesterol); PL (phospholipids)

In contrast, scavenger receptor class B, type I (SRB1) plays a more protective role as a key molecule in the reverse cholesterol transport, so-called because peripheral synthesized cholesterol is returned to the liver for excretion into the bile. The lipoproteins mainly involved in this sub-path belong to the class of HDL. They may be secreted by the liver or intestine as nascent HDL (preβ-HDL) with discoidal shape consisting mainly of apolipoprotein A-I and phospholipids. Mature HDL are formed by two progressive events: (i) taking up excess peripheral free cholesterol and phospholipids, e.g. facilitated by ABCA1, followed by (ii) the esterification of the cholesterol content, a reaction that is catalyzed by the enzyme lecithin:cholesterol acyl transferase (LCAT). The lipidation of apolipoprotein A-I is required for generating spherical HDL particles and clearing sterols from peripheral cells such as macrophages. SRB1 is expressed primarily in the liver and has been identified as an HDL receptor which promotes the selective uptake of esterified cholesterol into the liver (Acton et al., 1996). SRB1 has also been suggested to play a role in the efflux of excess peripheral free cholesterol. A second way of delivering esterified cholesterol to the liver occurs via the action of the cholesteryl ester transfer protein (CETP). CETP transfers preferentially cholesteryl ester (CE) from HDL to apoB-containing lipoproteins and triglycerides (TG) *vice versa*. At the beginning of this year, the crystal structure of this amazing protein has been published (Qiu et al., 2007) which provides detailed insights into the molecular mechanism of exchanging lipids among lipoproteins.

Another modulator of HDL is the phospholipid transfer protein (PLTP). Its role has been suggested to form preβ-HDL by transferring phospholipids from triglyceride-rich lipoproteins to HDL and at the same time to facilitate the remodeling of mature HDL by fusing small spherical particles to form larger particles (HDL2-like) (van Tol, 2002). HDL remodeling is also accompanied by the action of the hepatic lipase (HL). This enzyme, in contrast to LPL, hydrolyzes preferentially HDL triglycerides and phospholipids yielding the reformation of HDL3-like particles. In general, the life cycle of all lipoproteins is characterized by a continuous remodeling of the content, shape and size. From a philosophical point of view one could formulate: 'They never stand still, but if, they will die'.

2.2 Hypotheses of atherogenesis

In general, atherosclerotic events are characterized by the accumulation of lipids and fibrous material in the large arteries. These so-called fibrous plaques may already appear in the infancy without recognizable effects but may yield to serious cardiovascular diseases (CVD) like myocardial infarction in the elderly. An in-depth review about atherosclerosis is provided by (Glass and Witztum, 2001). Once, it has been suggested that the plaque formation is caused either by lipid disorders alone, or solely in response to injury. In that context mainly two hypotheses came up to explain this progressive atherosclerotic process (atherogenesis): (i) *response-to-injury* describes the process as a local, excessive inflammatory event in response to an injury of the vascular endothelial function (Ross, 1999). (ii) *response-to-retention* assumes an increased retention time of apoB-100 carrying lipoproteins (e.g. LDL, VLDL remnants) in the innermost layer of the artery wall, the intima (Williams and Tabas, 1998). For a schematic illustration of a normal artery see Figure 2.4.

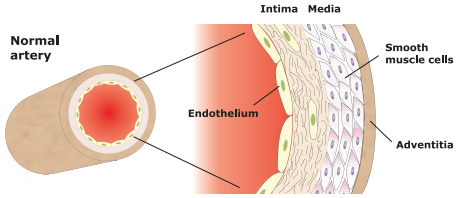

Figure 2.4: **Scheme of a normal artery.**

In recent years, the view has changed in that atherosclerosis is thought to be both, an inflammatory disease initiated and progressed by hypercholesterolemia (elevated cholesterol levels in the blood) (Steinberg, 2002). The prolonged retention of lipoproteins in the artery intima is assumed as the key pathogenic event instigating a cascade of inflammation and immune responses that lead to atherosclerotic lesions. For detailed reviews the reader is referred to (Getz, 2005; Libby, 2002).

In brief, the response cascade includes the following events: Retained lipoproteins are disposed for modifications, e.g. oxidation, which makes them to preferred substrates for a variety of scavenger receptors on the surface of macrophages. The presence of oxidized lipoproteins signals to endothelial cells to increase the expression of various adhesion molecules, like P-Selectin and VCAM-1 (Vascular cell adhesion molecule-1). They maintain contact with blood monocytes and T lymphocytes which, with the help of chemokines (e.g. MCP-1, Monocyte chemo-attractant protein-1), penetrate into the artery intima (Cushing et al., 1990). This process requires a specific receptor membrane-bound on monocytes called CC chemokine receptor 2 (CCR2, MCP-1 receptor) (Boring et al., 1998). Once resident there, mono-

cytes accelerated by M-CSF (Monocyte colony stimulating factor) differentiate to macrophages that bind and internalize modified lipoprotein particles by scavenger receptors. Macrophages accumulate large intracellular cholesteryl ester droplets leading eventually to so-called foam cell formation. Together with T lymphocytes they form the *fatty streak*, a hallmark of the artery lesion. The increased secretion of pro-inflammatory cytokines and chemokines amplifies the inflammatory response and stimulates the migration and proliferation of smooth muscle cells in the intima lesion. Following the synthesis of matrix proteins and proteoglycans a fibrous capsule is formed covering the fatty streak. In response to the death of macrophages, e.g. by necrosis or apoptosis, and to evolution of the atherosclerotic plaque the inflammatory process further propagates. Finally, plaque disruption causes thrombosis and acute clinical complications such as myocardial or ischemic infarction.

2.3 Clinical markers

It is widely accepted that elevated serum cholesterol values, in particular LDL cholesterol (LDL-C), are associated with an increased risk of cardiovascular diseases (CVD). Further, clinical indications traditionally provide the concentration of HDL cholesterol (HDL-C), the ratio of LDL-C/HDL-C and the total plasma triglyceride content. In the early 1970s, Donald S. Fredrickson has proposed an international classification of various types of hyperlipidemia based on the levels of the main lipoprotein classes (Fredrickson, 1971). It does not account for HDL and was later adopted by the World Health Organization. However, it is partly still in use today. The main features are summarized in Table 2.1.

2.3.1 Serum cholesterol

To reduce the risk for CVD monitoring serum cholesterol values is strongly recommended. European guidelines (Backer et al., 2003; Graham, 2005) propose the following boundaries for asymptomatic subjects: Total cholesterol (TC) $<$ 200 mg/dl specifying LDL-C $<$ 115 mg/dl and HDL-C $>$ 40 mg/dl as well as triglycerides $<$ 150 mg/dl. Recent recommendations plan to further reduce both the value of LDL-C and the LDL-C/HDL-C ratio lower than 70 mg/dl and 1.5, respectively. However, it is still unclear and controversial which boundaries make sense with respect to individuality. How high is too high? Moreover, diagnosis and treatment of men and woman who have common lipid abnormalities, but normal or low concentrations of LDL-

Table 2.1: **Fredrickson classification of hyperlipidemia.**

Type	Synonym	Defect	Phenotype	Treatment
I	Familial Hyperchylo-micronemia	Decreased LPL or altered apoC-II	Elevated chylomicrons	Diet control
IIa	Familial Hypercholest-erolemia	LDL receptor deficiency	Elevated LDL only	Bile acids sequestrant, Statins, Nicotinic acid
IIb	Combined Hyper-lipidemia	Decreased LDL receptor and increased ApoB	Elevated LDL and VLDL and Triglycerides	Statins, Nicotinic acid, Gemfibrozil
III	Familial Dysbetalipo-proteinemia	Defect in apoE synthesis	Increased IDL	Gemfibrozil
IV	Endogenous Hyper-lipidemia	Increased VLDL production and decreased elimi-nation	Increased VLDL	Nicotinic acid
V	Familial Hypertriglyc-eridemia	Increased VLDL production and decreased LPL	Increased VLDL, Chylomicrons	Nicotinic acid, Gemfibrozil

C remain difficult. Thus, it is obvious that other clinical markers beyond 'bad' and 'good' cholesterol are needed to precisely predict individual lipid disorders. In this context, a distinct sub-fraction of LDL called small-dense LDL, Lipoprotein (a), the apolipoproteins A-I and B-100 as well as various inflammatory markers are discussed.

2.3.2 Small-dense LDL

Krauss and Burke (Krauss and Burke, 1982) could show following high-resolution gradient gel electrophoresis (GGE) that distinct sub-fractions of LDL differing in size and density exist which may contribute differently to metabolic and pathological behavior. Today, LDL is commonly divided into three sub-species, large buoyant, intermediate and small dense LDL abbreviated with lbLDL, idLDL and sdLDL, respectively. Due to specific structural properties, sdLDL (density = 1.040-1.063 g/ml) have a prolonged residence time in the intima and is the preferred substrate for oxidative and chemi-

cal modifications. The predominance of the small-dense LDL sub-fraction is assumed to be particularly atherogenic and to be associated with a 3-7 fold increase in CVD risk (Berneis and Krauss, 2002; Griffin et al., 1994).

2.3.3 Lp(a)

A variety of case-control and prospective studies have been shown that an increased concentration of a LDL-like particle called Lipoprotein (a), Lp(a), strongly correlates to the risk of atherosclerosis and CVD. The first results on this issue were already published in the early 1980s (Kostner et al., 1981). Most of the studies describe in common cut-off levels for an increased risk between 25 and 30 mg/dl. Lp(a) was found in the density range of 1.05 and 1.08 g/ml consisting of a specific additional protein component named apolipoprotein-a (Apo(a)) which is bound to apoB-100 by disulfide linkage. For a comprehensive review on Lp(a) the reader is referred to (Maher and Brown, 1995).

2.3.4 ApoB-100/apoA-I ratio

More recently, several clinical prospective studies have been elucidated the predictive power of the apolipoproteins B-100, A-I, and the apoB-100/apoA-I ratio - Quebec Cardiovascular Study (Lamarche et al., 1996), Framingham Offspring Study (Schaefer et al., 1994a,b), INTERHEART (Yusuf et al., 2004) and the AMORIS (Apolipoprotein-related MOrtality RISk) study (Walldius et al., 2001). In consequence, it has been evidently shown that the apoB-100/apoA-I ratio is a new simple, strong and accurate risk factor for cardiovascular disease (Walldius and Jungner, 2006).

2.3.5 Lipoprotein-associated inflammatory markers

In face of tissue injury or infection, the host defends with a process termed the acute-phase response. An independent assessment of the risk for CVD was elucidated in a number of studies for acute-phase proteins such as the C-reactive protein (CRP) and other inflammatory proteins. In a variety of studies, CRP has been shown to better predict cardiovascular risk than traditional risk factors such as LDL-C (Ridker et al., 2002). Beside CRP, which was the first and thus even the best studied marker of inflammation in humans, also serum amyloid A (SAA), group II secretory phospholipase A_2 ($sPLA_2$), platelet-activating factor acetyl hydrolase (PAF-AH) and others may be potential markers or mediators of atherosclerosis (Chait et al., 2005).

2.4 Medication

Besides recommendations to change life style conditions, hyperlipidemia is treated with drugs. Most of the anti-atherogenic drugs aim at lowering the concentration of LDL-C. Widely used are so-called **statins** with approximately 400 millions of applications worldwide. *Atorvastatin*, also known as *Sortis* in German speaking countries is the largest selling drug in the world with about US $12.9 billion in 2006. Its cholesterol-lowering effect is documented, dose-dependent, up to 50 % (Rouleau, 2005).

2.4.1 Statins

Statins are competitive inhibitors of the HMG-CoA[1] reductase which catalyzes the reaction of HMG-CoA to mevalonate - the key process of cholesterol biosynthesis (Figure 2.5).

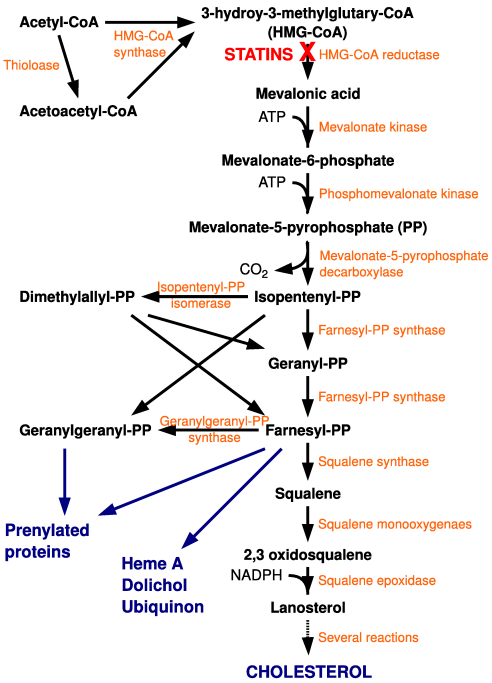

Figure 2.5: **Inhibition of cholesterol biosynthesis by statins.**

The intracellular cholesterol concentration inversely regulates the expression of the LDL receptor which supplies cholesterol through receptor-mediated endocytosis. When cellular cholesterol levels are low transcription factors of the class of sterol response element binding proteins (SREBP) are activated through potential proteolytic cleavage (Brown and Goldstein, 1986, 1997). The activated part enters the cell nucleus and binds to sterol response elements (SRE) in the promoter region of the LDL receptor gene. Thus, lowering the cholesterol concentration up-regulates the LDL receptor synthesis, increases the uptake of apoB-containing particles from the blood circulation and, subsequently, reduces the plasma LDL cholesterol level. Besides regulating the cholesterol biosynthesis, the SREBPs also coordinate the transcription of a number of genes involved in the fatty acid metabolism and

[1] 3-hydroxy-3-methylglutaryl-coenzyme A

uptake including fatty acid synthase (Magana and Osborne, 1996) and acetyl-CoA carboxylase (Lopez et al., 1996). However, the application of statins is controversial because of several side effects documented in the past, such as headache, nausea, vomiting, constipation, diarrhea, weakness and muscle pain. More serious side effects of myopathy and rhabdomyolysis are known in the context of *Lipobay*. Biochemically, this can be explained by the fact that inhibition of the HMG-CoA reductase not only reduces the intracellular level of cholesterol but rather all intermediates of the synthesis pathway, as well. Of main importance is farnesyl pyrophosphate that serves as the source for other essential cellular components, e.g. selenoproteins, ubiquinone (Co-enzyme Q10) and geranyl compounds. The latter plays a major role in post-translational glycosylation of proteins. It is assumed that more than 300 proteins are influenced by statins. The systemic effects of statins remain to be intensively studied. Only recently, a novel modulator of the LDL receptor mediated endocytosis was identified. The serine protease called PCSK9 (pro-protein convertase subtilisin/kexin type 9) provides a new therapeutic target to lower LDL cholesterol levels (Horton et al., 2007).

2.4.2 Fibrates, nicotinic acid and resorption inhibitors

Other lipid-lowering therapies include the treatment with fibrates (Fenofibrate, Gemfibrozil), nicotinic acid (Niacin) or resorption inhibitors (Ezetimibe). **Fibrates** are agonists of PPAR-α, specific transcription factors that belong to the nuclear hormone receptor super-family termed peroxisome proliferator-activated receptors. Intracellular enzymes of fatty acid and triglyceride synthesis are down-regulated by PPARs. In contrast, catabolic enzymes are up-regulated which together results in a substantial decrease in plasma triglycerides and a moderate decrease in LDL cholesterol. In turn, PPAR-α induces the transcriptional synthesis of the major HDL apolipoproteins, apoA-I and apoA-II, which increases the HDL cholesterol level (Staels and Auwerx, 1998).

The lipid-lowering effect of **nicotinic acid** has been mainly associated with the suppression of lipolysis from adipose tissue, however, the mechanism is not fully understood. The decreased release of free fatty acids is assumed to suppress triglyceride synthesis in the liver and VLDL secretion into the blood leading to reduction of LDL, accordingly (Karpe and Frayn, 2004). In addition, considerably reduced Lp(a) levels have been found under nicotinic acid medication (Carlson et al., 1989).

Another strategy is to directly block cholesterol absorption from diet. Inhibitors, like ***Ezetimibe***, bind to a specific cholesterol uptake mediating protein called Niemann-Pick Carrier 1 like Protein 1 (NPC1L1). The de-

creased cholesterol uptake again promotes the receptor-mediated endocytosis of plasma lipoproteins and lowers the plasma cholesterol level.

The lipid-modifying drugs currently available have generally modest effects on HDL-C levels. For example, fibrates and niacin raise HDL-C by only 5% to 10% (depending on the triglyceride levels) and 15% to 35%, respectively (Expert Panel on Detection, Evaluation, and Treatment of High Blood Cholesterol in Adults, 2001). Even more, despite aggressive treatment of LDL cholesterol a significant number of coronary events still occur. Thus, novel therapeutics targeting HDL are increasingly propagated as promising medication in the future. This implies not necessarily simply raising HDL-C levels but rather targeting the processes involved in HDL metabolism and reverse cholesterol transport. Current emerging therapies are excellently reviewed by (Duffy and Rader, 2006) and include fibrates' next generation, inhibitors of CETP (Tall, 2007), e.g. Torcetrapib (Nissen et al., 2007), and apoA-I directed therapeutics. A comprehensive review of pharmacotherapy for lipid disorders is given by (Knopp, 1999).

Chapter 3

Current *State of the Art* in the Analysis of Lipoprotein Metabolism

"To doubt everything or to believe everything are two equally convenient truths; both dispense with the necessity of reflection."

(Henri Poincaré)

3.1 Animal models

A number of genes encoding for proteins that directly interact with plasma lipids have been isolated, sequenced and mapped over the time. They serve as candidate genes to identify mutations associated with alterations in the lipoprotein phenotype. Using this knowledge, numerous animal models have been established to gain new insights in the abnormalities of lipoprotein metabolism. Guinea pigs are proposed to be appropriate models to study the effect of diet and drugs (Fernandez and Volek, 2006; West and Fernandez, 2004). In contrast, transgenic or knock-out mouse models have been widely used to analyze the effects of over- and underexpression of single genes (Breslow, 1993, 1996). Most common are knock-out mice that are deficient in apolipoprotein E (ApoE-/-) (Plump and Breslow, 1995) or the LDL receptor (LDLR-/-) (Powell-Braxton et al., 1998) as well as transgenic mice that express human apolipoprotein B (Kim and Young, 1998; Purcell-Huynh et al., 1995).

However, mouse as a species *per se* is highly resistant to atherosclerosis. In order to develop atherosclerotic disease selective mutations have to be induced. Thus, whether these models accurately mimic the human lipoprotein metabolism remain controversial. Even more, whereas some patients have indeed a monogenic defect, e.g. in the LDL receptor gene, it is widely accepted that atherosclerosis is a complex disease influenced simultaneously by a number of genes effecting the lipid values.

3.2 Pathway analysis in atherosclerosis

Analyzing the interaction of multiple genes may therefore contribute more effectively to the understanding of disease development. Several approaches already attend to this matter. King and her colleagues accounted for gene interactions by a network-based approach (King et al., 2005). They performed a comprehensive gene level assessment of coronary atherosclerosis by using a customized microarray platform to assay gene expression profiles of vessels from human hearts. They compiled lists of genes relevant to the cardiovascular system under subheadings that included 'atherosclerosis', 'smooth muscle cell', 'endothelial cell', 'apoptosis', 'cytokine' and 'adhesion molecule'. As a main result, they provide further support for the idea that smooth muscle dedifferentiation is a key process in the disease progression of atherosclerosis. However, they neglected genes which are more relevant to underlying disorders in the lipid metabolism.

Knoblauch et al. performed epidemiological studies to analyze single nucleotide polymorphisms (SNPs) and derived haplotypes within multiple lipid-regulatory genes (Knoblauch et al., 2002, 2004). They conclude from the results that the selected haplotypes explain most of the genetic variance in HDL and LDL cholesterol in a representative German population. As an example, ApoE shows the strongest influence on the variation in LDL (50%) and in the LDL/HDL ratio (36%). However, this approach does not tell us anything about the underlying molecular processes.

To analyze the interrelationship between the kinetics of individual biochemical processes and the dynamics of the whole lipoprotein population in a causative and quantitative manner mathematical models are needed. In 2000, a first kinetic model of the lipoprotein metabolism suitable to analyze the effects of genetic variations on blood lipid values was published by Knoblauch et al. (Knoblauch et al., 2000).

In addition, there exist a few mechanistic models for selected sub-systems of the lipid metabolism in the liver. Ratushny et al. have focused on the gene network involved in the hepatocellular biosynthesis of cholesterol and

its exchange with blood plasma cholesterol (Ratushny et al., 2003). Shorten and Upreti published a kinetic model that puts particular emphasis on how different fatty acid compositions influence the complex processes of lipid metabolism and lipoprotein assembly in human liver (Shorten and Upreti, 2005).

3.3 Tracer kinetic studies and compartment modeling

3.3.1 Methodological aspects

In general, mathematical models concerning the lipoprotein metabolism consider lipoprotein density classes as dynamic variables (=compartments) of the system. These models are commonly named *compartment models*. Endogenous labeling with stable isotopes and reasonable use of compartment models in the analysis of kinetic data are so far state of the art to describe the dynamics in lipoprotein metabolism. Recent publications given by Barrett et al. (Barrett et al., 2006), Parhofer et al. (Parhofer and Barrett, 2006) and Rashid et al. (Rashid et al., 2006) provide comprehensive overviews about these lipoprotein tracer kinetic studies and what has been learned for apoB and apoA kinetics, respectively. In order to facilitate the design of experiments and the analysis of lipoprotein tracer data using compartment models the SAAM software was developed (Barrett et al., 1998).

In brief, phenomenological forming and degrading processes govern the evolution of the compartments over time whose mass balance is described by a set of differential equations. Compartment modeling aims at quantifying the transition or transport rate of material either (i) into a compartment, (ii) from one compartment to another one or (iii) out of the system. The kinetic parameters for, e.g. synthesis and catabolism of a compartment are typically measured in terms of production rates (PR) and fractional catabolic rates (FCR), respectively. They are usually determined by radioactive or stable isotope tracer experiments. Herein, lipoproteins can be labeled either exogenously or endogenously. The former follows the procedure of isolating lipoproteins from plasma which are labeled in vitro and subsequently reinjected. The latter uses amino acids which are firstly labeled with stable isotopes (e.g. L-[^{13}C]leucine) and incorporated into the apolipoproteins under study as endogenous tracers by bolus or primed constant infusion. Taking leucine as an endogenous tracer offers the advantage of an essential amino acid that is readily available and not converted to other amino acids. The transition rates are obtained by analyzing the ratio between labeled and unlabeled material (tracer/tracee ratio) over time (Parhofer et al., 1991).

From the tracer kinetic data the coefficients of the underlying system of differential equations are determined deriving subsequently PRs and FCRs.

Details of the laboratory methodology are out of focus of this work and have been comprehensively reviewed elsewhere (Dwyer et al., 2002; Patterson et al., 1998).

3.3.2 Studies on the VLDL, IDL and LDL metabolism

In the last decades, numerous compartment models have been designed to quantify the synthesis, interconversion and catabolism of apoB100-containing lipoprotein classes in blood plasma, such as VLDL, IDL and LDL (Adiels et al., 2005; Beltz et al., 1985; Bilheimer et al., 1979; Chan et al., 2006; Cummings et al., 1995; Fisher et al., 1994; Packard et al., 1995, 2000; Parhofer et al., 1996; Tremblay et al., 2004; Winkler et al., 1999). PRs and FCRs have been determined in about 30 studies for healthy subjects and are comprehensively reviewed in (Marsh et al., 2002; Watts et al., 2000). The metabolism of VLDL and LDL has been also studied under several aspects including the effect of gender and age, under fasting, feeding or in dependence on dietary composition as well as under several pathological conditions and interventions by pharmacotherapy.

Studies indicate that an increase in VLDL and LDL production as well as a decreased VLDL and LDL catabolism correlates with age (Marsh et al., 2002). The difference between women and men may be related to differences in hormone constitution. An increased VLDL production was observed for the feeding state compared to the fasting state. One problem, however, in analyzing subjects under feeding is remaining because of the non-steady-state situation.

Especially, studies on subjects under pathological conditions such as familial hypercholesterolemia (FH), metabolic syndrome, type II diabetes, familial defective apoB (FDB), hypobetalipoproteinemia, mutant forms of PCSK9, enabled to identify the most determinant players in the VLDL secretion as well as the VLDL and LDL catabolism, namely the LDL receptor, apoB and an intracellular chaperone for the LDL receptor (PCSK9).

In a very early radiolabeling study, Bilheimer et al. provided the first evidence that FH is associated with a decreased clearance of LDL consistent to a defect in the LDL receptor (Bilheimer et al., 1979). They investigated the gene-dosage effect in 7 heterozygous and 7 homozygous FH patients compared to normal subjects using ^{125}I-radiolabeled LDL. For the latter, they observed a three-fold increase in apoB-LDL production and one third of normal fractional catabolic rate.

The phenomenon of increased VLDL synthesis was further supported by

studies of (Cummings et al., 1995) and (Tremblay et al., 2004) using stable isotopes. Cummings et al. found an increased hepatic secretion of VLDL in 6 patients with heterozygous FH (elevated LDL cholesterol and apoB levels) who received a primed, constant infusion of L-[^{13}C]leucine. The isotopic enrichment of VLDL apoB was measured using GC/MS (gas chromatography/mass spectrometry). They conclude from the results that a decreased LDL receptor activity is accompanied with an increased receptor-independent hepatic uptake of cholesterol. This leads to an increase in the absolute intracellular cholesterol pool and stimulates the synthesis and secretion of VLDL apoB.

In contrast, Fisher et al. observed a decreased VLDL production rate combined with a shift to the direct production of IDL/LDL species (almost 40% of overall apoB) in patients with heterozygous FH using endogenous labeling of VLDL with L-[^{3}H]leucine as the stable isotope (Fisher et al., 1994). Furthermore, VLDL apoB was fully converted to LDL as compared to about half of secreted apoB in normal subjects. The results have been explained by an adaptation to an increase in the hepatic cholesterol ester level rather than by the LDL receptor paradigm because an underlying mutation in the LDL receptor gene could not be observed.

Firstly, this may reflect the diversity of results which can be obtained by studies with similar or even the same phenotypic conditions. Secondly, it gives raise to another highly discussed point of interest in lipoprotein metabolism - is the liver capable of directly synthesizing apoB-containing lipoprotein particles other than of density of VLDL?

Several studies support the concept of producing apoB-containing lipoproteins of different densities. However, it remains controversial whether an increased LDL apoB concentration arise from a direct synthesis by the liver or a fast turning-over VLDL, which can shift newly secreted apoB directly to the LDL fraction (Demant et al., 1996). Although this topic is not fully clarified most of the compartment models include pathways allowing the direct production of IDL and LDL (see Figure 3.1).

Studies on hypobetalipoproteinemia (low LDL cholesterol and apoB levels), which attributes mainly to truncations of apoB, showed that the rate of secretion is closely linked to the length of apoB (Parhofer et al., 1996). In patients with metabolic syndrome and insulin resistance, free fatty acids induce hypersecretion of VLDL-apoB (Adiels et al., 2005; Chan et al., 2006; Cummings et al., 1995).

3.3.3 Studies on HDL metabolism

Like tracing apoB-100 in the metabolism of lipoproteins, such as VLDL and LDL, tracer kinetic studies for the HDL metabolism also use individual lipoprotein components (mainly apolipoproteins) as the tracee under study. Opposed to apoB-100, this implies several difficulties because HDL apolipoproteins readily exchange between lipoprotein species, occur in equilibrium with free plasma pool and can be taken up separately from a HDL particle (Ponsin and Pownall, 1985). This might make following the tracer and estimating the appropriate turnover rates more difficult.

The majority of studies have used labeled apoA-I to kinetically examine the metabolism of HDL (Batal et al., 1998; Chétiveaux et al., 2004; Frénais et al., 1999; Ikewaki et al., 1993; Ji et al., 2006; Miller et al., 2003; Pietzsch et al., 1998; Rader et al., 1991; Roma et al., 1993; Schaefer et al., 2000; Vélez-Carrasco et al., 1999; Winkler et al., 2000). They aimed at understanding the factors influencing the HDL metabolism and the key atheroprotective process of reverse cholesterol transport (RCT), in particular leading to low HDL cholesterol levels. Besides healthy subjects, much has been learned from studies in patients with several dyslipidemia, such as hypo- and hyperalphalipoproteinemia, insulin resistance, type 2 diabetes and obesity.

The results have provided the general suggestion that the clearance rather than the production rate of HDL apoA-I is the dominant process affecting plasma HDL-C levels (Brinton et al., 1994). Pietzsch et al. have reported intrinsic (HDL composition) as well as extrinsic (CETP and HL activities) factors leading to enhanced HDL apoA-I FCR in patients with insulin resistance (Pietzsch et al., 1998). The HDL particles were enriched in triglycerides and phospholipids as well as depleted of cholesteryl ester and protein. Whereas obesity and insulin resistance belong to common low HDL cholesterol disorders hypo- and hyperalphalipoproteinemia are rare human disorders. Hypoalphalipoproteinemia is caused by monogenic defects in one of the determinants for low HDL-C and apoA-I levels, such as ABCA1, apoA-I and LCAT. Studies in patients with defective ABCA1 have likewise reported an increased apoA-I catabolism at normal production rates (Batal et al., 1998; Miller et al., 2003).

Contrary, patients with hyperalphalipoproteinemia (e.g. HL or CETP deficiency) show slower apoA-I catabolism yielding high HDL-C and apoA-I levels compared to healthy subjects. For example, Ruel et al. have measured the *in vivo* kinetics of apoA-I and apoA-II in patients with complete (n=3) and partial (n=3) HL deficiency by primed constant infusion of deuterated leucine (Ruel et al., 2004). They have observed enlarged triglyceride-rich HDL particles and 21% lower apoA-I FCR which is also consistent to the

fact that HL deficiency causes hypertriglyceridemia. However, the results suggest that HL may be important for adequate HDL metabolism but may not be necessary for normal HDL mediated RCT.

Ikewaki et al. performed *in vivo* kinetic studies in patients with homozygous (n=2) and heterozygous (n=1) CETP deficiency by administering $^{13}C_6$-labeled phenylalanine by primed constant infusion for up to 16 h. They have found a delayed catabolism of apoA-I and apoA-II in the homozygous patients while production rates of these apolipoproteins were unaffected (Ikewaki et al., 1993).

Most interestingly, a mutant form of apoA-I, named apoA-I_{Milano}, and specific forms of LCAT deficiency indeed lower the HDL-C level but without associated risk of CVD (Roma et al., 1993). This phenomenon has been related to the possibly different metabolic fates apoA-I has in lipoprotein particles with apoA-I alone (LpA-I) and together with apoA-II (LpA-I:A-II) (Rader et al., 1991). While apoA-I levels are determined by its rate of clearance (as already mentioned above), apoA-II levels are predominantly affected by its rate of production. Ikewaki et al. have postulated that the production rate of apoA-II mainly regulates the distribution of apoA-I among HDL-classes. Thus, an increased production of apoA-II would shift apoA-I from LpA-I to LpA-I:A-II yielding a decrease in LpA-I and elevated levels of LpA-I:A-II, accordingly (Ikewaki et al., 1995).

Besides apoA-I and A-II, a few studies have investigated the role of other lipoprotein components such as apoC and apoE (Batal et al., 2000; Millar et al., 1998). Cohn et al. have measured turnover rates of the HDL-apolipoproteins A-I, C-I, C-III and E in 16 subjects using a primed constant (12 h) infusion of deuterated leucine and a three-compartment model (Cohn et al., 2003). From the data they postulated a metabolic link between apoC-III and apoA-I indicating a significant role of apoC-III in regulating HDL metabolism.

With respect to lipid components, some studies have been performed to examine the turnover of triglycerides (Patterson et al., 2002; Zech et al., 1979) and cholesterol (Ouguerram et al., 2002; Schwartz et al., 1982). Patterson et al. have investigated the VLDL-TG kinetics in healthy subjects using stable isotopically labeled glycerol and palmitate tracers in conjunction with a four-compartment model. The study was aimed at proving the necessity of introducing a tracer-recycling (e.g. hepatic glycerolipid pools) into the compartment model in order to accurately describe VLDL-TG kinetics. The results indicated that this together with a bolus injection of the tracer would indeed offer a reliable approach. However, especially with regard to these lipids it remains quite difficult to analyze kinetic data because of their rapid

exchange between apoB-containing lipoproteins and HDL (Barrett et al., 2006).

Combined multicompartment models provide a method to analyze the kinetics of several components simultaneously. They are quite rare due to experimental limitations. Nevertheless, Adiels et al. published a model that analyzes the kinetics of both apoB and triglycerides, simultaneously (Adiels et al., 2005). For this purpose, 17 subjects with normal lipid values were administered with [$^2H_3$]leucine and [$^2H_5$]glycerol as a bolus injection. The kinetic analysis was performed using a two-layer compartment model enabling to handle both tracers separately. Since they decided to define compartments of uniform particle size (uniform TG/apoB ratio) the model has been limited to four distinct particle sizes. As main results, they obtained $VLDL_1$ and $VLDL_2$ apoB and TG fractional catabolic rates as the major determinants of plasma TG concentration. Interestingly, they found significant differences in the delay times after synthesis of VLDL-TG and VLDL-apoB (21 vs. 33 min). This has been related to a sequential assembly model of VLDL in the liver.

In summary, most of the studies have been designed for both apoB-100 and apoA-I metabolism to investigate the cause of high LDL-cholesterol (major determinants of disorders: LDLR, apoB-100, PCSK9) and low HDL-cholesterol levels (major determinants of disorders: ABCA1, apoA-I, LCAT), respectively. Both have in common that the determinants of related disorders include processes in which receptor-mediated uptake or the appropriate ligand binding are defective. Furthermore, a number of studies suggest that dyslipidemia is not exclusively related to high LDL-C and low HDL-C. Even low LDL-C (hypobetalipoproteinemia) and high HDL-C (hyperalphalipoproteinemia) are likewise caused by underlying disorders and may increase the risk of cardiovascular disease (CVD). This supports the concept presented here that monitoring the distribution of the entire lipoprotein composition spectrum as well as changes in individual lipoprotein compositions may reveal more reliable information about the patients risk state.

3.3.4 Dynamics of individual lipoprotein complexes vs. compartments

In the early beginning of studying the lipoprotein metabolism using tracer kinetic data density classes have been assumed as a homogeneous population of lipoprotein particles. Since several studies, especially on VLDL and LDL metabolism, have shown that both comprise kinetically heterogeneous lipoprotein particles so-called multicompartment models became favorable.

As an example, Figure 3.1 shows a multicompartment model consisting of 15 different compartments (numbered circles). This model has been used to analyze the metabolism of apoB-100 containing lipoproteins, e.g. to evaluate the variation of production and clearance between VLDL1 and VLDL2, to examine the metabolism of IDL and LDL in dependence on the precursor VLDL kinetics and to understand the formation of small-dense LDL (Packard et al., 2000).

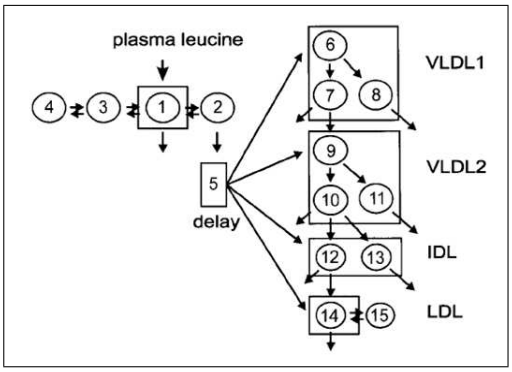

Figure 3.1: **Example of a compartment model (Packard et al., 2000).**

The arrows (→) specify the transition or transport rates (i) into a compartment (production rate, PR), (ii) from one compartment to another one (fractional transport rate, FTR) or (iii) out of the system (fractional catabolic rate, FCR). Trideuterated L-[5,5,5,-$^2H_3$]leucine (d_3-leucine) was used as tracer administered both by bolus and primed constant infusion.

The plasma leucine concentration is represented by compartment 1 which receives the tracer and distribute it to several body protein pools (compartments 3 and 4). This also includes the intracellular compartment 2 serving as the precursor for the synthesis of apoB-100. After a delay (compartment 5) the tracer appears throughout the lipoprotein multicompartments VLDL1, VLDL2, IDL and LDL which again consist of two or three sub-compartments (6-7, 9-11, 12-13 and 14-15, respectively).

As main results, Packard et al. found that the production rates of VLDL1 and VLDL2 are not correlated. This would indicate an independent assembly and secretion of both VLDL subclasses. Furthermore, they postulated from the estimated transition rates a diminished lipolysis of VLDL (lower VLDL1-apoB, VLDL2-apoB FTR and higher VLDL2-apoB PR at elevated levels of total plasma triglycerides) and a prolonged resistance of LDL (lower LDL-apoB FCR) as the cause of predominant levels of small-dense LDL. However, as long as the model does not take into account processes related

to the metabolic fate of individual lipoproteins or even components such as triglycerides, physiological conclusions should be handled carefully.

Multicompartment models not only fail to mimic the physiological reality in several ways but also may lead to incorrect interpretations of the estimated phenomenological rates. The number of sub-compartments chosen as well as the transition of one compartment into another one is physiologically completely unfounded as (i) still a sub-compartment combines a number of individual lipoprotein particles to a homogeneous population and (ii) each kinetic process affects its substrate on a molecular level rather than on a compartment level. The mistake one makes becomes very apparent by analyzing the kinetic behavior of a compartment compared with that of a single lipoprotein complex. Unlike the assumption compartment models act on, there is no simple kinetics which can describe the dynamics of a compartment as illustrated in the following simple example:

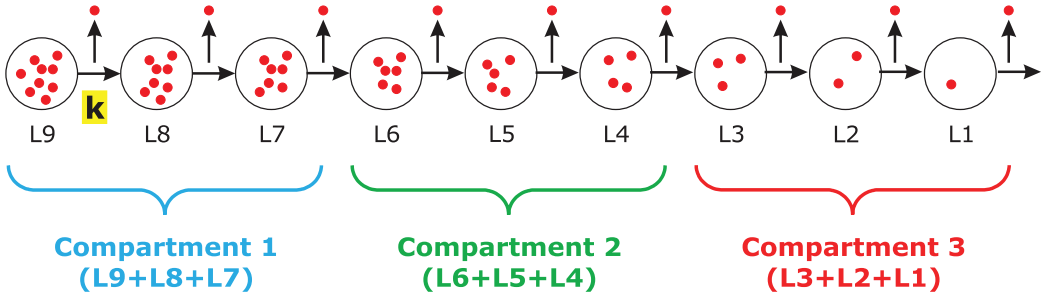

Figure 3.2: **Scheme of the delipidation cascade of 9 lipoprotein particles (L9 → L1).** The conversion from one lipoprotein complex into another one occurs by releasing one molecule triglyceride (red bullets). In the simplest example, the parameter k is assumed to be equal for all lipoprotein particles (homogeneous kinetics). In an extended version, the conversion rate additionally depends on the number of triglyceride molecules present in the corresponding lipoprotein particles (heterogeneous kinetics). A compartment, C1, C2 and C3 comprises three individual lipoprotein complexes, L9 to L7, L6 to L4 and L3 to L1, respectively.

The main process by which VLDL1 converts to VLDL2 or IDL and subsequently LDL is the removal of triglycerides from the lipoprotein complex in that fatty acids are released (hydrolyzed) from the glycerol backbone. Figure 3.2 schematically illustrates this process with 9 lipoprotein complexes of different triglyceride composition which successively lose their triglyceride content. Except for the lipoprotein complex *L9* the initial concentration of all lipoprotein complexes is zero. A compartment simply comprises a number of individual lipoprotein complexes, three in the example.

Mathematically, the process of delipidation is described by simple mass-

action kinetics, i.e. the rate with that one lipoprotein complex converts to another one (by losing one molecule triglyceride) depends linearly on the substrate concentration. The balance equations are formulated as follows:

Balance equations of delipidation cascade	*Solution of the balance equations*
$\dot{L}_9 = -k\ L_9$	$L_9 = C\ e^{-kt}$
$\dot{L}_8 = k\ L_9 - k\ L_8$	$L_8 = C\ (kt)\ e^{-kt}$
$\dot{L}_7 = k\ L_8 - k\ L_7$	$L_7 = C\ \frac{k^2t^2}{2}\ e^{-kt}$
$\vdots = \vdots$	$\vdots = \vdots$

The trajectories (Figure 3.3) show that the dynamic behavior on the basis of individual lipoprotein complexes differs remarkably from that using a compartmental description. The difference will be more pronounced with larger compartments, i.e. a higher number of individual lipoprotein complexes combined into one compartment.

Especially with respect to the trajectory of compartment 1, there is one distinctive feature. Using linear mass-action kinetics the degradation rate at non-zero substrate concentration levels can only be zero under steady state conditions (concentration does not change over time). However, this would contradict to the model definition made in this example. Although compartment 1 is at time t=0 present at sufficient concentration (non-zero value) its concentration remains unchanged (or marginally increases) during the first time period until the trajectory rapidly declines which accounts for a degradation rate of value zero.

Further support for the incorrectness of compartment modeling comes from the examination of the underlying kinetic rate law for both, a single lipoprotein complex and a compartment. Exemplarily, Figure 3.3(c) shows the time evolution dL/dt over substrate concentration $L(t)$ for L9 (black line) and compartment 1 (L9+L8+L7, blue line), respectively. As expected, the kinetic rate law of the single lipoprotein complex follows a linear mass-action kinetics. In case of the compartment the kinetic rate law might be expressed as a complex non-linear kinetic mechanism (e.g. quadratic or cubic).

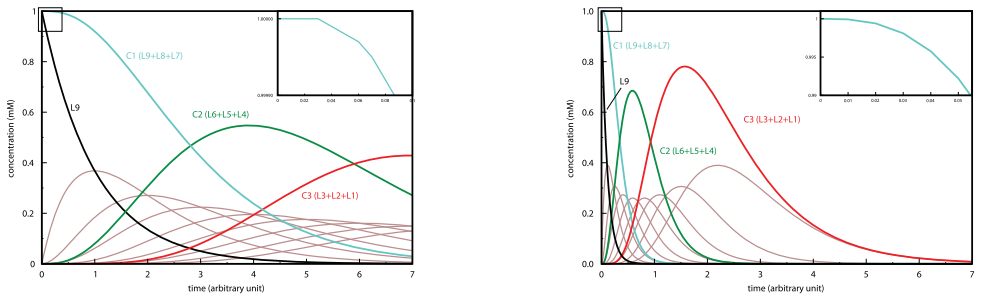

(a) Trajectories for homogeneous kinetics

(b) Trajectories for heterogeneous kinetics

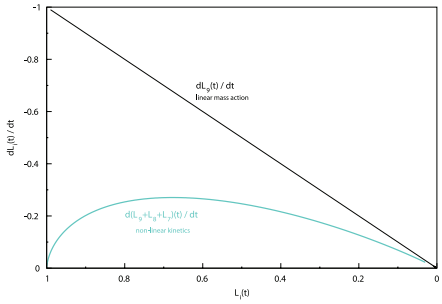

(c) Kinetic rate laws

Figure 3.3: **Single lipoprotein complex vs. compartment kinetics.** Trajectories by assuming kinetically (a) homogeneous and (b) heterogeneous lipoprotein complexes. Black line: time curve for the lipoprotein complex L9; Brown lines: time curves for individual lipoprotein complexes (L8 to L1); Blue, green and red line: Compartment 1, 2 and 3 each combine three individual lipoprotein complexes L9 to L7, L6 to L4 and L3 to L1, respectively. y-axis: concentration (mM), x-axis: time (arbitrary units). (c) The kinetic rate law for the dynamics of the individual lipoprotein complex (L9, black line) follows a linear mass-action kinetics whereas the dynamics of compartment 1 (L9+L8+L7, blue line) might be expressed as a complex non-linear kinetics. y-axis: dS/dt, x-axis: S(t), S=affected lipoprotein complex or compartment.

The same analysis was performed by considering lipoprotein complexes as kinetically heterogeneous in that the rate depends on the individual lipoprotein composition. The rate constant was additionally multiplied by the appropriate number of triglyceride molecules in each of the lipoprotein complexes. The trajectories appear differently as formerly observed (Figure 3.3(b)), the error one gets by combining lipoprotein complexes into compartments persists.

3.3.5 Summary of compartment modeling's limitations

Compartmental models may provide a useful phenomenological description of the lipoprotein dynamics. However, compartment models exhibit some serious limitations.

(i) By using density classes as system variables the composition and kinetic heterogeneity of lipoproteins are largely neglected.

(ii) The relative transition rates between compartments and the rate of the underlying molecular processes remain disparate. This could be shown on the example discussed before. It was the most simplest approximation to metabolic processes. Despite it's simplicity, a simple-minded translation into a compartment model will fail dramatically as there is no simple kinetics which can describe the dynamics of the compartments. This problem is not unique to the above model but will be more pronounced for realistic systems. More precisely, VLDL is not transformed into IDL by just one process but by a number of successive elementary reactions in which triglycerides are removed and apolipoproteins are exchanged.

(iii) Modeling of changes in the level of lipoprotein classes reflects the current experimental state of the art. However, it provides only a faint insight into the dynamics taking place in the full space of individual lipoprotein complexes.

(iv) Depending on the available kinetic data, compartment models have focused on specific parts of the lipoprotein metabolism, e.g. the metabolism of HDL based on kinetic measurements with labeled apoA-I and/or apoA-II or the metabolism of LDL and VLDL sub-fractions based on kinetic measurements with labeled apoB-100.

(v) Compartment modeling and tracer kinetic studies remain time consuming and even more difficult to perform. Methodological problems such as an adequate amino acid precursor kinetics are unsolved yet (Barrett et al., 2006).

—

Here, a novel modeling approach is presented that overcomes the limitations of traditional modeling techniques and experimental difficulties. The model itself is one of the major results of this work and is separately described in the following chapter.

Chapter 4

The *in silico* Model

"All models are wrong, but some are useful."

(George E. P. Box)

In the modeling approach, the use of predefined density classes is avoided, instead lipoproteins are characterized by their protein and lipid composition. As described below, the model takes into account essential lipoprotein constituents and processes involved in the lipoprotein metabolism in human blood plasma.

4.1 Lipoprotein components

A detailed description of the protein and lipid components considered in the model was provided in the introduction section 2.1.1. The lipoprotein complexes in the model are composed of three different types of apolipoproteins and lipids abbreviated with A, B, F and C, T, P, respectively (Table 4.1).

Table 4.1: **Model components.**

Model abbrev.	Lipoprotein component
A	Apolipoprotein A-I
B	Apolipoprotein B-100
F	Further Apolipoproteins
C	Total Cholesterol
T	Triglycerides
P	Phospholipids

The protein components A and B are thought to represent apoA-I and apoB-100, respectively. Each lipoprotein is either equipped with component A or component B. Thus, the terms of *A-particles* or *B-particles* are introduced, respectively. The protein component F (F = **f**urther apolipoproteins) is intended to lump together other apolipoproteins, mainly C apolipoproteins and apoE. The lipid components C, T and P represent total cholesterol (free cholesterol and cholesteryl esters), triglycerides and phospholipids, respectively. The dynamics of phospholipids is not directly considered. Instead, the number of phospholipid molecules in an individual lipoprotein complex is calculated such that - together with the apolipoproteins - full occupancy of the lipoprotein surface is achieved (appendix A).

The component's densities vary between 1.35 and 0.886 g/ml for apolipoproteins and triglycerides, respectively. The possible molecule number for each component goes up to several thousands (Table 4.2) and results by considering all stoichiometric combinations in a huge diversity of lipoprotein complexes in the system. Given a specific interval (min, max) of molecule numbers for each component one would get for A-particles $A \cdot (F+1) \cdot (C+1) \cdot (T+1)$ and for B-particles $B \cdot (F+1) \cdot (C+1) \cdot (T+1)$ about $4.8 \cdot 10^8$ lipoprotein complexes in total.

Table 4.2: **Composition properties of lipoprotein complexes.**

Lipoprotein species		A	B	F	C	T
				component particle number		
A-particle	*min*	1	0	0	0	0
	max	5	0	15	300	50
	packages	5	0	15	150	25
B-particle	*min*	0	1	0	0	0
	max	0	1	15	3000	10,000
	packages	0	1	15	150	500

min and *max* represent the lower and upper limit of component's number, respectively. Lipid (C,T) package sizes were defined as 2 and 20 molecules in A- and B-particles, respectively. Thus, in terms of *packages*: A-particles contain at most 150 packages of cholesterol molecules and 25 packages of triglyceride molecules, B-particles contain at most 150 cholesterol and 500 triglyceride packages.

To reduce the total number of lipoprotein complexes and to make the computation time required to obtain a steady state still tractable I refrained from considering the actual number of molecules for total cholesterol (C) and triglycerides (T). Instead, their content was quantified in terms of lipid

packages. Lipid packages of C and T comprise 2 molecules in A-particles and 20 molecules in B-particles, respectively, which finally results in two orders of magnitude less lipoprotein complexes.

4.2 Kinetic processes

From the reactions reported to affect the metabolism of lipoprotein in the human blood plasma, 20 elementary processes were selected. They cover the spectrum of synthesis and interconversions until receptor-mediated uptake of lipoproteins. Figure 4.1 illustrates the main processes taking place on lipoprotein complexes at a molecular level. These processes can be grouped into the 6 categories of:

(I) Birth and Death including the synthesis and holoparticle uptake of lipoproteins, *(II) Exchange with tissue cells*, *(III) Exchange of lipids* and *(IV), (V) of proteins among lipoproteins* as well as *(VI) Enzyme reactions* which are described in more detailed in the following. A more mechanistic representation of how the processes are formulated in the model is given in Figure 4.2.

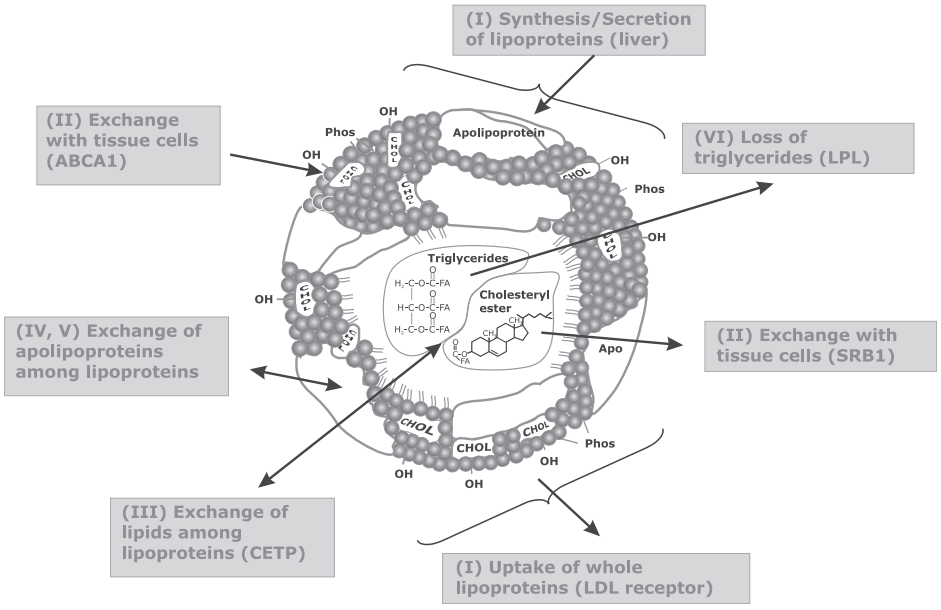

Figure 4.1: **Illustration of the main kinetic processes affecting a lipoprotein complex.** Roman numeral in parentheses denote the category the process is assigned to. For in-depth description of the processes see text.

I) Birth and Death. The total amount of lipoprotein complexes is the result of *de novo* synthesis by the liver and the receptor-mediated uptake of whole particles from the blood by tissue cells (Figure 4.2a). Separate kinetic parameters are used for the generation and elimination of A- and B-particles. The synthesis of B-particles is thought to reflect the synthesis and secretion of VLDL by the liver whereas synthesized A-particles represent preβ_1-HDL secreted by the liver, as well. The initial composition (initA, initB, initF, initC, initT) of the nascent particles was set to fixed values (1, 0, 0, 10, 0) and (0, 1, 10, 2000, 10000) for A- and B-particles, respectively. Thus, in terms of packages initial A-particles contain 5 packages of cholesterol molecules and initial B-particles contain 100 cholesterol and 500 triglyceride packages.

II) Lipoprotein-Tissue Exchange. Besides the synthesis and holoparticle uptake of lipoprotein complexes (see category I), individual lipoprotein components are selectively altered by exchange processes with various tissue cells. Processes of this category are among the important steps of the reverse cholesterol transport (from the periphery back to the liver). Here, the model takes into account the uptake of peripheral cholesterol by A-particles (named *Influx*) and the delivery of cholesteryl esters from both particle species (*EffluxA, EffluxB*) mainly to the liver (Figure 4.2b). The *Influx* is thought to be mediated by the ATP-binding cassette A1 (ABCA1) transporter and a monomolecular, preβ-migrating, lipid-poor or lipid-free form of apoA-I is described as the preferred acceptor in blood plasma (Rye and Barter, 2004). In the model, the latter would represent the initial A-particle. On the other hand, the scavenger receptor class B, type I (SRBI) is assumed to facilitate the *Efflux*. Whereas the contribution of SRBI to the selective uptake of cholesteryl ester from A-particles is well established (Acton et al., 1996; Thuahnai et al., 2001; Trigatti et al., 1999, 2000a,b), for B-particles, its function has been documented more sparsely (Rhainds and Brissette, 1999). Initially, Green and Pittman showed the selective uptake of LDL-CE in rat liver perfusates (Green and Pittman, 1991).

III) Inter-Lipoprotein Exchange of neutral lipids among lipoproteins is mediated by the cholesteryl ester transfer protein (CETP) which transfers preferentially cholesteryl esters from A- to B-particles and triglycerides *vice versa*. It is hypothesized that the mechanism of action follows a Ping-Pong Bi-Bi shuttle between the donor and acceptor lipoprotein molecules rather than via a ternary complex between CETP, the donor and the acceptor molecule (Mead et al., 2002). To model

this transfer, a non-lipid bound form of this carrier protein was introduced (called CETP(0) in the model) that can be loaded either with C (called CETP(C)) or T (called CETP(T)) shuttling between A- and B-particles (Figure 4.2c). The elementary steps of the bidirectional exchange are modeled as follows: (i) one package of component C is transferred from an A-particle to non-lipid bound CETP(0) ($ExchangeC_A$), (ii) CETP(C) releases the package of C to an apoB-containing lipoprotein ($ExchangeC_B$), (iii) one package of component T is transferred from a B-particle to non-lipid bound CETP(0) ($ExchangeT_{B1}$), (iv) CETP(T) releases its package of T to an apoA-containing lipoprotein ($ExchangeT_A$). A similar exchange of triglycerides may occur from VLDL to LDL playing a crucial role, for example in the accumulation of small-dense LDL (Lewis and Steiner, 1996) or during partial CETP suppression (Morton and Greene, 2007). In order to be aware of this physiology, triglyceride uptake of B-particles was allowed and separately defined ($ExchangeT_{B2}$).

IV) Exchange of apolipoprotein A. Central to lipoprotein metabolism is the transfer of apolipoproteins among lipoprotein. ApoA-I exchange between HDL species is well established and modeled by decomposing it into (i) a release step from a lipoprotein complex into a common apolipoprotein pool and (ii) an uptake process from this pool into a lipoprotein complex. The transfer process for the protein component A is restricted to A-particles and is thought to describe the remodeling of apoA-containing HDL (Figure 4.2d).

V) Exchange of apolipoproteins F. The transfer of those apolipoproteins (mostly apoE and apoC) lumped together into the component F may take place between arbitrary lipoprotein complexes (Figure 4.2e). Apolipoproteins C and E are described to be transferred from HDL particles to newly synthesized VLDL directly after secretion and *vice versa* after remodeling of VLDL (Eisenberg, 1984). These processes were named *TransferF* and *UptakeF*, respectively, which are treated in the model separately for either particle species (Figure 4.2e). Based on the work of (Boyle et al., 1999), all transfer processes are assumed to follow the mechanism of aqueous diffusion instead of a particle collision. Thus, plasma reservoirs of the appropriate components are introduced named $pool_A$ and $pool_F$.

VI) Enzymatic Conversion. One central enzymatic process effecting the remodeling of lipoproteins is the hydrolysis of triglycerides and phospholipids, i.e. removing fatty acids by cleavage of the ester bond

to the glycerol backbone. As this process is catalyzed by two different enzymes, lipoprotein lipase (LPL) and hepatic lipase (HL), it is treated in the model as two separate processes, accordingly (Figure 4.2f). Both enzymes exhibit different substrate specificity. LPL preferentially hydrolyzes triglycerides as compared to phospholipids contributing predominantly to the remodeling of triglyceride-rich lipoproteins (TRL), like VLDL. In contrast, HL does not favor one of the lipids and contributes mainly to the lipolysis of IDL, LDL and HDL (Deckelbaum et al., 1992; Zambon et al., 2003). With respect to this substrate specificity the processes are named *HydrolyzeA* acting on both A- and B-particles and *HydrolyzeB* exclusively subjected to B-particles.

A summary of the kinetic processes included in the model and their physiological meaning is shown in Table 4.3.

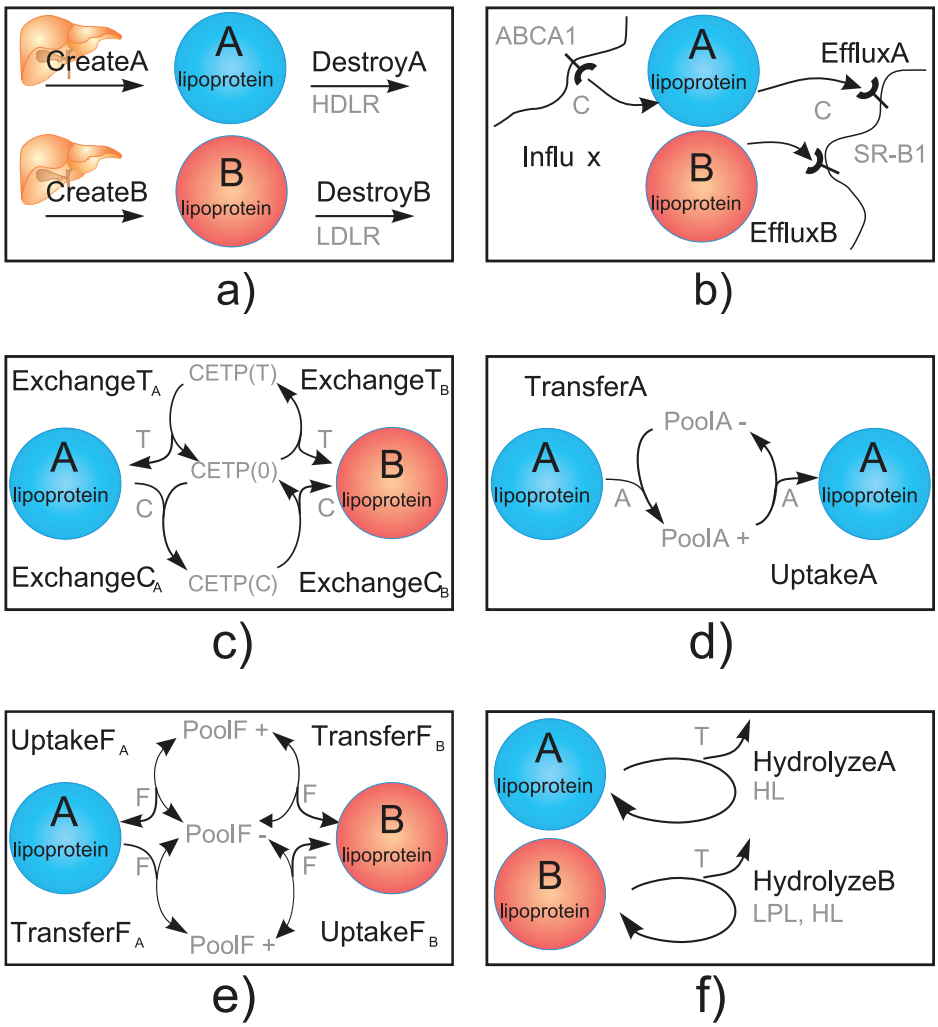

Figure 4.2: **Illustration of the kinetic processes defined in the model.** a) Synthesis of A- and B-particles and degradation via HDL and LDL receptors, respectively. b) Influx of peripheral cholesterol (C) into A-particles via the ATP-binding cassette A1 (ABCA1) receptor and selective efflux of cholesteryl ester (C) by the scavenger receptor B1 (SRB1). c) Elementary processes of the cholesteryl ester transfer protein (CETP) named mediating the exchange of triglycerides (T) and cholesteryl ester (C) between lipoprotein components. CETP(0), CETP(T) and CETP(C) represent non-lipid bound, T- and C-loaded form of CETP, respectively. d,e) Exchange of apolipoproteins (A, F) among lipoprotein complexes via free plasma pools (PoolA, PoolF). f) Hydrolysis of triglycerides (T) from A- and B-particles by hepatic and/or lipoprotein lipase (HL, LPL).

Table 4.3: **Description of the kinetic processes defined in the model.**

Lp Species	Process	Description
A-particle	*Death and Birth*	
	CreateA	Synthesis and secretion of lipid-poor apoA-I molecules by the liver
	DestroyA	Receptor-mediated particle uptake, e.g. by the HDL receptor (HDLR)
	Lipoprotein-Tissue Exchange	
	Influx	Peripheral cholesterol is transferred to plasma HDL particles mediated by e.g. ABCA1
	EffluxA	Selective uptake of cholesteryl ester from HDL facilitated by e.g. SRB1
	Inter-Lipoprotein Exchange	
	ExchangeC$_A$	Cholesteryl ester is transferred from HDL to the non-lipid bound exchange protein (*CETP(0)*)
	ExchangeT$_A$	*CETP(T)* releases its triglyceride content to HDL
	TransferA	Remodeling of apoA containing HDL particles by losing and
	UptakeA	Receiving a single molecule of apoA-I from the plasma pool
	TransferF$_A$	Delivery of apolipoproteins from HDL to newly synthesized VLDL via a free plasma pool
	UptakeF$_A$	Uptake of apolipoproteins by HDL particles
	Enzymatic Conversion	
	HydrolyzeA	Removal of triglycerides (hydrolysis of free fatty acids) by the action of Hepatic Lipase (HL)
B-particle	*Death and Birth*	
	CreateB	Synthesis and secretion of VLDL by the liver
	DestroyB	Receptor-mediated particle uptake, e.g. by the LDL receptor (LDLR)
	Lipoprotein-Tissue Exchange	
	EffluxB	Selective uptake of cholesteryl ester from e.g. LDL facilitated by e.g. SRB1
	Inter-Lipoprotein Exchange	
	ExchangeC$_B$	*CETP(C)* releases its cholesteryl ester to apoB-containing lipoproteins
	ExchangeT$_{B1}$	Triglyceride from apoB-containing lipoproteins is transferred to the non-lipid bound exchange protein (*CETP(0)*)
	ExchangeT$_{B2}$	*CETP(T)* releases its triglyceride content to apoB-containing lipoproteins
	TransferF$_B$	Release of apolipoproteins during the delipidation cascade of apoB particles
	UptakeF$_B$	Uptake of further apolipoprotein molecules, e.g. of apoE by newly synthesized VLDL
	Enzymatic Conversion	
	HydrolyzeB	Removal of triglycerides (hydrolysis of free fatty acids) by the action of Lipoprotein Lipase (LPL)

4.3 Simplifications

To keep the model tractable (in time) some simplifications regarding the number of components and the kinetic description of the processes were made:

- In face of known important regulatory functions different apolipoproteins may have (see section 2.1.1), distinguishing between several isoforms is refrained and various apolipoproteins are lumped together into one component. Hereby, apoF is thought to cover mainly apoC and apoE.
- As free cholesterol and cholesteryl ester were combined to one component C (=total cholesterol), esterification of free cholesterol by the lecithin cholesterol acyl transferase (LCAT) is not considered. Processes that would affect either free cholesterol or cholesteryl ester are addressed to total cholesterol, accordingly.
- The dynamics of phospholipids is not explicitly modeled, however, the amount is incorporated for density calculation in the end (see appendix A). From this, it also follows that LPL and HL solely hydrolyze triglycerides in the model.
- Setting the initial composition to fixed values rather than to deal with a distribution of different compositions is another simplification made in the model.
- Likewise, the receptor-mediated uptake is not further specified regarding the differentiation between several lipoprotein receptors. For example, the model does not distinguish between the LDL receptor (LDLR), LDL receptor related protein (LRP) and VLDL receptor (VLDLR) for B-particle uptake or between different HDL receptors (e.g. Cubulin, Scavenger) for the uptake of A-particles. Although receptors such as ABCG1 and ABCG4 have been reported to be involved in the uptake of peripheral cholesterol (Wang et al., 2004), even with respect to the impact of a disorder in ABCA1 to Tangier Disease, the model focuses on the ABCA1 mediated process only.
- Finally, despite CETP is proposed to bind phospholipids, cholesterol and other molecules (Connolly et al., 1996; Qiu et al., 2007), CETP was restricted to its main function - the exchange of neutral lipids.

4.4 Model equations

For most reactions considered in the model, the exact kinetic mechanism including all regulatory effects is not known. Therefore, we used simple rate equations based on mass action kinetics. They are summarized in Table 4.4.

A-particle		
$v_{createA}$	=	$v_{createA} = const$
$v_{destroyA}$	=	$c_{destroyA} \cdot X_i$
v_{influx}	=	$v_{influx} = const$
$v_{effluxA}$	=	$c_{effluxA} \cdot nC_i$
$v_{exchangeC_A}$	=	$c_{exchangeC_A} \cdot nC_i \cdot CETP(0)$
$v_{exchangeT_A}$	=	$c_{exchangeT_A} \cdot CETP(T)$
$v_{transferA}$	=	$c_{transferA} \cdot nA_i \cdot (A_{max} - A)$
$v_{uptakeA}$	=	$c_{uptakeA} \cdot A$
$v_{transferF_A}$	=	$c_{transferF_A} \cdot nF_i \cdot (F_{max} - F)$
$v_{uptakeF_A}$	=	$c_{uptakeF_A} \cdot F$
$v_{hydrolyzeA}$	=	$c_{hydrolyzeA} \cdot nT_i$
B-particle		
$v_{createB}$	=	$v_{createB} = const$
$v_{destroyB}$	=	$c_{destroyB} \cdot X_i$
$v_{effluxB}$	=	$c_{effluxB} \cdot nC_i$
$v_{exchangeC_B}$	=	$c_{exchangeC_B} \cdot CETP(C)$
$v_{exchangeT_{B1}}$	=	$c_{exchangeT_{B1}} \cdot nT_i \cdot CETP(0)$
$v_{exchangeT_{B2}}$	=	$c_{exchangeT_{B2}} \cdot CETP(T)$
$v_{transferF_B}$	=	$c_{transferF_B} \cdot nF_i \cdot (F_{max} - F)$
$v_{uptakeF_B}$	=	$c_{uptakeF_B} \cdot F$
$v_{hydrolyzeB}$	=	$c_{hydrolyzeB} \cdot nT_i$

Table 4.4: **Model equations.** v_μ and c_μ are rate and rate constant of reaction μ, respectively; nX_i denotes the amount of component X, X=(A,B,F,C,T) in a lipoprotein complex i; X_i is the amount of lipoprotein i in the system; A_{max}, F_{max} and A, F are the maximal and actual number of free A and F in the plasma pool, respectively. $CETP(0)$ and $CETP(C)$, $CETP(T)$ denote the non-lipid bound and lipid bound (either with C or T) transport forms of the cholesteryl ester transfer protein (CETP), respectively.

Chapter 5

Methods - Experiments and Modeling Work

"It doesn't matter how beautiful your theory is, it doesn't matter how smart you are. If it doesn't agree with experiment, it's wrong."

(Richard Feynman)

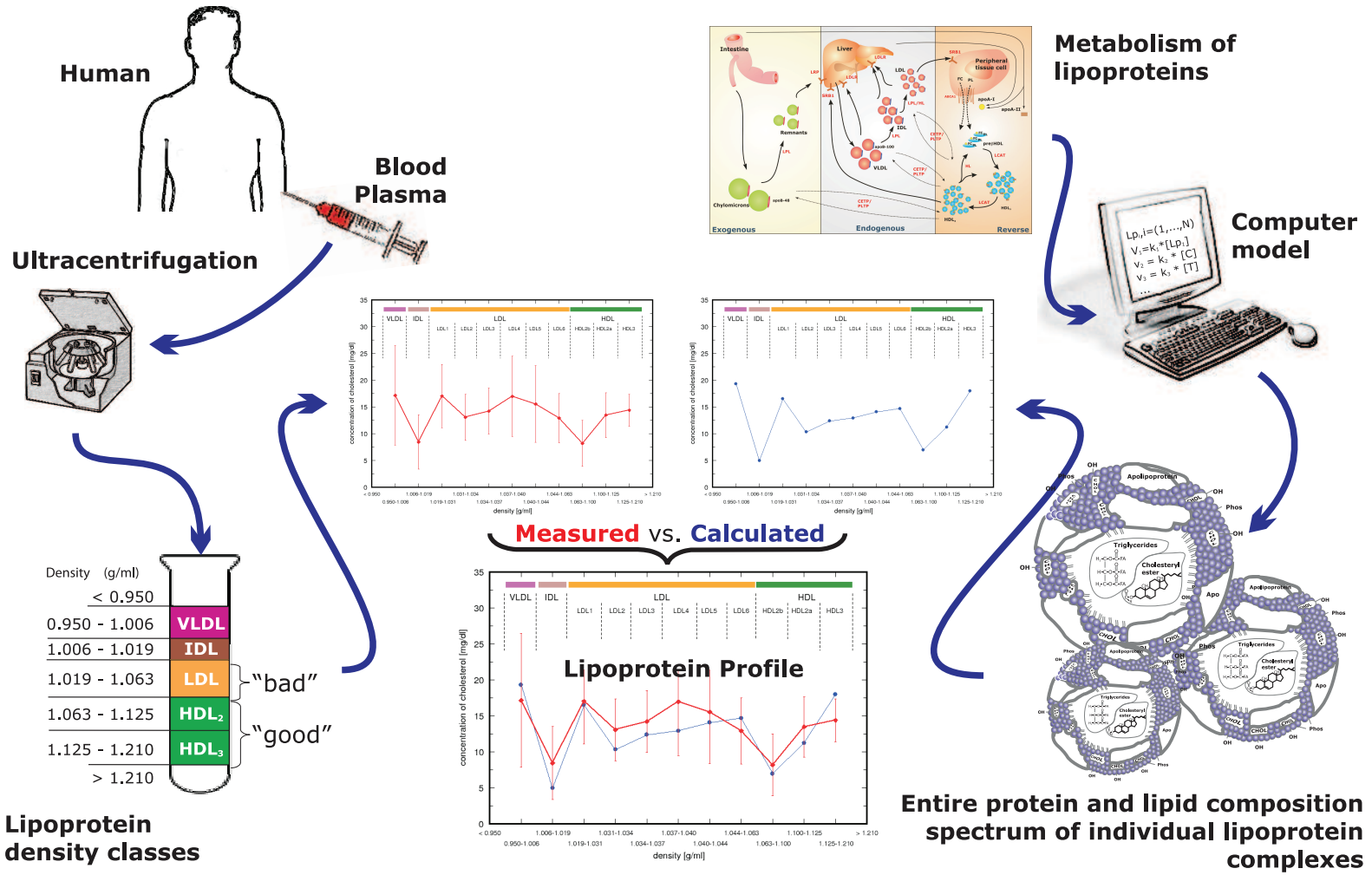

Figure 5.1: Schematic overview of experimental and modeling methods.

5.1 Experiments

5.1.1 Subjects

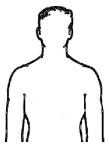

All laboratory assessments were performed at the Department of Clinical Chemistry, University Hospital of Freiburg, Germany. Normolipidemic concentration ranges of total plasma lipoprotein components are given as follows: 120-240 mg/dl total cholesterol, 25-200 mg/dl triglycerides, 40-80 mg/dl free cholesterol, 80-160 mg/dl cholesteryl ester, 100-300 mg/dl phospholipids and 90-200 mg/dl for apolipoprotein (apo) A-I, 40-70 mg/dl apoA-II, 30-150 mg/dl apoB-100, 1-10 mg/dl apoC-II, 5-15 mg/dl apoC-III and 4-12 mg/dl apoE.

5.1.2 Lipoprotein separation

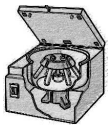

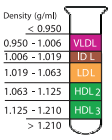

Main classes of lipoproteins (VLDL, IDL, LDL, HDL) and subfractions of LDL and HDL were isolated from plasma by sequential preparative ultracentrifugation according to Baumstark et al. (Baumstark et al., 1990). The LDL class was separated into six density sub-fractions (LDL1-6) whereas HDL was subdivided into fractions of $HDL2_b$, $HDL2_a$ and HDL_3. Recoveries of cholesterol after centrifugation of all lipoproteins were > 95 %. The interassay coefficient of variance of the determination of apoB in each of the six LDL subfractions was ≤ 5 % (Winkler et al., 2000).

5.1.3 Lipoprotein chemistry

Cholesterol, triglyceride and phospholipid concentrations were determined enzymatically with the CHOD-PAP, GPO-PAP and PLD-PAP methods (Roche Diagnostics, Mannheim, Germany), respectively. Concentrations of apolipoproteins were determined by turbidimetry on a Wako 30 R analyzer (Wako Chemicals, Japan) using polyclonal antisera (Rolf Greiner Biochemica, Germany) specific for the respective antigens. For experimental details the reader is referred to (Winkler et al., 2000).

5.1.4 Lipoprotein composition profile

The concentration of the lipoprotein components in each separated lipoprotein density class (see Table 5.1) are averaged values from 11 randomly selected normolipidemic subjects under fasting conditions. ApoC isoforms and apoE were lumped together into one component named apoF.

Table 5.1: **Experimental lipoprotein composition data.**

Lp fraction	Density (g/ml)		Total	A	B	F	C	T	P
	min	*max*	*concentration in mg/dl (± SD)* (n=11)						
Plasma	0.950	1.400	755.8 (102.6)	122.3 (21.7)	68.3 (17.3)	20.87 (3.8)	164.9 (30.1)	109.9 (44.6)	181.9 (23.0)
VLDL	0.950	1.006	120.9 (70.9)	0.0	5.1 (2.1)	7.12 (3.8)	17.1 (9.3)	69.5 (42.8)	22.0 (11.9)
IDL	1.006	1.019	33.4 (10.4)	0.0	3.7 (1.7)	0.54 (0.2)	8.4 (5.1)	12.1 (2.6)	8.6 (3.4)
LDL	1.019	1.063	217.34 (56.1)	0.0	47.5 (12.7)	0.45 (0.4)	89.6 (24.4)	19.7 (5.6)	60.1 (14.6)
LDL1	1.019	1.031	41.8 (12.5)	0.0	7.8 (2.2)	0.05 (0.1)	17.0 (5.9)	5.1 (1.5)	11.8 (3.5)
LDL2	1.031	1.034	30.4 (8.7)	0.0	6.2 (1.7)	0.0	13.0 (4.3)	2.5 (0.7)	8.6 (2.6)
LDL3	1.034	1.037	33.4 (10.0)	0.0	7.3 (2.2)	0.0	14.2 (4.3)	2.6 (1.1)	9.4 (2.7)
LDL4	1.037	1.040	39.7 (17.3)	0.0	9.2 (4.1)	0.0	17.0 (7.5)	2.8 (1.5)	10.8 (4.5)
LDL5	1.040	1.044	36.9 (16.8)	0.0	8.9 (4.1)	0.0	15.5 (7.2)	2.5 (1.2)	10.0 (4.5)
LDL6	1.044	1.063	33.4 (11.6)	0.0	8.4 (3.1)	0.34 (0.2)	12.9 (4.6)	3.0 (1.1)	8.8 (3.0)
HDL	1.063	1.400	216.1 (50.5)	89.4 (19.9)	0.0	5.12 (2.0)	41.8 (10.9)	10.5 (2.0)	64.8 (18.3)
HDL2	1.063	1.125	96.13 (33.1)	34.9 (12.0)	0.0	0.38 (0.5)	21.61 (8.0)	5.63 (1.0)	33.80 (12.9)
HDL2b	1.063	1.100	31.1 (16.8)	9.4 (5.5)	0.0	0.38 (0.4)	8.1 (4.3)	2.0 (0.4)	11.3 (6.5)
HDL2a	1.100	1.125	65.1 (18.6)	25.5 (7.3)	0.0	0.0	13.5 (4.2)	3.6 (0.8)	22.5 (7.2)
HDL3	1.125	1.210	84.2 (17.3)	42.8 (9.1)	0.0	0.48 (0.4)	14.4 (3.0)	3.6 (1.1)	23.2 (5.4)
preβ-HDL*	1.210	1.400	40.8 (20.0)	30.6 (8.0)	0.0	2.57 (1.5)	0.0	0.0	29.7 (1.3)

Data are averaged values from 11 randomly selected normolipidemic subjects under fasting conditions. *The density fraction of so-called preβ-HDL (1.210-1.400 g/ml) was not directly measured in the experiment. Therefore, this fraction was assumed and calculated as the difference between total plasma and total HDL values for apoA-I, cholesterol and phospholipids. Abbreviations: VLDL, IDL, LDL, HDL (very low, intermediate, low, high density lipoproteins); A, B, F, C, T, P (apoA-I, apoB-100, apoC+apoE, total cholesterol, triglycerides, phospholipids)

5.2 Modeling and simulation

Setting up a model aims at presenting a simplified view of reality, however, in most cases complex enough that its analysis can only occur *in silico* (on a computer).

A schematic illustration of the incremental and sometimes iterative steps of model building and simulation up to getting the results and performing analyses is given in Figure 5.2. Broadly, a model describes in an adequate manner all components of a system under investigation and the interactions between them which is called *model definition*. In case of the lipoprotein metabolism this concerns the *lipoproteins* as well as their constituents and the *kinetic processes* involved in the permanent remodeling of lipoproteins, respectively. The model definition made in this work (see Chapter 4) arose from an intensive study of the current *state of the art* literature knowledge as presented in-depth before. If the processes are known the *model equations* are formulated. They permit to describe the time evolution of each of the components in the system.

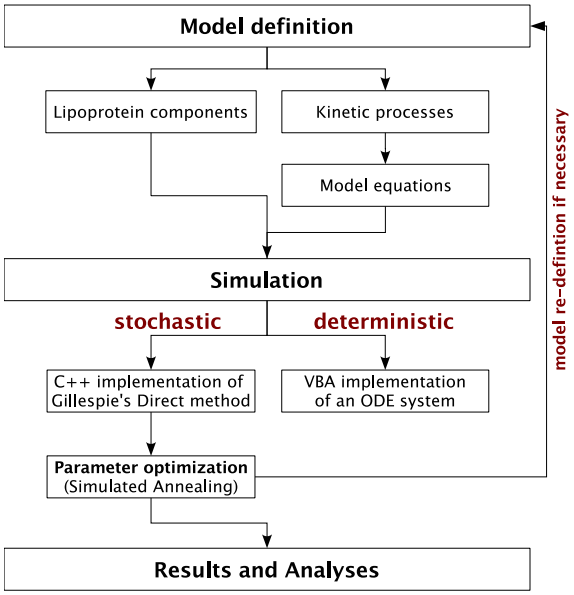

Figure 5.2: **Steps in modeling and simulation of the lipoprotein metabolism.**

The model was simulated by two different approaches, a stochastic and a deterministic one, which are described in the following.

5.2.1 Stochastic simulation

The stochastic model is simulated based on Gillespie's Direct algorithm (Gillespie, 1976) considering a system of N chemical species, in this model lipoproteins $\vec{Lp_i}$, $i = (1, \ldots, N)$, which are affected by M different kinetic processes R_μ, $\mu = (1, \ldots, M)$ in a unit volume V.

Each lipoprotein complex $\vec{Lp_i}$ is unique with respect to its composition $\vec{Lp_i}(nX_i))$ where nX_i is the number of molecules of component X, $X \in \{A, B, F, C, T\}$ in a lipoprotein i (Figure 5.3).

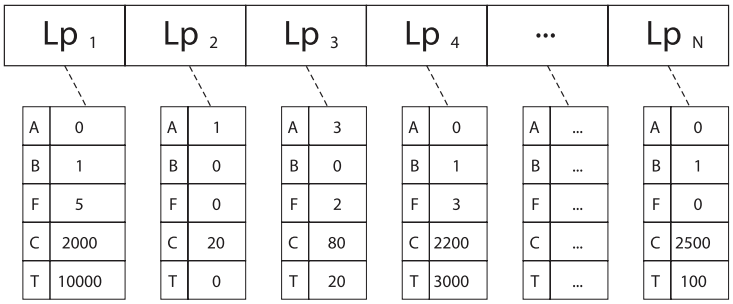

Figure 5.3: **Lipoprotein complexes in the system.** Each lipoprotein complex has an individual composition $\vec{Lp_i}\,(nA, nB, nF, nC, nT)$.

All lipoprotein complexes $\vec{Lp_i}$ may be present with n_i identical copies. The n_i may be any non-negative integer number. As the model includes the exchange of the components A and F with plasma pools of free A and free F, respectively, and the exchange of the components C and T by the cholesteryl ester transfer protein ($CETP$) the numbers n_A, n_F, $n_{CETP(0)}$, $n_{CETP(C)}$ and $n_{CETP(T)}$ were also introduced which denote the numbers of the respective component in the plasma pool. The state of the system is uniquely characterized by the vector $\vec{n}$ of all numbers n_i and of all pool components.

$$\vec{n} = \Big(n_1, n_2, \ldots, n_N, \quad n_A, n_F, \ldots, n_{CETP(T)}\Big) \tag{5.1}$$

The set of all thinkable vectors $\vec{n}$ constitutes the *s*tate space of the system. Let $P(\vec{n}', t)d\vec{n}$ be the probability to observe the system in a small volume $d\vec{n}$ in the state space, i.e. the probability to find

$$\begin{aligned}
n_1' \leq \quad & n_1 < n_1' + dn_1 \\
\vdots \quad & \\
n_N' \leq \quad & n_N < n_N' + dn_N \\
n_A' \leq \quad & n_A < n_A' + dn_A \\
\vdots \quad & \\
n_{CETP(T)}' \leq \quad & n_{CETP(T)} < n_{CETP(T)}' + dn_{CETP(T)}
\end{aligned}$$

The function $P(\vec{n}, t)$ is the probability density of state $\vec{n}$. It contains all information about the evolution of the stochastic system over time. N_{from}

denotes the set of states which may be transformed to state $\vec{n}$ by a single reaction and with N_{to} the set of all states which may be produced from $\vec{n}$ by a single reaction. Consider, for example the reaction "EffluxA$_i$" representing the uptake of cholesteryl ester from an A-particle of type i. The event of this reaction would be to transform a particle of type i to type i_{-C} which has one C less than i. Therefore, by action of the considered reaction the number n_i is reduced by one. At the same time, the number $n_{i_{-C}}$ is increased by one (the total number of A-particles in the system is not affected by the considered reaction). Therefore, the set N_{to} created by a reaction of type "EffluxA" (with arbitrary i) is the set of all states where one arbitrary A-particle is missing and in exchange, an A-particle with one less C is added. In the same manner the action of the other reactions has to be considered. The equation governing the evolution of the probability density $P(\vec{n},t)$ – the master equation – can be written

$$\frac{\partial P(\vec{n},t)}{\partial t} = \sum_{\vec{n}' \in N_{from}} r_{\vec{n}' \to \vec{n}} P(\vec{n}',t) - \sum_{\vec{n}' \in N_{to}} r_{\vec{n} \to \vec{n}'} P(\vec{n},t) \tag{5.2}$$

Here, $r_{\vec{n} \to \vec{n}'}$ denotes the rate of the reaction transforming the state $\vec{n}$ to $\vec{n}'$. The explicit expression for this would be very complicated as one has to consider all possible results of the action of 20 different reaction types and will, therefore, be omitted here.

The Master equation (Eq. 5.2) cannot be analytically solved. Therefore, approximate numerical solutions were determined using Gillespie's stochastic simulation algorithm (Gillespie, 1976).

Gillespie algorithm. The time evolution of the system is described as a sequence of events taking place at discrete time points. In each event, only one of the elementary processes is carried out instantaneously thereby changing the state of the system. In principle, the algorithm computes the probability a_μ for each reaction μ to occur in the next infinitesimal time step $(t, t+\Delta t)$. The total probability $a_0 = \sum a_\mu$ is a measure for the total activity in the system. Two random numbers, r_1 and r_2, uniformly distributed over unit interval (0,1) are generated. The first is used to determine the waiting time until the next reaction occurs:

$$\tau = \frac{1}{a_0} \ln \frac{1}{r_1} \tag{5.3}$$

The probability for a reaction to occur is proportional to its rate. Accordingly, the index μ of the reaction, which is carried out next, is chosen in that

$$\sum_{k=1}^{\mu-1} a_k < a_0 r_2 \leq \sum_{k=1}^{\mu} a_k \tag{5.4}$$

Finally, one of the lipoproteins is randomly assigned as substrate for the chosen reaction μ. Given the reaction index μ, a third random number r_3 was calculated in order to select one of the lipoprotein particles in the system with its specific composition. The determination of the appropriate lipoprotein equals the calculation of the reaction index μ (see Eq. (5.4)), except the index μ now denotes a specific lipoprotein particle. Execution of the reaction changes the state of the system either by changing the number of lipoproteins or by altering the composition of one of them. Thus, recalculation of the reaction probabilities for the new state is needed, however, only for those a_μ which were actually influenced by the system change.

After updating the system the simulation time is set to $t = t + \tau$. The process is continued by iteratively drawing pseudo-random numbers for the next time interval, the next reaction to be executed and the lipoprotein affected. As illustrated in Figure 5.4 the simulation starts in a system state being lipoprotein-free.

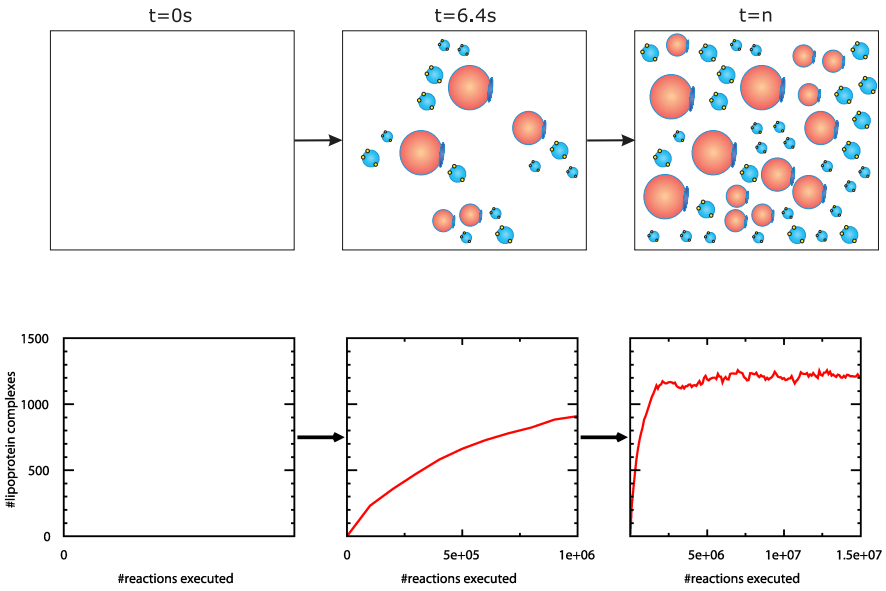

Figure 5.4: **System development.** The stochastic simulation starts with a system being lipoprotein free. After approximately five millions of reactions a steady state is reached.

Executing approximately five millions of such consecutive single reactions (one per time step), a steady state was reached, i.e. the average number of lipoproteins and their composition in the systems remained constant. Further 10 millions of executions sampled the stationary distribution of individual lipoprotein complexes in that the lifetime of each lipoprotein in the system

is monitored. This allows to calculate the average number of an individual lipoprotein complex in the steady state.

5.2.2 Deterministic simulation

If the probability density function $P(\vec{n};t)$ is known, expectation values $c_i(t)$ for the concentration of lipoprotein complexes can be calculated according to

$$c_i(t) = \frac{1}{V} \sum_{\vec{n}} n_i \; P(\vec{n};t). \tag{5.5}$$

The summation goes over all possible states of the system, i.e. over all legal combinations of n_i.
Carrying out the calculation of the expectation values using the Master equation (Eq. 5.2) one obtains a system of first-order differential equations for the time evolution of the concentration vector $\vec{c}(t)$:

$$\vec{c}(t) = \Big(c_1(t), \cdots, c_N(t), c_A(t), c_F(t), c_{CETP(0)}(t), c_{CETP(C)}(t), c_{CETP(T)}(t)\Big) \tag{5.6}$$

The differential equation for the time-evolution of the concentration of the i-th lipoprotein complex has the general form (similar to the form of the master equation)

$$\frac{dc_i}{dt} = f_i^{(+)}\left(\vec{c}\right) - c_i \cdot f_i^{(-)}\left(\vec{c}\right) \tag{5.7}$$

where $f_i^{(+)}$ and $f_i^{(-)}$ comprise all processes that increase or decrease the concentration c_i, respectively. The stationary solution of this system obeys the fix-point equation Eq. 5.8

$$c_i = \frac{1}{\lambda} \; \frac{f_i^{(+)}\left(\vec{c}\right)}{f_i^{(-)}\left(\vec{c}\right)} + \left(1 - \frac{1}{\lambda}\right) \; c_i \tag{5.8}$$

which was solved iteratively. $\lambda \geq 1$ is an integer factor that helps to stabilize convergence, i.e. to overcome oscillations that may occur during iteration procedure.

5.3 Calculation of the density profile

The density d (in g/ml) of a lipoprotein complex is calculated as the sum of the component's molecular weights w_i divided by the sum of the component's molecular volumes v_i

$$d = \frac{\sum w_i \; n_{i,j}}{\sum v_i \; n_{i,j}} \tag{5.9}$$

where i specifies the components (A, B, F, C, T, P) and $n_{i,j}$ is the number of molecules of component i in the lipoprotein complex j. The number of phospholipid molecules is estimated to fill the calculated free volume within the lipoprotein surface (see appendixA).

Values of the molecular weights and volumes were taken from literature and are listed in Table 5.2. From its amino acid composition, apoB-100 is estimated to have a molecular mass of 513 kDa. The somewhat higher apparent molecular mass (approximately 550 kDa) of the native protein is the result of glycosylation. For the lipid components CE, PL and TG average values were used, because the molecular weight and volume may vary depending on the chain length and type (saturated, mono- or polyunsaturated) of the esterified fatty acids.

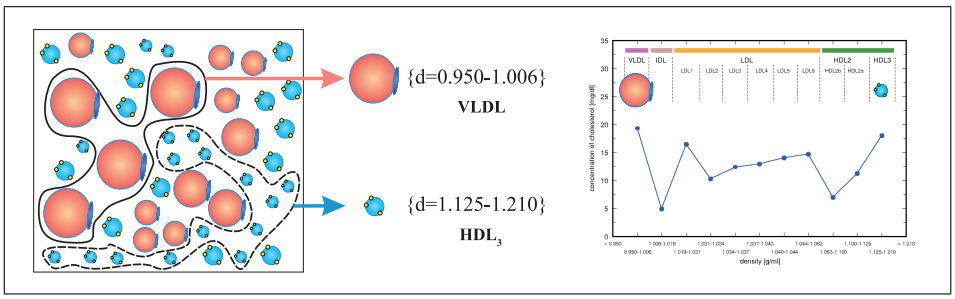

Figure 5.5: **Calculation of the lipoprotein profile by assigning every single lipoprotein according to its density to one of the common density classes.**

Each of the lipoprotein complex is assigned according to its density to one of the density classes typically determined in clinical investigations (Figure 5.5). Finally, according to the concentration the lipoprotein complexes occur in those density classes the distribution over density is calculated.

Table 5.2: **Data for density calculation.**

Component	**Molecular weight**	**Molecular volume**	**Reference**
	g/mol	*ml/mol*	
A	28,500	21,087	(Kostner and März, 1996)
B	546,340	404,292	(Teerlink et al., 2004)
F (ApoC + ApoE)	15,000	11,100	
C (FC+CE)	583	605	
T	859	947	(Teerlink et al., 2004)
P	786	773	(Teerlink et al., 2004)

The molecular weight of component F is averaged by taking individual molecular weights (see also (Kostner and März, 1996)) of apoC isoforms, predominantly apoC-II (8.8 kDa) and C-III (8.9 kDa), and apoE (34 kDa) in a specific set ratio. Similarly, a 1:2 ratio for cholesterol:cholesteryl ester (molecular weights of 386 and 648 Da, respectively) is used for the average molecular weight of component C. Molecular volumes were calculated using appropriate component's specific volumes (Teerlink et al., 2004).

5.4 Optimization

Mathematical optimization can be used as a computational engine to arrive at the best solution for a given problem in a systematic and efficient way. Parameter estimation is one important application of it and yields to reproduce a given experimental data set in the best possible way (Moles et al., 2003).

5.4.1 Parameter estimation

The model parameters were obtained in that predicted and experimental lipoprotein profiles were compared by measuring the distance

$$(\mathbf{p}) = \sum_i w_i \left(x_i^{exp} - x_i^{pred}(\mathbf{p}) \right)^2 \tag{5.10}$$

where $\mathbf{p}$ is the vector of the model parameters. $x_i^{pred}(\mathbf{p})$ and x_i^{exp} correspond to the simulated and measured concentrations of lipoprotein constituents in the i-th density class (see Table 5.1), respectively. w_i is a weight used to achieve that all the data points contribute equally to the distance. Model parameters are adjusted by minimizing the distance function (Eq. 5.10). In this two complications have to kept in mind: (1) the error measure is a stochastic quantity since the underlying process is stochastic and (2) the problem is high-dimensional. This precludes the use of steepest descent methods. To avoid trapping of the minimization procedure in local minima Simulated Annealing (SA) was used to find the global optimum (Kirkpatrick et al., 1983).

5.5 Hardware and software utilities

The stochastic model was implemented in C++ and simulations were performed under a LINUX distribution (Suse 10.1) on a PC (Intel Duo Core). On this machine, a single simulation run (15 millions of events) takes approximately 45 sec. Programs were written in *Octave* (version 2.1.72-16) to facilitate selected system analyses. Octave is a high level programming language designed for the solution of numeric problems and the open-source clone of *MATLAB*. Graphical illustrations were created using graphics software *CorelDraw* (version 12.0). Representation of the results was designed using *xmgrace* (version 5.1.19-13), a 2D-plot-program for visualization of scientific data.

Chapter 6

Results

"The whole of science is nothing more than a refinement of everyday thinking."

(Albert Einstein)

6.1 Stochastic vs. deterministic simulation

The dynamics of the lipoprotein system was simulated by two different approaches, a stochastic and a deterministic one, which have been described in-depth in section 5.2. In brief, the stochastic approach describes the time behavior of the system as a kind of random walk process governed by a sequence of events taking place at discrete time points. The stationary distributions of lipoprotein compositions are calculated by tracking the life of a number of molecules (individual lipoprotein complexes). On the other hand, the deterministic approach regards the time behavior of the system as a continuous process governed by a set of ordinary differential equations and considers concentrations of the variables. Here, the number of variables is specified by the combinatorial diversity of lipoprotein compositions which determines, in principle, the number of differential equations one has to deal with. The possible molecule number for each of the lipoprotein components (lower and upper limit) was chosen very sparsely to cover a sufficient number of different lipoprotein compositions. Noteworthy, the concentrations of a large number of lipoprotein complexes were observed to be practically zero. This might argue for the existence of only a small space of lipoprotein compositions the elementary processes of the lipoprotein metabolism generally act on. However, the solution of very large equation systems even poses serious numerical problems.

For the stochastic simulation, this enormous complexity is not a problem as the Gillespie algorithm computes only stochastic trajectories for those lipoprotein complexes which are effectively observed during simulation. Hence, Gillespie's direct method does not suffer from the type of combinatorial explosion as the deterministic approach. Furthermore, using the stochastic simulation algorithm permits (within a reasonable computation time) to deal with smaller package sizes for the lipid components, i.e. the number of lipid molecules per package, which is important since small package sizes are needed to achieve a sufficiently high coverage of possibly small physiologically relevant density intervals, i.e. containing a sufficient number of lipoprotein complexes.

One problem, however, with the Gillespie algorithm is to conclude from the stochastic trajectories at which time point of the simulation the true stationary regime has been reached and a representative sampling of the state space has been accomplished. To test whether the criteria used to assess stationarity work well the lipoprotein distributions calculated for one and the same set of kinetic parameters have been compared with both model variants (Figure 6.1). To keep the deterministic model numerically tractable the package sizes for cholesterol (C) and triglyceride (T) were set in case of A-particles to two molecules, for B-particles to 100 and 250 molecules, respectively. The maximal molecule number of the components A, B, F, C and T was restricted to (4, 0, 5, 100, 40) for A-particles and to (0, 1, 5, 5,000, 10,000) for B-particles. Using the package sizes given above, the possible C and T content in terms of packages for A-particles decomposes into 50 and 20 packages, for B-particles to 50 and 40 packages, respectively.

As the number of all components, with exception of A and B, can become zero, the total number of different lipoprotein complexes in this example is given by $4 \cdot (5+1) \cdot (50+1) \cdot (20+1)$ for A-particles plus $1 \cdot (5+1) \cdot (50+1) \cdot (40+1)$ for B-particles = 38,250 spanning a density range between 0.92 and 1.4 g/ml. Arbitrary values of the kinetic parameters (not shown) were chosen and the stationary concentration of lipoprotein complexes was computed using either Gillespie's algorithm or iterating the fix-point equation (Eq. 5.8).

In order to compare the two solutions the total density range covered by the 38,250 lipoprotein complexes was subdivided into 30 intervals and the occupancy of these density intervals was calculated by cumulating the calculated concentrations of the corresponding lipoprotein complexes.

As shown in Figure 6.1, with increasing number of time steps used in the Gillespie simulation the stochastic solution converges toward the numerical solution of the deterministic model. For 10^7 steps both are virtually the same.

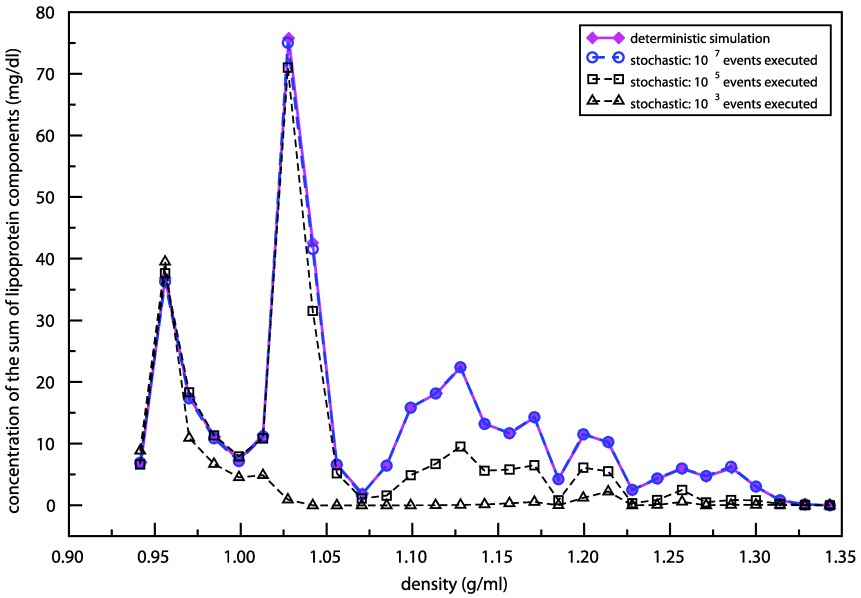

Figure 6.1: **Stochastic vs. deterministic simulation.** Density distributions of the concentration of the sum of lipoprotein components (mg/dl) obtained by using the Gillespie algorithm with different numbers of simulation steps (events) and by the iterative solution of the deterministic equation system using the same parameter set. The density space (0.9-1.4 g/ml) was subdivided into 30 equally sized intervals.

The striking advantage of performing stochastic simulations of the master equation by means of Gillespie's algorithm is that increasing the number of lipoprotein components (e.g. by including cholesteryl ester) or using smaller package sizes results only in a moderate increase of computing time because this algorithm *per se* only deals with such lipoprotein complexes that effectively occur. In contrast, the deterministic model has to deal with all possible complexes despite the fact that most of them never reach discernible concentrations. All subsequent results were therefore obtained using the stochastic simulation algorithm and the much smaller package size of 20 molecules for C and T in B-particles.

6.2 Lipoprotein profiles in healthy subjects

In the experiment, mean concentrations of the lipoprotein components (e.g. total cholesterol, Figure 6.2) in main lipoprotein density classes (VLDL, IDL, LDL, HDL) and sub-fractions of LDL and HDL were measured after separation from blood plasma by ultracentrifugation. The LDL class was separated into six density sub-fractions which can be again grouped into the commonly named large buoyant (lb, LDL1/2), intermediate dense (id, LDL3/4) and small-dense LDL (sd, LDL5/6). The HDL class was subdivided into fractions of HDL_{2b}, HDL_{2a} and HDL_3. The experimentally measured concentration values have been already presented in Table 5.1.

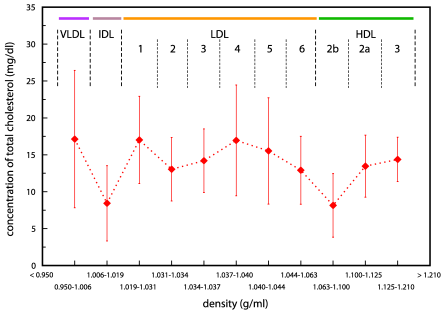

Figure 6.2: **Clinically measured lipoprotein profile.** Shown is the distribution of total cholesterol over common density classes including sub-fractions of LDL1-6, HDL_{2b}, HDL_{2a} and HDL_3.

In the simulation, stationary distributions of individual lipoprotein complexes and their components (e.g. total cholesterol, Figure 6.2) over density were computed, as outlined in section 5.2.1, by using Gillespie's stochastic simulation algorithm. The simulation starts with a system being lipoprotein-free. Executing approximately five million elementary reactions (one per time step), a steady state was reached, i.e. the average number of lipoproteins and their composition in the system remained constant. Further 10 million executions sampled the stationary distribution of individual lipoprotein complexes. Subsequently, each of the lipoprotein complexes in the system is assigned according to its density to one of the experimentally defined density classes yielding lipoprotein density profiles as typically determined in clinical investigations.

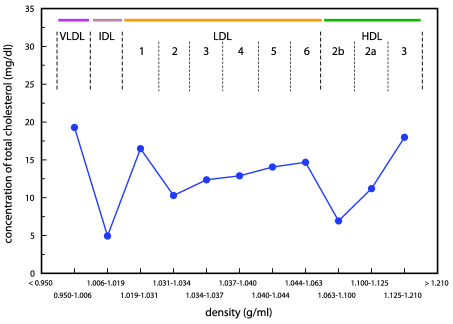

Figure 6.3: **Simulated lipoprotein profile.** Shown is the distribution of total cholesterol over common density classes including sub-fractions of LDL1-6, HDL_{2b}, HDL_{2a} and HDL_3.

6.2.1 Parameter values

The set of model parameters that entail best agreement between the computed lipoprotein profile and the experimental data was determined as follows. To keep the number of lipoprotein complexes in the simulation tractable the system was scaled with an appropriate volume factor yielding a reaction volume of one tenth femto-liter. Parameter values for the synthesis of A- and B-particles were taken from (Schaefer et al., 2000) and (Maugeais et al., 1997), respectively, and fixed during parameter optimization. Numerical values of all other model parameters were obtained by minimizing the discrepancy between simulated and clinically measured lipoprotein profiles (see section 5.4.1). They are listed in Table 6.1.

The estimated parameter values are in most cases in a reasonable agreement with experimentally determined kinetic data found in the literature taking into account the difficulties to extract rate constants of elementary processes from kinetic measurements based on compartment analyses. The underlying reaction mechanism can either be monomolecular (e.g. *EfluxA*) or bimolecular (e.g. $ExchangeC_A$) which is important to know while comparing the stochastic rate constants with rate constants obtained from, e.g. tracer kinetic studies. There is a simple relationship between the values of the rate constants used in the stochastic and the deterministic model. In case of monomolecular reactions both constants are equal. In the case of bimolecular reactions, the stochastic rate constant c_μ derives from the deterministic rate constant k_μ by

$$c_\mu = \frac{k_\mu}{N_A\, V} \tag{6.1}$$

where N_A is the Avogadro constant and V denotes the small sample volume used in the stochastic simulation. Most of the reactions in the model, e.g. the transfer and exchange processes in the plasma, are bimolecular.

As can be taken from Table 6.1, the rate constant estimated for the uptake of A-particles (0.21 day^{-1}) corresponds well to the reference value (0.20 day^{-1}) obtained by various studies (Cohn et al., 2003; Maugeais et al., 1997; Ouguerram et al., 2002; Schaefer et al., 2000). In case of B-particles, the uptake parameter value (=1.31 day^{-1}) lies in the range of fractional catabolic rates (FCR = 0.5 - 6.0 day^{-1}) estimated for VLDL and LDL, respectively, by Maugeais and colleagues using a compartment model (Maugeais et al., 1997). Ikewaki et al. obtained similar ranges (Ikewaki et al., 1995).

Table 6.1: **Model parameter values.**

Rate constants (c_μ)	Unit	Model value	Experiment value	Reference
A-particle				
$c_{createA}$	mM· day^{-1}	8.0e-3	8.4e-3 to 9.2e-3	(Maugeais et al., 1997), (Schaefer et al., 2000), (Cohn et al., 2003)
$c_{destroyA}$	day^{-1}	0.21	0.20	(Maugeais et al., 1997), (Schaefer et al., 2000), (Ouguerram et al., 2002), (Cohn et al., 2003)
c_{influx}	mM· day^{-1}	1.1e-3	2.5e-3	(Fielding et al., 1983)
$c_{effluxA}$	day^{-1}	0.01	0.312	(Ouguerram et al., 2002)
$c_{exchangeC_A}$	day^{-1}	397.1	110.1	(Jarnagin et al., 1987) [a)]
$c_{exchangeT_A}$	day^{-1}	0.65	-	
$c_{transferA}$	day^{-1}	2.0e-4	5.3e-5	(Cohn et al., 2003) [g)]
$c_{uptakeA}$	day^{-1}	0.02	0.14	(Cohn et al., 2003) [h)]
$c_{transferF_A}$	day^{-1}	9.4e-4	7.6e-3	(Batal et al., 2000) [c)]
$c_{uptakeF_A}$	day^{-1}	1.9e-3	3.9e-3	(Batal et al., 2000) [d)]
$c_{hydrolyze_A}$	day^{-1}	5.6	27.72	(Hime et al., 1998)
B-particle				
$c_{createB}$	mM· day^{-1}	1.0e-3	1.0e-3, 1.4e-3	(Ikewaki et al., 1995), (Maugeais et al., 1997)
$c_{destroyB}$	day^{-1}	1.31	0.5 - 5.5 0.4 - 6.9	(Maugeais et al., 1997) (Ikewaki et al., 1995)
$c_{effluxB}$	day^{-1}	0.5	-	
$c_{exchangeC_B}$	day^{-1}	1.7	-	
$c_{exchangeT_{B1}}$	day^{-1}	887.75	1.2	(Jarnagin et al., 1987) [b)]
$c_{exchangeT_{B2}}$	day^{-1}	55.7	-	
$c_{transferF_B}$	day^{-1}	2.0e-3	1.6e-3	(Batal et al., 2000) [e)]
$c_{uptakeF_B}$	day^{-1}	3.5e-3	0.061	(Batal et al., 2000) [f)]
$c_{hydrolyze_B}$	day^{-1}	8.3	7.52	(Ouguerram et al., 2002)

Comparison of estimated model parameter values with measured rate constants found in the literature. Indexes from a) to h) see explanations in appendix B.

The estimated value for the monomolecular process of selectively removing HDL cholesteryl ester (CE), in our model called *EffluxA*, is a magnitude less than what is proposed in published data (0.01 vs. 0.31 day^{-1}, respectively) (Ouguerram et al., 2002). This might be partially caused by summarizing free cholesterol and cholesteryl ester in one component. The preferred physiological substrate of that efflux reaction is cholesteryl ester and the rate depends proportionally on its concentration. Taking the sum of total cholesterol instead increases the substrate concentration available. To transport equal amounts of substrate (e.g. per day) out of the plasma a lower fractional catabolic rate would compensate a higher substrate concentration.

An attempt to relate measured kinetic data of bimolecular processes to the estimated model parameters is exemplarily proposed in the following for the transfer of cholesteryl ester from HDL to apoB-100 carrying lipoproteins, e.g. VLDL, by the CETP. This process is comparable with the bimolecular reaction modeled in $ExchangeC_A$ which follows the rate law

$$v_{exchangeC_A} = c_{exchangeC_A} \cdot nC_i \cdot CETP(0) \tag{6.2}$$

Jarnagin et al. characterized the specificity of a cholesteryl ester transfer protein from human plasma with a molecular weight of 74,000 Dalton Jarnagin et al. (1987). The total transfer activity $v_{exchangeC_A}$ was assayed with 110.52 $\text{mg/dl} \cdot \text{day}^{-1}$ as the rate of loss of H^3-labeled cholesteryl ester in HDL (50 μg/ml in 0.5 ml incubation volume). The CETP mass is given with 0.049 mg/dl ($= 6.6 \cdot 10^{-6}$ mmol/l). The kinetic rate constant $k_{exchangeC_A}$ equals according Eq. 6.2 the total transfer activity divided by the concentration of cholesteryl ester in HDL and by the CETP mass being in its non-lipid bound form *CETP(0)* (in our calculations approximately 25.3 % of total CETP mass). Most of the CETP is loaded with C while the T-loaded form of CETP is very rare with approximately 73.3 % and 1.4 %, respectively.

$$\begin{aligned} k_{exchangeC_A} &= \frac{v_{exchangeC_A}}{[CE] \cdot [CETP(0)]} \\ &= \frac{110.52 \ (\text{mg/dl} \cdot \text{day}^{-1})}{10 \ (\text{mg/dl}) \cdot 1.67 \cdot 10^{-6} \ (\text{mmol/l})} \\ &= 6.63 \cdot 10^{6} \ (\text{l/mmol} \cdot \text{day}) \end{aligned}$$

According to Eq. 6.1 the kinetic rate constant is scaled to the volume (factor 60,220 l/mmol) in that the simulation takes place and agrees in the order of magnitude to the calculated stochastic rate constant $c_{exchangeC_A}$ in our model (110.6 vs. 397.1 day^{-1}). However, the reference HDL-CE concentration is approximately one third of that in our simulation and the CETP

mass is much less even. Thus, comparing the fluxes (total transfer activities) instead being 110.52 vs. 72.13 mg/dl $\cdot$ day^{-1} might be more useful.

Similarly, Jarnagin et al. provide the rate value of the transfer of triglycerides (TG) from VLDL to HDL by CETP relative to the CE transfer (0.11 nmol TG relative to 1 nmol CE per ml per h). This bimolecular process represents $ExchangeT_{B1}$ in the model and follows the rate law

$$v_{exchangeT_{B1}} = c_{exchangeT_{B1}} \cdot nT_i \cdot CETP(0) \tag{6.3}$$

The total transfer activity $v_{exchangeT_{B1}}$ is 15.87 mg/dl $\cdot$ d^{-1}, accordingly. From the given CE (100 μg in 0.5 ml incubation volume) to TG ratio for VLDL (0.15) follows the VLDL-TG concentration of 133.3 mg/dl. By taking the CETP(0) mass given above the (volume scaled) kinetic rate constant is more than two magnitudes less than the estimated model parameter (1.2 vs. 887.75 day^{-1}). However, in this case the reference VLDL-TG concentration is approximately double of that in our simulation and even the CETP mass is less. Thus again, comparing the fluxes (total transfer activity) instead being 15.87 vs. 297.45 mg/dl $\cdot$ day^{-1} might be more useful.

In general, another reason for discrepancies in these processes might be due to the fact that we modeled the exchange of CE and TG uncoupled. That means, triglycerides (component T) of B-particles can be transferred as long as triglycerides and an appropriate acceptor (non-lipid bound CETP) are available independent on the amount of CE (component C) in A-particles. Moreover, the experimental values reflect the overall transfer whereas the model parameter value addresses one elementary step of the entire process.

In case of the transfer and uptake processes of component F the parameters are only slightly interpretable with the current state of the model because it does not specify a particular apolipoprotein. However, Batal et al. investigated the plasma kinetics of VLDL and HDL apoC-III and apoE, both are potential candidates for component F (Batal et al., 2000).

For the in-depth description of how measured rate constants were related to the estimated model parameters even for bimolecular processes such as the exchange of apolipoproteins the reader is referred to appendix B.

6.2.2 Calculated vs. clinically measured lipoprotein profiles

The lipoprotein density profiles for each of the lipoprotein components calculated from the parameter values given in Table 6.1 are, to a large part, in a remarkable agreement with the clinical data (Figure 6.4). However, with respect to the distribution of apolipoprotein B-100 (Figure 6.4b) and of triglycerides (Figure 6.4e) some discrepancies remain.

The total amount of apoB-100 predicted by the model (41.8 ± 0.45 mg/dl) is lower than the mean value of 56.6 mg/dl determined experimentally for apoB-100, but within the expected interval ($\pm$ 21.4 mg/dl). In the model, the calculated concentration of apoB-100 is higher in the VLDL sub-fraction but lower in IDL and all LDL sub-fractions as compared to the laboratory values. This might be due to the simplifications made in the model for the kinetics of the receptor-mediated uptake of B-particles because regulatory influences of the apolipoproteins C and E are ignored. Likewise, the simplified kinetics of triglyceride removal from B-particles might also explain the too low triglyceride content predicted for the IDL sub-fraction since the high rate of triglyceride hydrolysis obtained by the parameter optimization procedure yields a rapid delipidation of newly synthesized B-particles.

The simplification to assume a definite initial composition of newly synthesized lipoproteins in the model might be another reason for the remaining discrepancy in the distribution of apoB-100.

The calculated distribution of model component F was compared with the clinical concentration values of the C apolipoproteins I-III and apoE. However, experimental data for component F are questionable as only about one half of the total plasma concentration of apoC and apoE (20.87 ± 3.8 mg/dl) is associated with lipoprotein complexes. The other half represents a free apolipoprotein pool in the plasma, whose value is about 10-fold higher than 1.2 mg/dl reported by (Batal et al., 2000). This might result from experimental difficulties, because it is well documented that apoE may dissociate from the surface of apoB-containing particles during prolonged ultracentrifugation (Blum et al., 1980; Gibson et al., 1983). This may account for the fact that the model predicts higher levels of component F in almost all lipoprotein density classes as compared to the available experimental data (Figure 6.4c). In fact, the calculated distribution of F agrees much better with the experimental total plasma concentration (19.0 mg/dl) as well as with the concentration observed for the free plasma pool (1.2 mg/dl) by Batal et al.

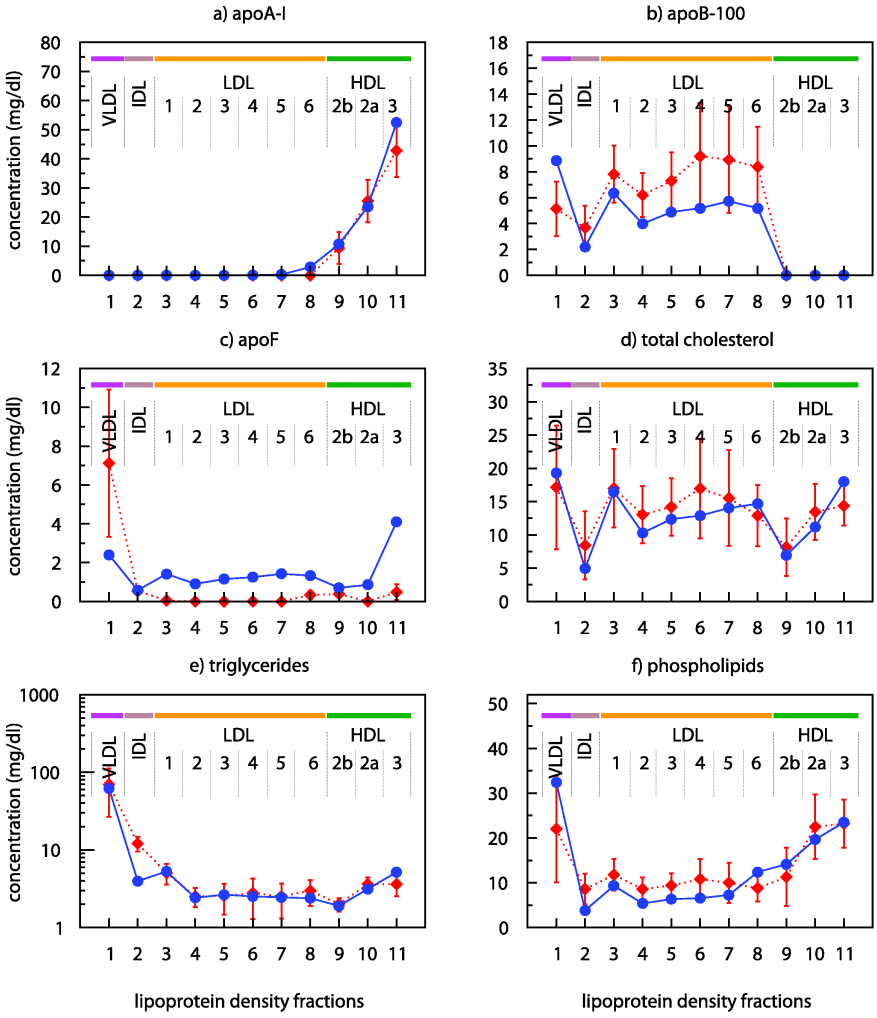

Figure 6.4: **Simulated (blue ○) vs. clinically measured (red ♢) distributions of all lipoprotein components over common density classes including sub-fractions of LDL_{1-6}, HDL_{2b}, HDL_{2a} and HDL_3.** The graphs show the concentration (mg/dl) of a) apolipoprotein A-I, b) apolipoprotein B-100, c) sum of further apolipoproteins, d) total cholesterol, e) triglycerides (logarithmic) and f) phospholipids in each of the density fractions (g/ml). The error bars show the standard deviation of the experimental values from eleven randomly selected subjects.

6.2.3 Event frequencies

In total, 20 different processes (called events) were defined in the model and 15 millions of such events have been executed during simulation, one single event in one time step. The frequency with which one of the events was executed relates to the reaction probability that arises from the appropriate model equation and the parameter value obtained by optimization.

For example, assuming the following composition of a lipoprotein complex i: A=1, B=0, F=2, C=180 and T=20 molecules. Two processes compete for this A-particle, the selective uptake of one molecule of component C (event $EfluxA$) and the removal of one molecule of component T by hydrolysis (event $HydrolyzeA$). The kinetic equations are formulated as $v_{efluxA} = c_{efluxA} \cdot nC_i$ and $v_{hydrolyzeA} = c_{hydrolyzeA} \cdot nT_i$, respectively. nC_i and nT_i are the number of molecules of component C (=180) and T (=20) in the lipoprotein complex i, respectively. The estimated parameter values are $c_{efluxA} = 0.01$ day^{-1} and $c_{hydrolyzeA} = 5.6$ day^{-1} yielding a total activity of 1.8 and 112.0 molecules per day. Thus, for this lipoprotein complex the probability for an $EfluxA$ event is lower than for the event $HydrolyzeA$. With respect to the entire lipoprotein composition spectrum in the system, the selective uptake of cholesterol from A-particles occurred about 100-fold less than the hydrolysis of triglycerides. The absolute frequency values for each of the events are listed in Table 6.2. Figure 6.5 shows the frequencies (in %) relative to the total number of events (15 million) executed during simulation.

According to their frequencies each of the events was classified either as frequent ($> 1\%$, class 1) or as seldom ($< 1\%$, class 2). Notably, class 1 covers about 99% of all executed reactions. The most frequent of all events is the cholesterol uptake from peripheral tissue by A-particles (*Influx*, 22.3%) followed by the transfer of cholesterol from A- to B-particles mediated by the CETP ($ExchangeC_A$, 20%). However, this is quite intuitive as it arises directly from the model equations. The more cholesterol is taken up from the periphery, the higher the cholesterol content of an A-particle and even the higher the probability that cholesterol can be subsequently transferred. Both events already cover almost one half of all executed reactions. Except for the event *EffluxA*, all lipid transfer or exchange processes belong to the class of frequent events. The exchange of proteins as well as the lipoprotein synthesis and degradation processes belong to the class of seldom events. This is likewise intuitive as the number of lipid molecules in a lipoprotein complex is a multiple higher as compared to the number of protein molecules.

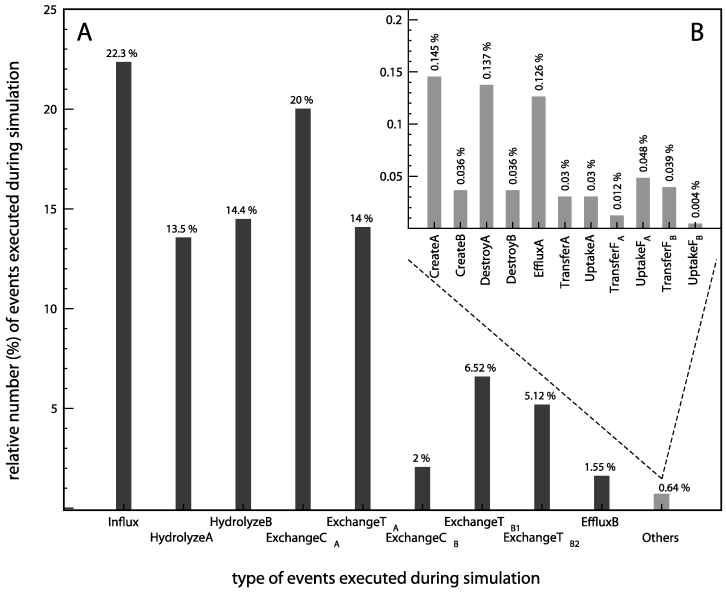

Figure 6.5: **Relative frequency of events executed during simulation.** Shown are the frequencies (in %) relative to the total number of events (15 million) that have been executed during simulation. According to their frequency the events were assigned to classes of frequent (figure A) and seldom events (insert B). The former covers about 99% of all executed reactions.

Table 6.2: **Absolute numbers of executions for each event.**

#	Frequent events (class 1)	Executions	#	Seldom events (class 2)	Executions
1	Influx	3,342,800	10	CreateA	21,693
2	HydrolyzeA	2,023,140	11	CreateB	5,421
3	HydrolyzeB	2,163,461	12	DestroyA	20,528
4	ExchangeC$_A$	2,992,831	13	DestroyB	5,372
5	ExchangeT$_A$	2,102,189	14	EffluxA	18,840
6	ExchangeC$_B$	299,285	15	TransferA	4,551
7	ExchangeT$_{B1}$	978,544	16	UptakeA	4,546
8	ExchangeT$_{B2}$	768,323	17	TransferF$_A$	1,799
9	EffluxB	233,046	18	UptakeF$_A$	7,189
			19	TransferF$_B$	5,911
			20	UptakeF$_B$	531

Moreover, all processes affecting the lipid content of A-particles show a higher frequency as compared to those affecting B-particles which arises from the up to 10-fold higher number of A-particles in the system, however, with two exceptions. The hydrolysis of triglycerides from B-particles (*HydrolyzeB*, 14.4%) occurred with comparably same frequency as from A-particles (*HydrolyzeA*, 13.5%). This results from the high number of triglyceride molecules (up to 10,000) in a single B-particle whereas A-particles contain only up to 100 triglyceride molecules. The higher frequency of *EffluxB* as compared to *EffluxA* can be explained by the same reason.

6.2.4 Dependency on initial composition

As default values, the initial composition of A- and B-particles have been chosen as reported in the literature for an average particle of nascent HDL and VLDL, respectively (see Table 4.2). They have been kept constant during simulation. However, the synthesis of a lipoprotein complex in the liver requires a close coordination of synthesizing lipids as well as proteins and their subsequent assembly to lipoprotein complexes. Depending on a variety of factors including nutrition or cellular and regulatory processes it is most likely that the liver may generate a certain spectrum of different lipoprotein compositions.

To admit a broader spectrum of initial lipoprotein compositions is of particular interest and would facilitate the examination of the lipoprotein distribution in blood plasma under several conditions such as fasting, feeding or hormone regulation. To analyze the impact of different initial compositions on the lipoprotein distribution I was asking: "How does the system change in response to initial compositions different from that of the default value?". This way, the molecule numbers of the lipoprotein components F, C and T of B-particles were randomized from a normal distribution by taking the default composition as the mean value. 100 different initial compositions (Figure 6.6) were analyzed in 100 independent simulation runs. The compositions obtained by randomization provide ranges for F, C and T between 0-18, 760-2934 and 6654-14784 molecules, respectively. The variation of each of the random compositions relative to the default composition was quantified using the euclidean distance (Eq. 6.4).

$$d(x,y) = \sqrt{\sum_{i=1}^{n} \left(\frac{x_i - y_i}{i_{max}} \right)^2} \tag{6.4}$$

where x_i and y_i represent the random and the default initial composition according to section 4.2 of component i, respectively. To ensure that all

components contribute equally to the distance relative changes were used, i.e. each component value (including the default composition) was divided by the maximum value the appropriate component reached (i_{max}) in the random sample.

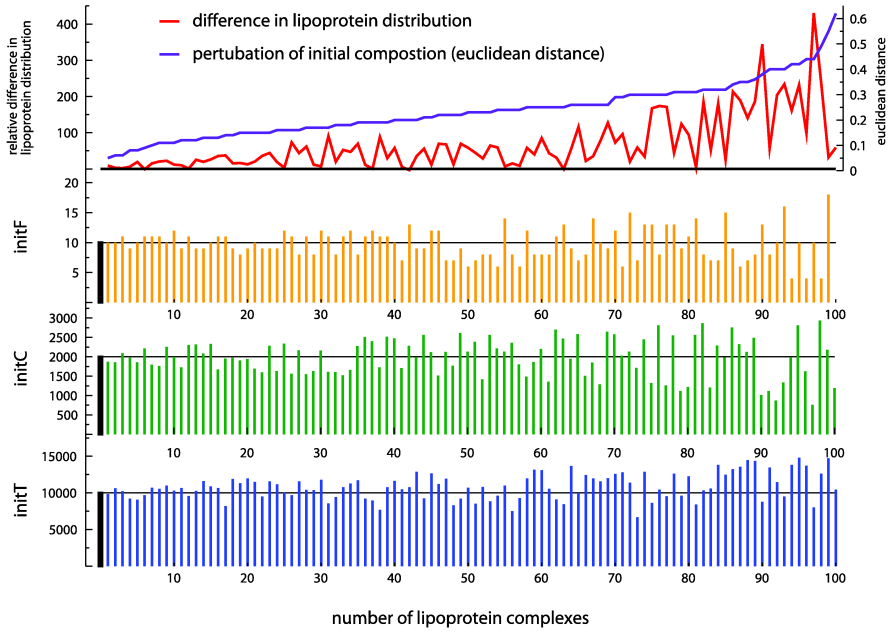

Figure 6.6: **Variation in the initial composition of B-particles.** The initial composition of B-particles, i.e. the molecule numbers of component F (orange), C (green) and T (blue), was randomized. The black bars mark the default B-particle initial composition (F=10, C=2000, T=10000). 100 different compositions (each peak in the graph) were obtained by 100 independent simulation runs. The graphs are sorted by the euclidean distance (topmost sub-graph, violet line). The change in the error measure (discrepancy between calculated and experimental lipoprotein distribution data) relative to the value obtained for the default composition is shown in the topmost sub-graph (red line).

The more distant the composition from the default the more different the lipoprotein distribution should be from the experimental one. In other words, one would expect an increasing discrepancy between calculated and experimental lipoprotein distribution data with increasing euclidean distance. As Figure 6.6 illustrates, this expectation is confirmed at least partly. The composition (F=10, C=1871, T=9821, #1) of slightest euclidean distance (d=0.0456) exhibits also only a slight increase in the error measure (+9.01) whereas a composition (F=10, C=760, T=8004, #97) considerably

away from the default composition (high euclidean distance value, d=0.4437) reaches the largest value of the error measure (+430.58).

However, a number of compositions (more than expected) of high euclidean distance fit comparably well or even improve the agreement with the experimental data (see lipoprotein composition #81 and #63, respectively). The results might account for at least two things. Firstly, the parameter set obtained by optimization seems to be very specific for the original initial composition because changing the composition worsen the agreement between simulation and experiment in most cases. Secondly, equal quality of agreement (relative change < 5-fold) is achieved by random compositions even if they are quite distant from the default values. The results suggest that certain variability in the initial composition can be partially compensated by the kinetic processes in the LP metabolism.

Table 6.3: **Initial compositions of B-particles with comparable agreement between simulation and experiment**

B	F	C	T	error measure*	Euclid distance
1	13	2285	10759	-3.46	0.200
1	11	2211	9662	-1.16	0.094
1	13	2466	8444	-0.66	0.253
1	12	2398	8956	0.45	0.189
1	11	2302	9566	1.04	0.121
1	11	2089	10202	2.18	0.065
1	10	1858	10631	3.08	0.065
1	12	2335	10056	3.17	0.159
1	14	2564	8418	3.82	0.313
...					

*relative change < 5-fold

Notably, this concerns initial compositions that are increased mainly in the amount of component F and C (see Table 6.3). In other words, the system relaxes more efficient to its normal state at higher initial amount of component F and C than at lower values as compared to the default values. This effect might also be caused by specific combinations of elevated or decreased amounts of the three components compared to other ones (not shown).

6.2.5 Influence of the lipid package size

Each lipoprotein complex is assigned according to its density to a specific density interval. In order to compare the model calculations with experimental data these density intervals correspond to those commonly obtained from clinical measurements. The density interval of a single lipoprotein density class can be very small, especially in case of the LDL sub-fractions. For example, the size of LDL2, 3 and 4 span only a density range of 0.003 g/ml. The density of a lipoprotein complex is calculated based on the particular lipoprotein composition (number of proteins and lipids). Using single lipid molecules, the density shift may keep within 0.003 g/ml by going from one lipoprotein complex of composition A to the next neighboring lipoprotein composition B (e.g. $\pm$ one molecule triglyceride). By comprising a number of lipid molecules in packages the transition of one lipoprotein composition to another one occurs between two packages and the density shift could overleap one or more density classes. Therefore, the lipid package size had to be chosen carefully to avoid sparsely or even non-occupied density ranges.

Another crucial point is, the simulation time needed to reach a steady state also depends on the package size. In general, the smaller the package size the longer it takes to reach the steady state. In the model, I defined a package as consisting of 2 and 20 lipid molecules cholesterol (C) and triglycerides (T) for A- and B-particles, respectively.

The influence of the lipid package size on both the lipoprotein profile and the simulation time is shown in Figure 6.7 for four different cases, (i) package size of 1 (single molecules), (ii) half of package size used in the model, (iii) double of package size used in the model and (iv) minimal package size feasible for the deterministic approach.

It is apparent, that with increasing lipid package size the small density intervals of LDL2-5 continuously contain less lipoprotein complexes while the amount of lipoprotein complexes in LDL6 increases accordingly. Nevertheless, the computation using single molecules needs about 10-fold in simulation steps to reach the steady state leading to about 7.5-fold increase in absolute computation time (3.3 vs. 0.43 min). On the other hand, dealing with larger package sizes does not substantially decrease the absolute computation time (0.39 vs. 0.43 min). Taking single molecules or half of the package size used in the model may potentially improve the fit but is computationally very expensive. Therefore, the package size chosen in the model provide a reasonable solution between sufficient occupation of density classes and computation time.

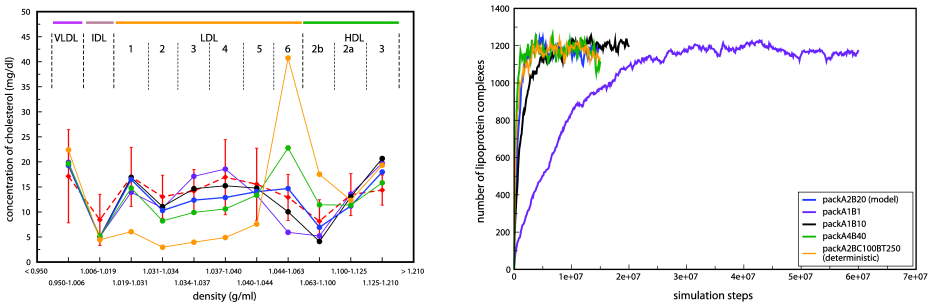

(a) lipoprotein profiles (b) simulation time

Figure 6.7: **Dependency of simulation results on lipid package size.** (a) The distribution of lipoproteins was calculated with varying package sizes for the lipid content (C, T). The nomenclature packA2B20 (blue curve) refers to package sizes of 2 for A-particles and 20 for B-particles, packA1B1 (violet), packA1B10 (black) and packA4B40 (green), accordingly. packA2BC100BT250 dedicates different lipid packages sizes of the C (100) and T (250) content for B-particles. y-axis: concentration of total cholesterol in mg/dl; x-axis: density in g/ml. (b) The smaller the package size, the more simulation steps are needed to achieve a steady state. y-axis: number of lipoprotein particles in the system; x-axis: number of simulation steps

6.2.6 Sensitivity analysis

Analyzing the sensitivity of a system aims at finding the most influential parameters by answering the question: 'How sensitively reacts the model, i.e. the lipoprotein distribution, to changes of the system parameter values?'. Each of the 28 model parameters was either decreased or increased by 10% of its normal value yielding 56 different simulation runs. All other parameters were kept constant. To provide average values and standard deviations for the error estimates each run was performed 100 times. Figure 6.8 shows the relative change in the error measure (distance between calculated and experimental lipoprotein distribution data) as compared to the standard parameter set (red line).

Most significant changes in the lipoprotein distribution are attributed to the processes of holoparticle uptake (parameters $c_{destroyA}$ and $c_{destroyB}$), of selective uptake of cholesterol from the periphery and B-particles (parameters c_{influx} and $c_{effluxB}$, respectively), of hydrolysis of B-particle's triglycerides ($c_{hydrolyzeB}$) as well as of lipid exchange among lipoproteins (parameters ($c_{exchangeC_B}$) and *CETP(tot)*). In other words, these parameters are the most sensitive ones of the system which argues for the importance of the

underlying processes. Changing the *destroy* parameters alters the total number of lipoproteins in the system. Interestingly, in dependence on the type, A- or B-particles, different effects were obtained. Decreasing the number of A-particles ($c_{destroyA-10}$) would decrease the quality of the fit by 3 times as much as for a 10 % increase ($c_{destroyA+10}$).

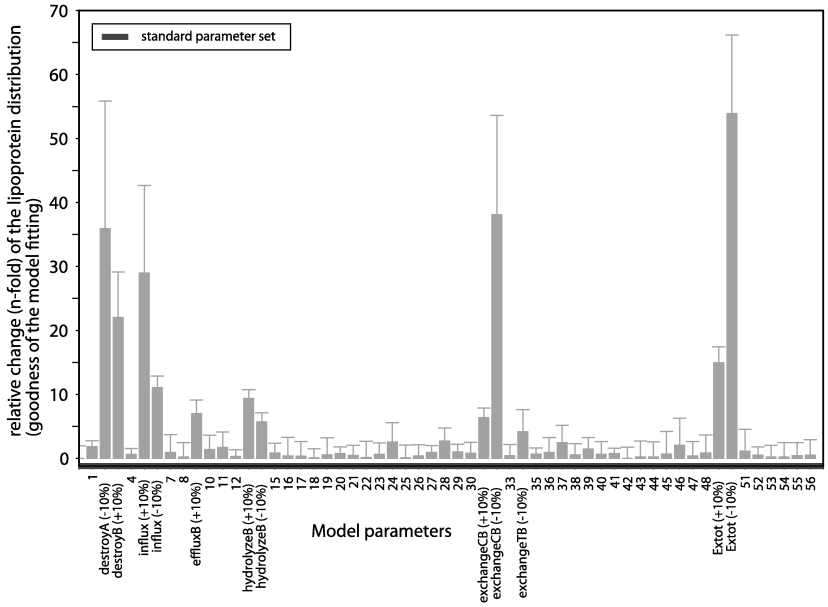

Figure 6.8: **Sensitivity of the model parameters.** y-axis: relative change in the quality of the model fit (n-fold), x-axis: parameters ± 10 %

Varying the 'destroy' parameters for B-particles show the opposite. The *Influx* process was already identified as the most frequent event during simulation. This might be the reason that the system also reacts considerably sensitive to a change in the parameter value of this process. This argument may also be applied to the hydrolysis and exchange process. Most sensitively, the system reacts to changes in the total amount of CETP available for the lipid exchange between lipoprotein complexes. Since B-particles can acquire cholesterol only through the CETP transfer activity decreasing the CETP concentration would limit the transfer capacity and influences the lipoprotein distribution substantially. The results even suggest that one ($ExchangeC_B$) of the five elementary processes included to model the lipid exchange among lipoproteins seems to be more influential than the others.

6.3 High-resolution density sub-fractions

Characterizing the distribution of lipoproteins in the blood plasma by quantifying their abundance in a limited number of main density classes such as chylomicrons, VLDL, IDL, LDL, HDL (= classical lipoprotein density profile) appears feasible as long as the distribution of lipoprotein components within these classes is sufficiently smooth. That means any alteration in the kinetic properties of the underlying elementary processes ultimately gives rise to changes in the relative occupation of these density classes. On the other hand, alterations in the kinetic processes may not necessarily lead to visible changes in the average value of a density class while the concentration and composition of individual lipoproteins within the class may vary significantly - an important fact that might crucially influence the medical interpretation of lipoprotein profiles.

To reveal the lipoprotein distribution within the main density classes experimentally used the width of each of them was decomposed into five equally sized sub-intervals. Subsequently, the amount of lipoprotein components in these narrow density classes, for which I introduce the name of *high-resolution density sub-fractions* (hrDS), was quantified. As an example, Figure 6.9 shows the distribution of cholesterol across the *hrDS*. On behalf of a better visualization scaled values of the *hrDS* cholesterol concentration are shown (Figure 6.9(a)), i.e. multiplied by the number of sub-intervals chosen (5 in this case).

The high resolution allows to clarify whether there is indeed a smooth distribution of lipoprotein components within main density classes or not, and even to quantify the moiety each of the *hrDS* contributes to the average concentration of the main class. Monotonically increasing and decreasing distributions clearly appear within a number of density classes, such as IDL, LDL1, LDL2 and HDL2b as well as LDL5, LDL6 and HDL3, respectively. More precisely, e.g. in LDL6 (density d = 1.044-1.063 g/ml), the calculated mean concentration of cholesterol amounts to 15.1 $\pm$ 0.1 mg/dl. The five *hrDS* named LDL6(I), (II), (III), (IV) and (V) relatively contribute with 53.1%, 25.7%, 11.7%, 5.5%, 4.0% to the average cholesterol concentrations, respectively.

It has to be mentioned, that the apparent saltus of the cholesterol concentration at the intersection of two density classes (Figure 6.9(a)), e.g. between LDL5 and LDL6, is somehow artificially due to the inequality of the density interval size of main density classes. Mostly, it occurs whenever two classes of considerably different size, e.g. LDL5 of size=4 (1.040-1.044) vs. LDL6 of size=19 (1.044-1.063), are neighbored. By normalizing the high resolution

lipoprotein profile to the density interval size indeed the leaps disappear, nonetheless, the formerly observed intra-class distribution patterns persist (Figure 6.9(b)).

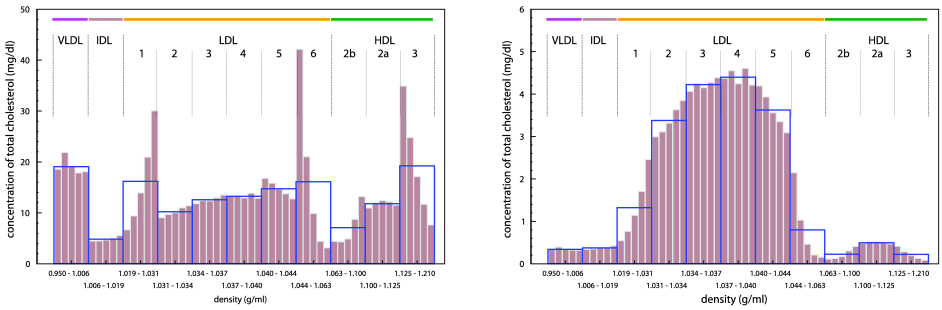

(a) non-metrical (b) metrical

Figure 6.9: **High-resolution distribution of total cholesterol within main density classes including sub-fractions of LDL1-6, HDL2b, HDL2a and HDL3.** Each of the main density classes was further decomposed into five equal-sized sub-fractions (the high-resolution density sub-fractions, *hrDS*). Scaled cholesterol concentrations are shown, i.e. the sum of *hrDS* cholesterol values divided by the number of *hrDS* (=5) equals the mean cholesterol concentration of the appropriate main density class obtained by simulation (blue). x-axis: density (g/*ml*) displayed as (a) equal-sized and (b) metrical density intervals; y-axis: concentration of total cholesterol (m*g*/*dl*)

Within HDL2a cholesterol seems to be normally distributed and shows its maximum value regarding the entire HDL (A-particles) density range. The distribution of cholesterol within VLDL, LDL3 and LDL4 seems to be irregular as leaps, in particular concerning VLDL(II), LDL3(II), LDL4(II) and LDL4(IV), between the *hrDS* occur. The latter captures in addition the maximal cholesterol value of the entire B-particle density range.

The specific intra-class variations of certain main density classes show similar patterns for all the other lipoprotein components (see Figure 6.10). Some, even if apparently marginal differences, occur within VLDL and LDL4.

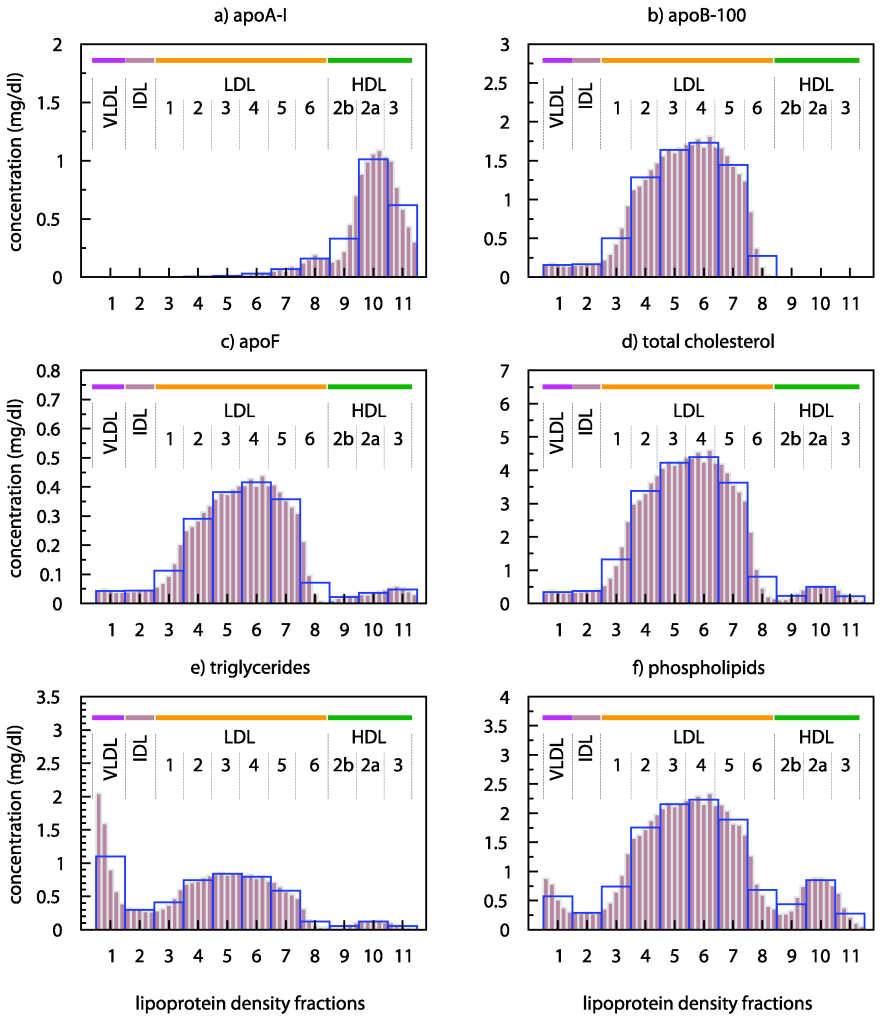

Figure 6.10: **High-resolution distribution of lipoprotein component concentrations within main density classes including sub-fractions of LDL1-6, HDL2b, HDL2a and HDL3.** Each density class (blue bars) was further decomposed into five equally sized sub-fractions (brown bars). The concentration values of a) apolipoprotein A-I, b) apolipoprotein B-100, c) sum of further apolipoproteins, d) total cholesterol, e) triglycerides and f) phospholipids were normalized to metrical density interval sizes. x-axis: metrical density intervals (g/ml); y-axis: concentration (mg/dl)

Regarding the distribution of triglycerides across the *hrDS* (Figure 6.10e) VLDL(I) and LDL4(II) instead of VLDL(II) and LDL4(IV) mainly contributes to the average concentration. VLDL and IDL intra-class distributions of triglycerides appear as monotonically decreasing and HDL2b(IV) instead of HDL2b(III) captures the cholesterol maximum of the HDL density range.

One may hypothesize that the amount and distribution of lipoprotein sub-populations differ due to inter-individual variations. Concerning that issue all parameters were tested for their capability to shift the high resolution distribution within a major density class either to lower or higher densities while the concentration value of the major class remained nearly unchanged. Parameter values have been only moderately altered, equally to the sensitivity analysis by ± 10%. The results indicate that inter-individual variations in the delipidation process (*HydrolyzeB*, Figure 6.11), the selective cholesteryl ester uptake from B-particles (*EffluxB*) and the amount of CETP available can shift the intra-class distribution significantly.

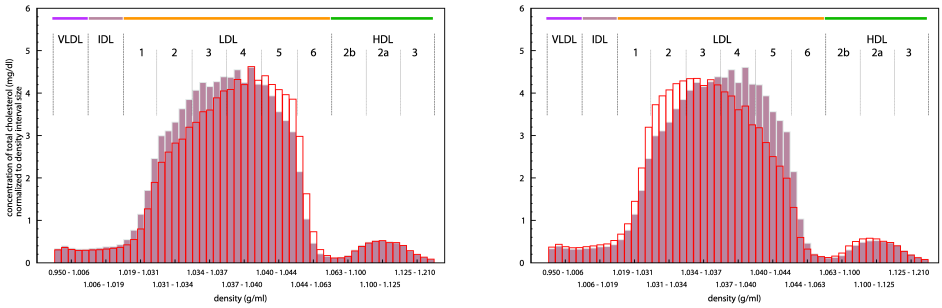

(a) hydrolyzeB+10 (b) hydrolyzeB-10

Figure 6.11: **Variation in the distribution of *hrDS*-cholesterol at moderately altered parameter values.** Alteration of the normal *hrDS*-cholesterol distribution (brown bars) by (a) increasing and (b) decreasing the parameter value of the *HydrolyzeB* process by 10% of its normal value (red bars). x-axis: metrical density intervals (g/*ml*); y-axis: concentration of total cholesterol normalized to density interval sizes (m*g*/*dl*)

But what degree of density resolution is necessary to identify all relevant fluctuations in the concentration of lipoprotein components? To answer this question, the number of *hrDS* was successively increased from 10 up to 50 sub-intervals (6.12).

The location of the overall maxima of the cholesterol values for A- and B-

particles does not considerably alter by using higher resolution as compared to five *hrDS*.

Nevertheless, with increasing resolution the distribution patterns become more and more irregular and additional leaps appear between *hrDS* most distinctly within LDL2-5 and HDL2a.

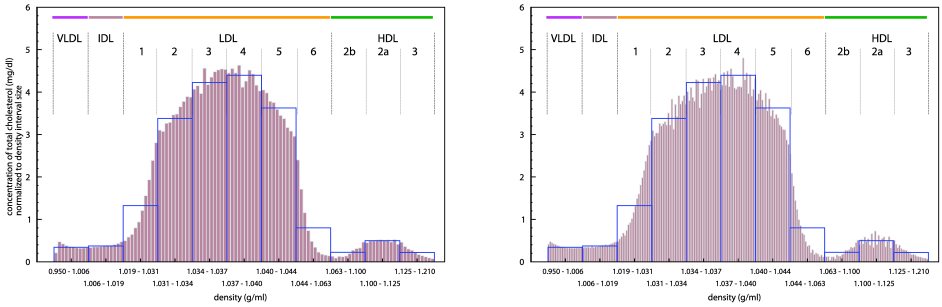

(a) 10 sub-fractions (b) 20 sub-fractions

Figure 6.12: **Distribution of *hrDS*-cholesterol with different density resolutions.** x-axis: metrical density intervals (g/ml); y-axis: concentration of total cholesterol normalized to density interval sizes (mg/dl)

Aside from stochastic effects one may hypothesize that these intra-class distribution patterns differ between individual healthy subjects or even pathological conditions. In conclusion, providing lipoprotein distributions in higher resolution than on the basis of major density classes may stimulate future experimental and modeling work aimed at identifying new subfractions of potential clinical relevance and improving the characterization of a patients risk state for CVD.

6.4 Analysis of the lipoprotein composition spectrum

The model is valuable to reveal the heterogeneity of the entire lipoprotein composition spectrum. One way to illustrate that is to calculate the lipoprotein composition (weight per cent) of a lipoprotein complex relative to the total lipoprotein mass as shown in Figure 6.13 for both the main density classes as well as for the *hrDS* within the main density classes.

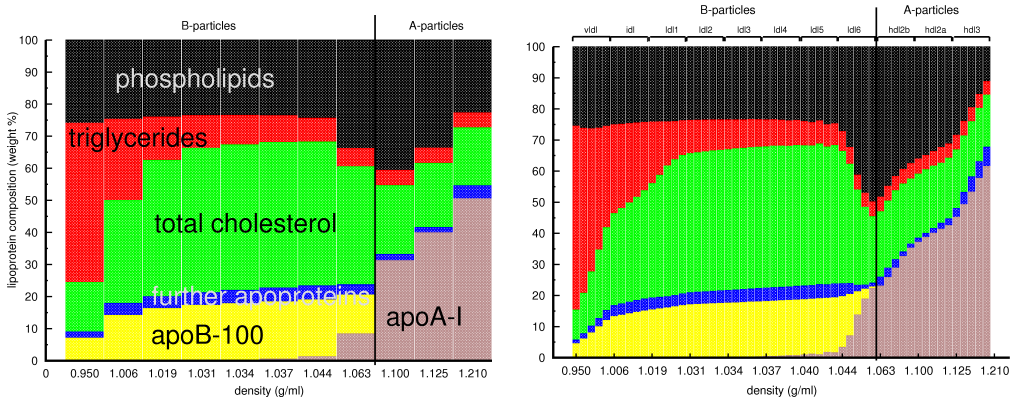

(a) main density classes (b) hrDS

Figure 6.13: **Lipoprotein compositions (weight %) of (a) main density classes and (b) *hrDS* within main density classes (resolution factor 5).** x-axis: density in g/*ml*; y-axis: % composition of lipoproteins consisting of apoplipoprotein A-I (brown), apolipoprotein B-100 (yellow), further apolipoproteins (blue), total cholesterol (green) triglycerides (red) and phospholipids (black)

With increasing density the composition shifts from triglyceride-rich lipoprotein complexes (VLDL) to lipoproteins that are enriched either in cholesterol (LDL) in case of B-particles or phospholipids and apolipoproteins in case of A-particles.

However, considering the relative lipoprotein composition does not adequately reflect the heterogeneity of lipoprotein complexes in terms of variable numbers of component molecules per lipoprotein complex. Figure 6.14 and 6.15 show therefore the entire spectrum of different lipoprotein compositions within the commonly used density classes for B- and A-particles, respectively. Each peak specifies the relative frequency of a single lipoprotein complex unique in its composition.

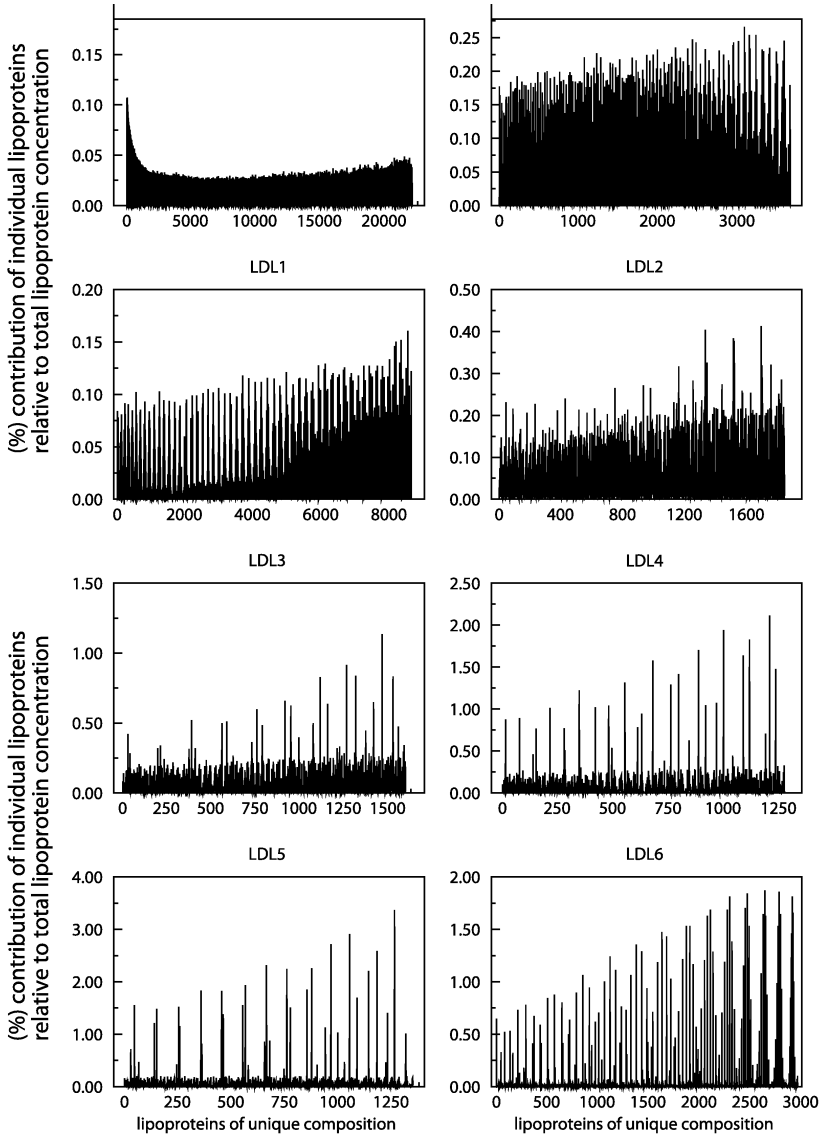

Figure 6.14: **Number of different B-particle compositions.** Contribution (%) of specific lipoprotein compositions to the total lipoprotein concentration within common density classes. Each peak specifies a single lipoprotein complex unique in its composition. y-axis: frequency (in %); x-axis: individual lipoprotein complexes with unique composition of (nA=0, nB, nF, nC, nT, nP)

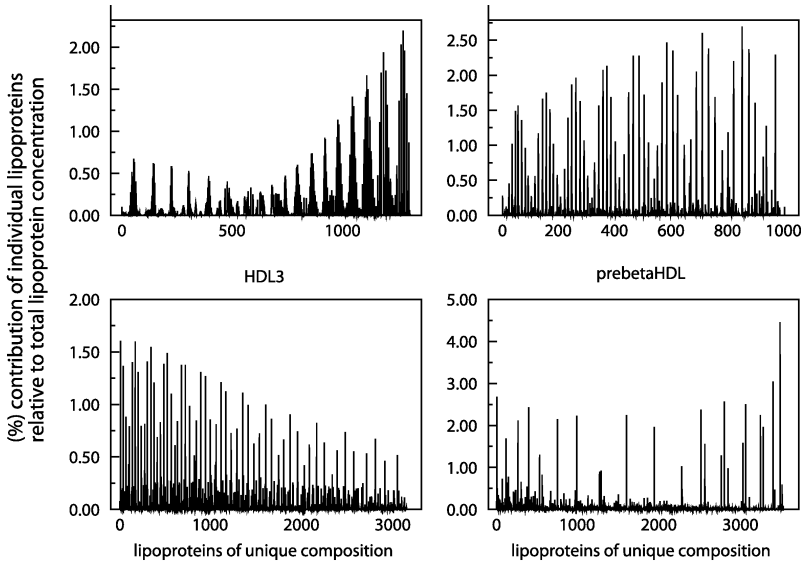

Figure 6.15: **Number of different A-particle compositions.** Contribution (%) of specific lipoprotein compositions to the total lipoprotein concentration within common density classes. Each peak specifies a single lipoprotein complex unique in its composition. y-axis: frequency (in %); x-axis: individual lipoprotein complexes with unique composition of (nA, nB=0, nF, nC, nT, nP)

The entire composition spectrum comprises in total 52,316 individual lipoprotein complexes of unique composition ever observed during simulation. As shown in Table 6.4, the total number of different lipoprotein compositions varies for B- and A-particles (43,370 vs. 8,946) and correlates within a density class likewise to the size of the density interval itself. For example, VLDL covers a larger density interval ($\Delta = 0.056$ g/ml) as compared to LDL6 ($\Delta = 0.019$ g/ml) and comprises approximately 10-fold more different individual lipoprotein compositions (22,072 vs. 2,963). On the other hand, lipoproteins of the LDL6 class occur 10-fold more frequent during simulation than lipoproteins of the VLDL class. As a general observation, A-particles are about 10-fold more frequent than B-particles.

Table 6.4: **Number of different lipoprotein compositions.** Frequency specifies the occurrence of lipoprotein complexes averaged over time, e.g. lipoprotein complexes of the LDL6 class occur over time about 10-fold more frequent as compared to the VLDL class.

Lp class	# comp.	frequency	Lp class	#comp.	frequency
B-particles			*A-particles*		
VLDL	22,072	9.87	HDL2b	1,303	178.53
IDL	3,659	2.39	HDL2a	987	284.07
LDL1	8,619	6.85	HDL3	3,141	481.04
LDL2	1,839	4.46	preβHDL	3,515	112.05
LDL3	1,595	6.13			
LDL4	1,274	7.99			
LDL5	1,349	12.92			
LDL6	2,963	70.53			
$\sum$	43,370	121.14	$\sum$	8,946	1,056.0

6.4.1 Further macroscopic properties

The macroscopic structure of a lipoprotein complex is widely described as a multicomponent aggregate having a spherical micellar shape and consisting of two so-called *phases* - the core and the surface. Both fulfill specific functionality which is enabled by having the right composition of appropriate chemical components.

The surface mediates the water-solubility and various regulatory functions, whereas the core permits to protect components from the surrounding water milieu. According to their physico-chemical properties the lipoprotein components distribute between these two phases, named *phase distribution*. In a very rough approximation, the core contains exclusively neutral lipids (cholesteryl esters, triglycerides), whereas the surface consists of apolipoproteins, phospholipids and free cholesterol. Miller and Smith have proposed a more detailed model for the phase distribution (Miller and Smith, 1973). It suggests that a tiny portion of neutral lipids can also be present in the surface necessary to provide better access to neutral lipids during the exchange process mediated by the CETP. In the opposite way, free cholesterol is to some extent present in the core. I have adapted and extended this model in my diploma thesis. For details the reader is referred to (Hübner, 2000). In brief, it allows for calculating the phase distribution from the composition (weight %) and the total mass of a lipoprotein complex. For the work presented here, the calculation of the phase distribution was automatized using GNU

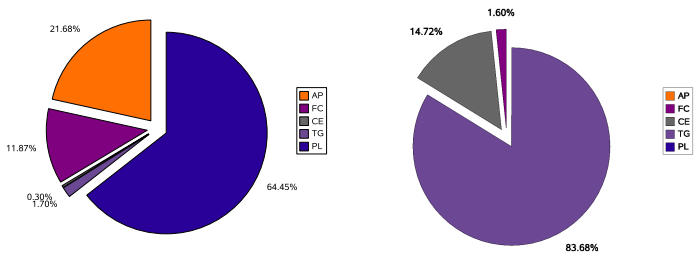

(a) Surface composition (b) Core composition

Figure 6.16: **Distribution of lipoprotein components between the surface and core of a lipoprotein complex.** (a) and (b) show the relative content (weight %) of the lipoprotein components in the surface and core, respectively, exemplarily for the common density classes VLDL. Abbreviations: apolipoproteins (AP), free cholesterol (FC), cholesteryl ester (CE), triglycerides (TG), phospholipids (PL)

Octave, version 2.1.72 and coupled to the simulation output. To illustrate the results, Table 6.5 as well as Figure 6.17 shows the phase distribution exemplarily for selected density classes.

Table 6.5: **Calculated phase distribution of lipoprotein components.** Abbreviations: apolipoproteins (AP), free cholesterol (FC), cholesteryl ester (CE), triglycerides (TG), phospholipids (PL)

	surface					*core*				
LP	AP	FC	CE	TG	PL	AP	FC	CE	TG	PL
	weight %					*weight %*				
VLDL	21.68	11.87	0.3	1.7	64.45	0	1.6	14.72	83.68	0
IDL	33.81	10.03	0.76	0.92	54.47	0	2.49	44.26	53.26	0
LDL1	35.81	19.46	0.93	0.41	43.39	0	1.41	68.4	30.2	0
LDL6	37.56	9.47	1.32	0.27	51.39	0	1.84	81.33	16.82	0
HDL2b	41.49	8.87	1.11	0.38	48.15	0	0.77	73.81	25.42	0
HDL2a	52.78	7.16	0.91	0.3	38.86	0	0.66	74.84	24.49	0
HDL3	68.29	4.81	0.61	0.19	26.1	0	0.71	75.4	23.89	0

Besides calculating the phase distribution, this provides the possibility of a fully characterization of the entire lipoprotein spectrum in human blood plasma with further macroscopic properties including volume and particle size. Incorporating these characteristic lipoprotein information can even stimulate a more precise description of the kinetic processes in the future.

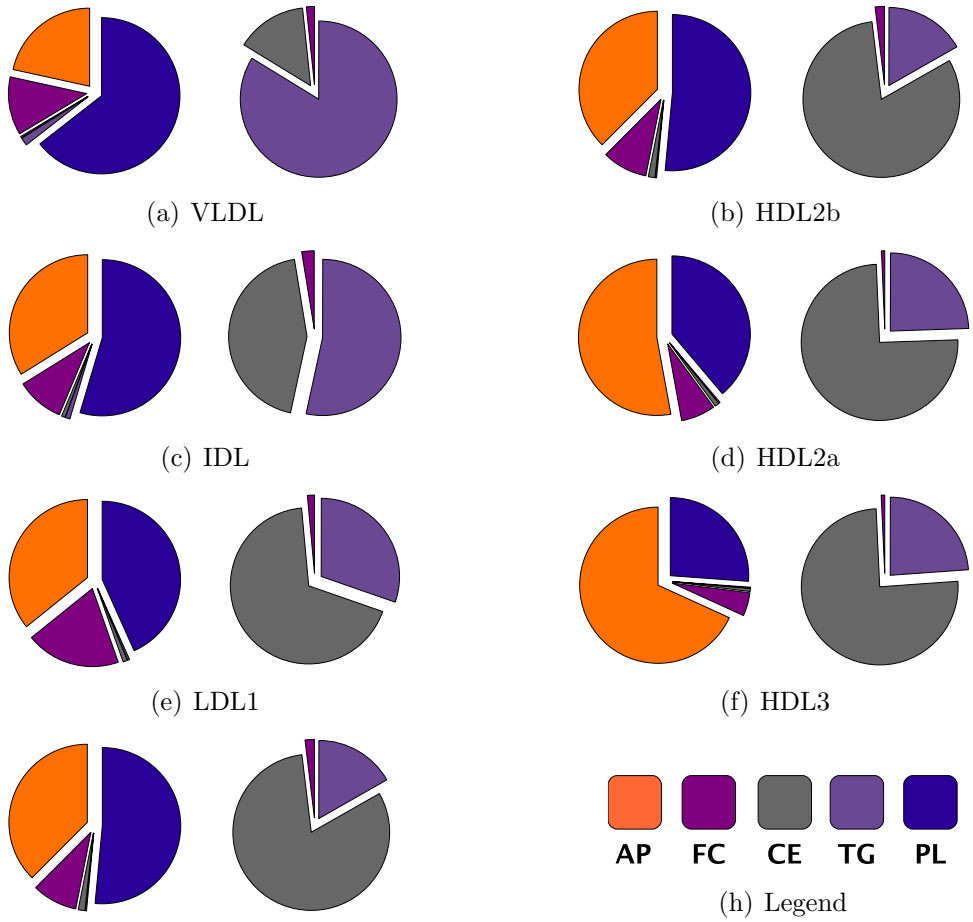

(a) VLDL (b) HDL2b (c) IDL (d) HDL2a (e) LDL1 (f) HDL3 (g) LDL6 (h) Legend

Figure 6.17: **Phase distribution of lipoprotein components in selected common density classes.** For each lipoprotein class % composition of the surface (left) and the core (right) is illustrated. Abbreviations: apolipoproteins (AP), free cholesterol (FC), cholesteryl ester (CE), triglycerides (TG), phospholipids (PL)

6.5 Simulated pathological profiles

To check the predictive capacity of the model the impact of disorders in the kinetic properties of the LDL receptor (LDLR), the lipoprotein lipase (LPL) and ATP-binding cassette A1 (ABCA1) on the stationary density distribution of lipoproteins was simulated (Figures 6.18, 6.19, 6.20).

6.5.1 Hypercholesterolemia

Elevated plasma cholesterol levels, mostly LDL, represent one of the major risk factors that contribute to diseases such as atherosclerosis. The LDL receptor (LDLR) mediates the uptake and lysosomal degradation of plasma LDL. Mutations disrupting the function of this receptor produce Familial Hypercholesterolemia (FH), an autosomal dominant hereditary disease. To date, more than 300 different variations in the LDL receptor gene have been found in FH subjects. Thereunder, the mutations show different serum lipid phenotypes ranging from extreme to only moderate hypercholesterolemia (Gudnason et al., 1994). This implies that the particular type of the underlying genetic variation influences the LDL receptor activity differently, however, the functional relation between mutation and residual LDL receptor activity is not fully understood.

In this work, the impact of a reduced LDLR activity on the distribution of lipoproteins was simulated by decreasing the parameter for the holoparticle uptake (process *DestroyB*) to 50 % of its normal value. As shown in Figure 6.18d, the resulting lipoprotein distribution exhibits a markedly increased cholesterol concentration, predominantly in the density range of LDL (82.06 vs. 136.68 mg/dl, +66.5%) at nearly unchanged cholesterol levels of density classes such as VLDL and IDL. It is suggesting that this arises from lowering the receptor-mediated uptake while maintaining a sufficient apoB-synthesis leading likewise to elevated LDL-apoB levels (Figure 6.18b). The findings are qualitatively in concordance to the majority of clinical observations in FH subjects.

In carriers of the FH-Keuruu mutation (Asp235->Glu) who have familial moderate hypercholesterolemia, Kovisto et al. found approximately 50% higher LDL cholesterol levels than in noncarriers of the same family (Koivisto et al., 1997). They also obtained slow catabolic rates of LDL and an efficient synthesis of apoB that seems to explain very high levels of LDL cholesterol and apoB in serum. Furthermore, they found slow cholesterol to apoB ratios in LDL particles suggesting that LDL particles are small and dense.

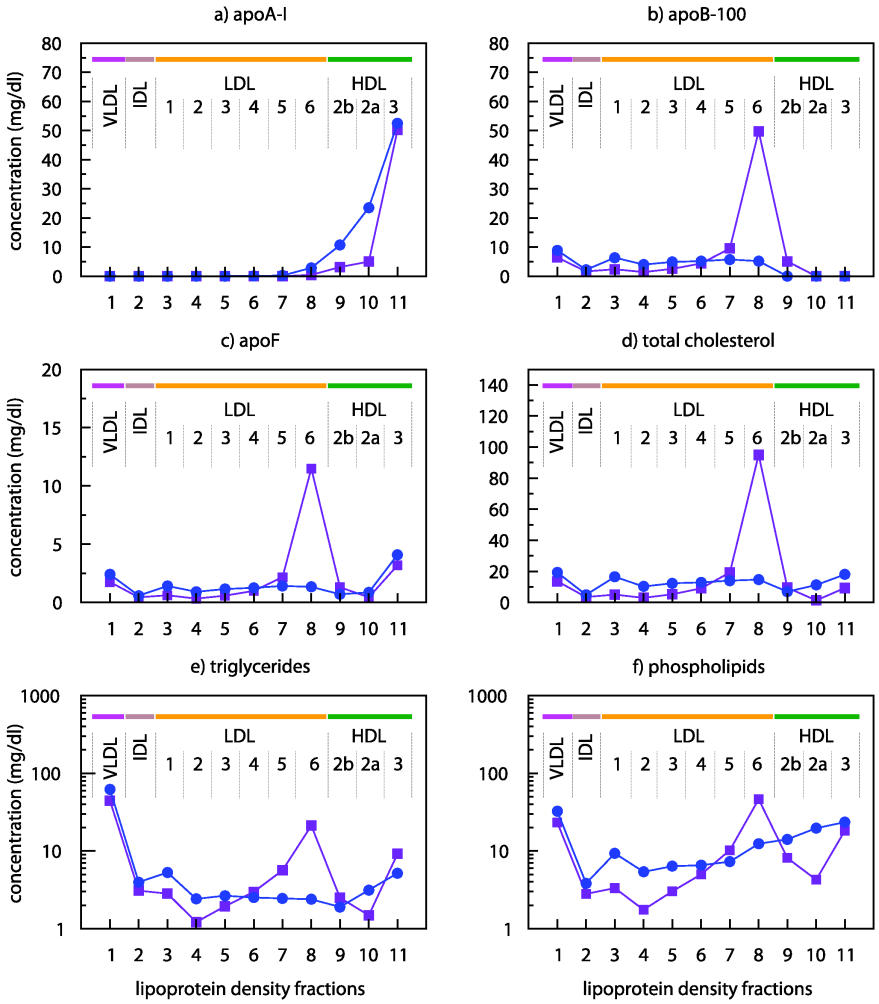

Figure 6.18: **Simulated distributions of lipoprotein components of pathological states: LDL receptor deficiency (50%).** Calculated normal (○) vs. pathological (■) concentrations of lipoprotein components in the commonly used density classes including sub-fractions of LDL1-6, HDL2b, HDL2a and HDL3. The graphs show the concentration (mg/dl) of a) apolipoprotein A-I, b) apolipoprotein B-100, c) sum of further apolipoproteins, d) total cholesterol, e) triglycerides (logarithmic) and f) phospholipids (logarithmic) over lipoprotein density fractions (g/ml)

The latter coincides with ratios observed during simulation in both cases, normolipidemic and LDLR deficiency (cholesterol/apoB ratio: 2.6 vs. 1.9, respectively), and is even reflected in elevated cholesterol levels especially in the density range of small-dense LDL (LDL5+6).

Within LDL, the sub-fractions LDL1-6 behave differently. Compared to normolipidemic values approximately 3-fold and 1.5-fold decreased cholesterol levels of lbLDL (LDL1+2, 26.8 vs. 8.0 mg/dl) and idLDL (LDL3+4, 25.2 vs. 14.4 mg/dl) are observed, respectively, as well as considerably higher amounts of sdLDL (LDL5+6, 29.7 vs. 114.3 mg/dl).

The different behavior of the LDL sub-fractions is also similar to findings by März et al. in a patient with FDB (Familial defective apolipoprotein B-100) who has a mutation in codon 3500 of the apoB gene substituting glutamine for arginine (März et al., 1993). They have found LDL1 and LDL2 almost unchanged, a slight and remarkable increase in idLDL and sdLDL, respectively, and have addressed the findings to a dependency on apolipoprotein E (apoE). Although the model does not include any regulatory influences of apoE in the receptor binding the tendency to accumulate small-dense LDL was clearly confirmed. Reducing the LDLR activity to 75% of its normal value the calculations reproduce more closely the specific behavior of lbLDL and idLDL reported by März et al. (data not shown).

The model calculations would therefore indicate a combined hyperlipidemia as the underlying molecular disease rather than solely FH or FDB. Discussing FDB in this context poses an additional and even more general issue. In fact, an impaired interaction between B-particles, such as LDL, and the receptor may be due to several reasons. Most obviously, there is either indeed a defect in the receptor itself due to mutations that cause a reduced expression or binding activity. Or, the ligand (potentially apolipoprotein B-100) carries a mutation. Since the process of the holoparticle uptake is effectively determined by solely one parameter in the model discriminating between these two possible defects is not yet possible.

The distributions of the remaining lipoprotein components of B-particles (apoF, triglycerides and phospholipids) show the same particular tendency within the LDL sub-fractions. With respect to component F the calculated distribution is consistent with the observations of Blum et al. who found that normal subjects and hypercholesterolemic patients have similar distribution patterns of apoE among lipoproteins (Blum et al., 1980), however, with considerable variability between individuals. This variability has been mainly referenced to a density shift of apoE-HDL to lower density ranges, most strikingly in some patients even to the major LDL range (1.019-1.050 g/ml). The latter is confirmed by the model calculations which show elevated and appropriate decreased apoF levels in the density ranges of LDL

and HDL, respectively. However, this seems to be only a minor part as the elevation of apoF levels in the LDL range arise mainly from apoB-particles carrying substantial amounts of apoF which coincides with the calculated distribution of apoB.

Regarding the distribution of A-particles (equivalent to HDL) the model predicts a moderate decrease in HDL cholesterol (Figure 6.18d) compared to the normolipidemic profile (20.19 vs. 38.64 mg/dl). This is in good agreement with the reduced overall HDL cholesterol level observed in seven heterozygous FH patients by (Frénais et al., 1999). They have studied these subjects by constant infusion of deuterated leucine as stable isotope and have used a monocompartment model for kinetic analysis. As a further result, they found, although apoA-I FCR was increased, the plasma apoA-I concentration maintained because of an increased HDL apoA-I production rate. The calculated plasma concentration of apoA-I is compared to the normal state maintained in the simulation, as well (106.43 vs. 107.8 mg/dl). Regarding the kinetic rates for apoA-I the model calculations show the opposite as (even if marginal) less executions occur for both events, *CreateA* and *DestroyA* (21,372 vs. 21,490 and 20,246 vs. 20,309, respectively).

In conclusion, as shown in-depth above a number of fundamental clinical characteristics concerning hypercholesterolemia (FH and FDB) were successfully reproduced.

6.5.2 Hypertriglyceridemia

Besides plasma cholesterol, even elevated levels of plasma triglycerides, called hypertriglyceridemia - a common form of dyslipidemia - are frequently associated with premature coronary artery disease (Brunzell, 2007). With regard to the Fredrickson classification, all but one of the dyslipidemia (type IIa) are characterized by elevated triglyceride levels, but with particular differences. For example, type IIb patients show a classic mixed hyperlipidemia (high cholesterol and triglycerides) by elevations in both LDL and VLDL, and patients of type III, also known as dysbetalipoproteinemia, have elevations characteristically in VLDL and remnant lipoproteins, such as IDL.

Genetically, two causes of severe hypertriglyceridemia are known, deficiency of lipoprotein lipase (LPL) and apoC-II. Both play a key role in the catabolism of triglyceride-rich lipoproteins (TRL) by removing (hydrolyzing) triglycerides. The former is the catalyzing enzyme, the latter its main activator. Concerning type III dyslipidemia receptor binding-defective forms of apolipoprotein (apo) E have been also discussed as the common denominator (Mahley et al., 1999) for elevated levels of remnant lipoproteins. In fact, more than 90% of type III patients are homozygous for apoE2 (Blom et al., 2005).

In case of lipoprotein lipase, about 100 gene polymorphisms have been identified associated with either decreased (Asp9Asn, Gly188Glu, and Asn291Ser) or increased (Ser447Ter) LPL activity due to changes in the amount of enzyme produced, the specific activity, or enzyme binding to lipoproteins (Fisher et al., 1997; Merkel et al., 2002). The consequences of an impaired LPL activity were simulated by lowering the parameter value for the process *HydrolyzeB* to one half of the original value.

The calculated lipoprotein distributions clearly display markedly elevated levels of lipoprotein components such as triglycerides (Figure 6.19e) and cholesterol (Figure 6.19d), predominantly in the density range of VLDL, IDL and early LDL. The total plasma concentration of triglycerides (159.5 vs. 95.2 mg/dl) is about 67.4% and of cholesterol (153.7 vs. 144.5 mg/dl) only moderately increased as compared to the simulated normolipidemic profile.

The model calculations show, as compared to normolipidemic LDL cholesterol values, a strong reduction in idLDL (25.2 mg/dl vs. 1.8 mg/dl, -92%) and to a lower degree of sdLDL (28.7 mg/dl vs. 5.1 mg/dl, -82%). Indeed, elevated levels of sdLDL implicated with mild to moderate hypertriglyceridemia (Packard, 2003) cannot be found in the model simulations. Likewise, reduced HDL cholesterol are not observed as reported by (Babirak et al., 1989) for the phenotype of heterozygous LPL deficiency or for the Asn291Ser mutation in the LPL gene (Reymer et al., 1995). In contrast, the calculated distribution shows increased HDL cholesterol levels which have been reported for other LPL mutations, such as the Ser447-termination (Ter) mutation at the exon 9 (Kuivenhoven et al., 1997).

With respect to component F (equivalent to apoE and apoC) the model also calculates elevated levels in VLDL which corresponds to (Blum et al., 1980) who have found in hypertriglyceridemic patients, by using radioimmuno assays, nearly all plasma apoE associated with triglyceride-rich lipoproteins.

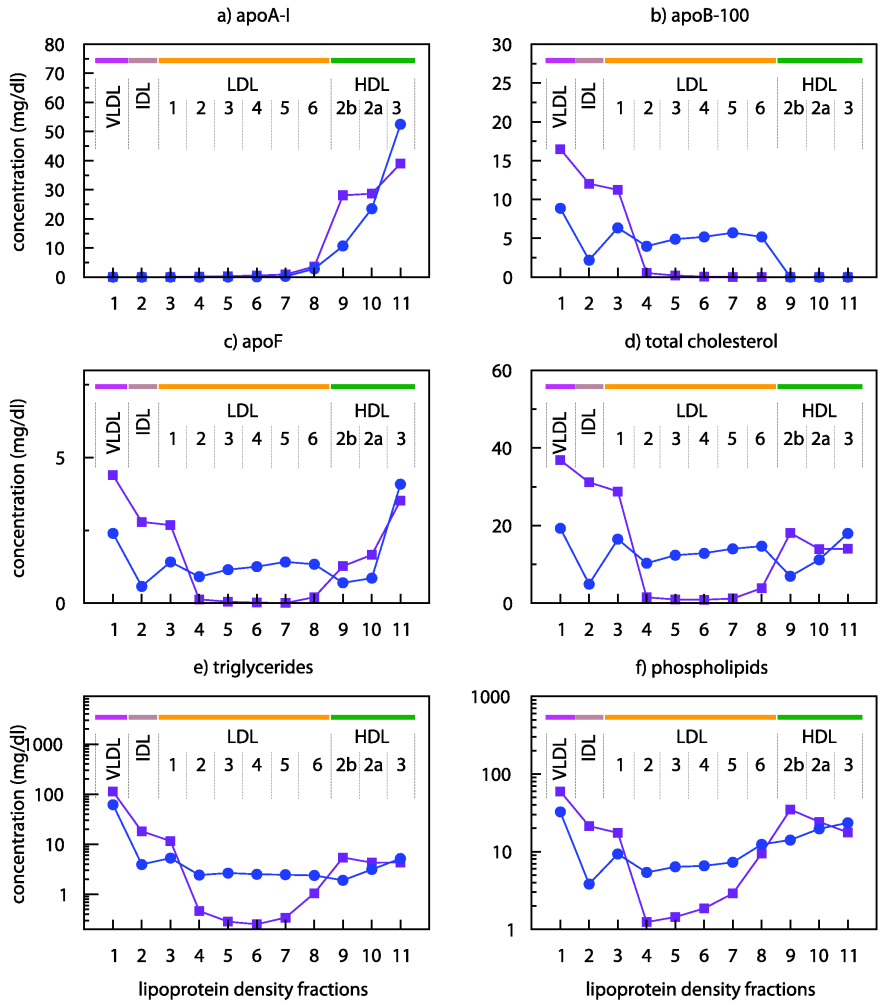

Figure 6.19: **Simulated distributions of lipoprotein components of pathological states: LPL deficiency (50%).** Calculated normal (○) vs. pathological (■) concentration of lipoprotein components in the commonly used density classes including sub-fractions of LDL1-6, HDL2b, HDL2a and HDL3. The concentrations (mg/dl) of a) apolipoprotein A-I, b) apolipoprotein B-100, c) sum of further apolipoproteins, d) total cholesterol, e) triglycerides (logarithmic) and f) phospholipids (logarithmic) over density (g/ml) are shown.

The calculated distributions can be mechanistically explained as follows. Due to the decreased hydrolysis parameter, the *HydrolyzeB* process is executed about 1.2fold less leading to the accumulation of triglyceride enriched lipoprotein complexes during simulation. Elevated triglyceride levels in VLDL, in turn, promote the transfer of triglycerides to HDL mediated by the CETP (1.4-fold higher frequency of the processes $ExchangeT_B$ and $ExchangeT_A$). Likewise, the more CETP is loaded with triglycerides the less lipid-unloaded CETP is present in plasma being capable to transport CE back from HDL to VLDL. Subsequently, lipoprotein complexes in the density range of HDL become enriched in cholesterol and triglyceride .

A 1.4-fold higher frequency is also observed for executing the *HydrolyzeA* process implicating a higher HL activity, the enzyme that catalyzes the hydrolysis of triglycerides from small B-particles and A-particles. That may explain the low triglyceride content in all LDL sub-fractions.

Overall, the results rather indicate dyslipidemia of type III (dysbetalipoproteinemia) than one of the other types due to the following reasons. First, the phenotype of patients with dysbetalipoproteinemia is characterized by both, hypercholesterolemia and hypertriglyceridemia. It has been widely proposed that the former is caused by impaired receptor-mediated clearance due to defective apoE, whereas the latter is caused primarily by impaired lipolytic processing of remnants and increased VLDL production associated with increased levels of apoE (Mahley et al., 1999). Second, LDL cholesterol has been found to be usually low in individuals with dysbetalipoproteinemia apparent in Figure 6.19d.

Although the calculations largely correspond to type III dyslipidemia an underlying defective binding of apoE cannot be implicated as the mathematical description of the modeled receptor-mediated uptake still neglects any regulatory influences, depends only on apoB and is thus nearly equal probable for all B-particles.

6.5.3 Hypoalphalipoproteinemia

Hypoalphalipoproteinemia (HA) are rare human metabolic disorders characterized by low HDL cholesterol and apoA-I levels. Causing factors are often mutations in one of the genes involved in the early step of the reverse cholesterol transport (RCT), such as ABCA1, apoA-I and LCAT. Regarding the ABCA1 gene to-date a large number of sequence variations have been identified (Miller et al., 2003) (OMIM 600046).

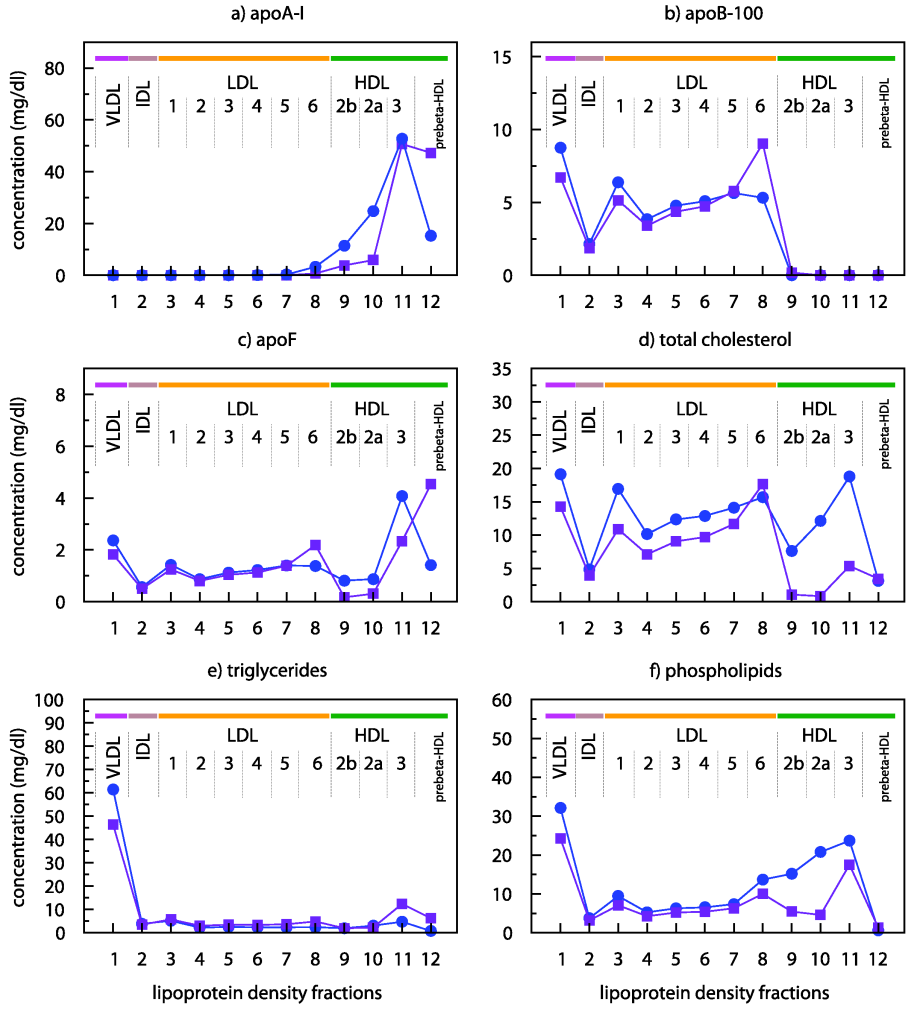

Figure 6.20: **Simulated distributions of lipoprotein components of pathological states: ABCA1 deficiency (50%).** Calculated normal (○) vs. pathological (■) concentration of lipoprotein components in the commonly used density classes including sub-fractions of LDL1-6, HDL2b, HDL2a and HDL3. The concentrations (mg/dl) of a) apolipoprotein A-I, b) apolipoprotein B-100, c) sum of further apolipoproteins, d) total cholesterol, e) triglycerides and f) phospholipids over density (g/ml) are shown.

It has been reported that, e.g. Tangier Disease (TD) is caused by defects in both alleles of the ABCA1 transporter gene (Bodzioch et al., 1999; Brooks-Wilson et al., 1999; Rust et al., 1999), the key mediator of the RCT by transferring cholesterol and phospholipids from peripheral cells to acceptor lipoproteins in the plasma. A heterozygous ABCA1 defect (one defective allele) concerns to the disorder known as familial hypoalphalipoproteinemia (FHA).

In this work, an impaired activity of ABCA1 was simulated by reducing the rate constant for the cholesterol uptake by A-particles (process *Influx*) to 50% of its normal value. Compared with normolipidemic values the model predicts low plasma cholesterol concentrations (144.5 vs. 95.47 mg/dl, -34%). As reported for FHA, a remarkable reduction of cholesterol levels appears in all HDL fractions (Figure 6.20d). HDL cholesterol accounts for only $\sim$ 10 mg/dl at nearly normal total plasma triglyceride levels (95.2 vs. 96.8 mg/dl). As a consequence, considerable levels of apoA-I (Figure 6.20a) occur in the density range d $>$ 1.21 g$/ml$ which argues for the accumulation of preβ-migrating lipoproteins. The model predicts further a marginal reduction in apoA-I within the HDL3 fraction, while in HDL2b and HDL2a apoA-I levels are severely depleted. As comparable results from clinical studies, a predominance of HDL particles being poor in cholesterol, but enriched in apoA-I have been found in patients with heterozygous TD (Asztalos and Schaefer, 2003; Asztalos et al., 2001).

The distributions of apoB, apoF, cholesterol and triglycerides of B-particles display a characteristic shift to lipoproteins in the density range of LDL6 (Figure 6.20b-e). Analyzing the stochastic trajectories of the model simulations exhibits that the *Influx* process occurred approximately 2-fold less frequent (2,501,067 vs. 1,333,287 executions). The reduced uptake of peripheral cholesterol by A-particles causes, in turn, a diminished cholesterol transfer to B-particles mediated by CETP (processes $ExchangeC_A$ and $ExchangeC_B$). Since less CETP molecules are thus loaded with cholesterol the rate for the back transfer of triglycerides is forced to increase from triglyceride-rich B-particles to A-particles or cholesterol-rich B-particles. Accordingly, the model calculations show reduced concentrations of VLDL triglycerides and an increased triglyceride level in, e.g. HDL3 and LDL6.

Overall, the simulated pathological profile corresponds well to data observed for patients with FHA. However, as discussed above for hypercholesterolemia, the simulated defect in the uptake of cholesterol can be caused by defective apoA-I or ABCA1, and discriminating between the two is not possible in the current status of the model.

Chapter 7

Discussion

"Prediction is very difficult, especially about the future."

(Niels Bohr)

7.1 Changing the perception of conventional experimental and modeling approaches

The work proposes a novel model to examine the dynamics of the lipoprotein metabolism in blood plasma. The pioneering idea of this model is to calculate the distribution of plasma lipoproteins on the basis of individual lipoprotein complexes. This changes the perception of conventional experimental and modeling approaches undertaken so far which described the dynamics on the basis of a few predefined density classes (= compartments). Previous models of the lipoprotein metabolism have therefore never taken into account the enormous diversity of lipoprotein compositions that physiologically can occur in blood plasma.

The model developed and presented here puts particular emphasis on this heterogeneity of lipoproteins. In other words, the model considers each of the lipoproteins as unique with respect to its composition of proteins and lipids eventually determining the kinetic behavior and macromolecular properties such as volume, size and density. The distribution of all lipoproteins over density yields a certain lipoprotein density profile. Most importantly, lipoproteins were defined in the model without *a priori* density classification. To compare the calculations with experimental data lipoprotein complexes were

assigned according to their density to common density classes *a posteriori* as the outcome of the model.

As the greatest benefits the approach (i) enables to include in an adequate manner the elementary reactions involved in lipoprotein metabolism, (ii) provides entire information on the lipid and protein composition of lipoproteins and (iii) reveals the distribution of lipoproteins in high resolution. The approach was designed to be able to reproduce lipoprotein density profiles of predefined density classes experimentally obtained from healthy subjects. Furthermore, disturbing one of the underlying molecular processes was aimed at simulating the impact of disorders in lipoprotein metabolism.

7.2 Simulated lipoprotein profiles reproduce experimental data with remarkable accuracy

To introduce the method and to deal with a manageable set of unknown kinetic parameters a core model was presented. The model was restricted to a representative number of lipoprotein components and important elementary biochemical processes involved in lipoprotein metabolism which use simplified rate equations of the mass-action type. Therefore, it is obvious that some inconsistencies between calculated and measured lipoprotein distributions occur. Nevertheless, even based on this simplified core model it succeeded to simulate with remarkable accuracy experimentally determined density profiles of lipid and protein components in normal and pathological situations. As experimental information on the composition of lipoproteins so far is only available for the main lipoprotein classes (= lipoprotein compartments), the only way to estimate unknown parameters of the model and to compare the computations with the experiment was to condense the calculated profiles of individual lipoprotein complexes into profiles of the commonly known density classes.

Numerical values of model parameters could be determined which to a large degree are in good agreement with experimental data taken from a larger set of independent kinetic experiments. Based on this parametrization, lipoprotein density profiles of normolipidemic subjects were computed. The remaining deviations pertain mostly to the distribution of apoB-100 whose calculated concentration is higher in VLDL and lower in the IDL and LDL classes than measured in the blood of normolipidemic patients.

Discrepancies between model and experiment may, at least partially, also result from experimental uncertainties. To our knowledge, it cannot be ex-

cluded that density fractionation of VLDL is incomplete so that VLDL particles are present in IDL sub-fractions or even in early LDL sub-fractions. This would give rise to an apparently higher content of triglycerides and apoB-100 in these sub-fractions and a lower content in VLDL. Furthermore, due to the integral property of apoB-100 (one molecule per lipoprotein) one would assume that the measured total plasma concentration of apoB-100 equals the sum of apoB-100 obtained in the lipoprotein fractions. Contradictory, the underlying experimental data provide a higher total plasma concentration of apoB than what has been measured for apoB associated to lipoproteins (68.3 ± 17.3 mg/dl vs. 56.6 ± 21.4 mg/dl, respectively). The reason could not be clarified, yet. Also with respect to the distribution of component F experimentally caused discrepancies cannot be (fully) excluded as, e.g. in case of apoE, it has been described that composition artifacts are possibly induced by multiple-sequential ultracentrifugation leading to apolipoprotein dissociation from circulating apoB-containing particles (Blum et al., 1980; Gibson et al., 1983).

Nevertheless, refinement of the model, for example, by including regulatory effects in the description and mathematical formulation of the kinetic processes (e.g. activation of LPL by apolipoprotein C-II) will certainly help to further overcome the discrepancy. A number of extensions and refinements are thinkable. I will come back to them in detail later on.

Another issue might also be of importance. It is widely accepted that the liver represents the major synthesis source of plasma lipoproteins such as VLDL and HDL (about 80 %) with the reminder being supplied by the intestine (Wu and Windmueller, 1979). Nevertheless, several tracer kinetic studies have proposed compartment models which could explain the experimental data even better by allowing additional synthesis of apoB-containing lipoproteins with compositions characteristic for IDL and LDL (Packard et al., 2000).

In general, the composition of newly synthesized lipoproteins can be described as the result of a complex regulatory machinery of the liver involving (i) coordination of the synthesis of each of the lipid and protein components, (ii) aggregation (assembly) of these components in the required proportions and (iii) movement of the aggregates from their site of assembly through the secretory route and into circulation. The contribution of two cellular membranes has been reported, the endoplasmic reticulum and the Golgi apparatus as the major site of lipid synthesis and lipoprotein assembly as well as site of further protein processing (e.g. glycosylation), respectively. Subsequently, secretory vesicles releases the Golgi, move to and fuse with the plasma membrane and nascent VLDL are secreted into circulation. Vance and Vance have proposed that newly synthesized lipids are preferred substrates, or even

required for lipoprotein assembly. However, *de novo*-synthesis compared to re-circulation is assumed to contribute the minor part of the intracellular lipid pool which argues for its role as rate limiting. The composition, mechanism of assembly and secretion of plasma circulating lipoproteins are affected by a variety of factors including fasting or feeding (Shorten and Upreti, 2005) as well as intracellular levels of cholesterol and hormone regulation (Vance and Vance, 1990). Thus, it is likely that the liver may produce particles whose density extends the entire VLDL spectrum. Allowing the hepatic synthesis of a broader spectrum of lipoproteins, possibly even belonging to the IDL and LDL type, may therefore contribute to improve the agreement between simulation and experiment. As a pilot study, this potential was analyzed by elucidating the impact of different initial compositions on the distribution of lipoprotein complexes in blood plasma. It could be shown, that for some even substantially altered initial compositions nearly equal quality of agreement between simulated and experimentally measured lipoprotein profiles can be achieved. This would suggest for the capability of the plasma lipoprotein metabolism to compensate specific changes in the initial composition of lipoproteins synthesized due to different liver conditions or dietary interventions leading, nevertheless, to normal blood lipid values.

A sensitivity analysis has displayed the determining parameters of the lipoprotein system modeled in this work. It was strikingly apparent that the most influential parameters of the model belong to those processes even major defects have been described for, namely hypercholesterolemia caused by an impaired uptake of B-particles ($c_{destroyB}$), hypertriglyceridemia derived from a reduced LPL activity ($c_{hydrolyzeB}$ and hypoalphalipoproteinemia as the result of an impaired peripheral cholesterol uptake (c_{influx}). The strong influence of CETP may approve the recently proposed role as a potential new drug target, e.g. for inhibitors like Torcetrapib (Brousseau et al., 2004) to lower the risk of atherosclerosis. The fact, that Pfizer has recently stopped all Torcetrapib clinical trials because of increased rate of mortality in patients receiving a combination of Torcetrapib/Atorvastatin, however, does not alter the putative clinical importance of CETP as a key protein in lipoprotein metabolism.

7.3 Lipid values in high resolution might be valuable to improve risk characterization

Monitoring the major lipoprotein classes, particularly low-density lipoproteins (LDL) and high-density lipoproteins (HDL), for characterizing risk of

cardiovascular disease (CVD) is well-accepted and routine in clinical practice. However, it is only one-half of the truth as lipoprotein classes comprise non-homogeneous populations of individual lipoprotein particles, and various studies have shown differing metabolic behavior and contribution to CVD of individual lipoprotein sub-populations.

First evidence for the existence of discrete LDL sub-populations have been reported by Krauss and Burke (Krauss and Burke, 1982). In various following studies a predominance of the sub-population of smaller, dense LDL (called *Pattern B*) has been proposed to be more atherogenic than of larger, buoyant LDL (called *Pattern A*) (Berneis and Krauss, 2002; Gardner et al., 1996; Griffin et al., 1994; Lamarche et al., 1997). The atherogenic effect has been primarily attributed to a composition-caused diminished clearance due to a lower affinity for LDL receptor binding (Nigon et al., 1991) and higher susceptibility to oxidative modifications (Dejager et al., 1993). Although the majority of previous studies have examined LDL sub-populations, more recently, also HDL has been found to be especially complex with at least 5 and perhaps as many as 12 or more subclasses (Asztalos et al., 2005a) showing differing metabolic behavior (Asztalos et al., 2005b) and redistribution in pathological conditions (Asztalos and Schaefer, 2003).

Nevertheless, the superiority of detailed lipid fractionation is still a matter of debate as experimental separation and analysis is an elaborate, time-consuming and expensive venture and not yet worthwhile for routine measurements. Experimental methods established for lipid fractionation include gradient density ultracentrifugation (Baumstark et al., 1990; Chapman et al., 1981; Griffin et al., 1990), non-denaturing polyacrylamide gradient gel electrophoresis (GGE) (Nichols et al., 1986), nuclear magnetic resonance (NMR) spectroscopy (Otvos, 2002; Otvos et al., 1992) and high-performance liquid chromatography (HPLC) (Carroll and Rudel, 1983; Hirano et al., 2003), each with particular assets and drawbacks (Winkler, 2004). Especially GGE and NMR spectroscopy are capable to measure both, lipoprotein particle numbers (LDL-P) and size. Either methods have been favored in the last decade, since prospective studies have emphasized stronger association between LDL-P and/or size and CVD risk compared with LDL-C (Sniderman et al., 2003). Today, even controversy exist whether the number of lipoprotein particles or the size actually matters (Berneis and Rizzo, 2004; Cromwell and Otvos, 2004). Recent findings of El Harchaoui et al. may further challenging the efforts of detailed lipoprotein sub-population analyses. They have investigated the value of LDL particle number and size as predictors of CVD in the EPIC-Norfolk prospective population study and the results do not support routine use of LDL-P in CVD risk assessment strategies (Harchaoui et al., 2007). In contrast, Asztalos et al. have demonstrated that specific HDL sub-

populations were definitely either significant positive or significant negative predictors of recurrent CVD events in the Veterans Affairs HDL Intervention Trial (Asztalos et al., 2005a).

It is obvious that the composition, number and size of lipoprotein particles argues for differing metabolic behavior and contribution to CVD. In fact, the cholesterol content per particle exhibits large inter-individual variation and distributions of LDL subclasses have been shown to vary largely among individuals independent of total LDL cholesterol (Krauss and Siri, 2004). A fact, that emphasizes the importance of the concept presented here as the work permits to calculate the distribution of lipoproteins across any narrow density interval of choice. Monitoring the distribution of the entire lipoprotein composition spectrum as well as changes in individual lipoprotein compositions reveal more sufficient information that may improve the characterization of a patients lipid risk state.

The model allows to indicate small alterations in one of the underlying processes, e.g. depending on the genetic disposition, among individuals leading subsequently to inter-individual variability. The latter has been proven by model calculations which clearly displayed altered distribution of the *hrDS* cholesterol within LDL at nearly same total LDL-C values. Only moderate changes in one of the underlying processes, exemplarily shown for the process *HydrolyzeB*, were able to shift the distribution of cholesterol, between *Pattern A* and *Pattern B*.

The analysis of high-resolution lipoprotein profiles may preferentially aim at understanding the reasons for inter-individual variability in subjects of normal or intermediate risk state, but possibly even in distinct pathological conditions. This work offers the possibility for that analysis on the basis of the entire spectrum of lipoprotein particles in plasma differing in size, composition, physiological function and possibly contribution to CVD. This way, the model may provide together with analytical lipid diagnostics a useful tool to improve the risk characterization of patients at normal or even intermediate risk state. It might be further helpful in planning prevention strategies as well as in guiding the extent and choice of therapeutic (drug and dietary) interventions. However, validation of the high resolution distribution, at best provided by detailed experimental lipid fractionation, will be one of the indispensable things needed to do in future work.

7.4 Simulated pathological states correspond well to clinical observations

Several gene products play major roles in the metabolism of lipoproteins as enzymes, transfer proteins, receptors and apolipoproteins. Variations or disorders in the underlying genes are associated with abnormal lipoprotein concentrations mainly addressed to LDL and HDL in the clinical routine. The model was applied to calculate the distribution of lipoproteins of subjects suffering from a defined molecular defect in one of the underlying elementary kinetic processes.

(a) Hypercholesterolemia, (b) Hypertriglyceridemia and (c) Hypoalphalipoproteinemia were exemplarily simulated by modifying the appropriate model parameters for the LDL receptor mediated uptake of B-particles, the LPL mediated hydrolysis of B-particle triglycerides and the ABCA1 mediated uptake of peripheral cholesterol, respectively. In all cases, the simulated pathological states could nicely reproduce fundamental clinical characteristics of the selected dyslipidemia.

(a) Hypercholesterolemia: The model calculations indicate a combined hyperlipidemia showing characteristics from FH (Familial Hypercholesterolemia, LDL receptor defect) and FDB (Familial Defective Apolipoprotein B-100) patients. The LDL receptor defect is associated with an increased level of LDL, whereas VLDL and triglycerides remain typically unchanged Brown and Goldstein (1986). With particular respect to LDL, accumulation of small-dense LDL has been found which coincides to observations in carriers of a LDL receptor gene Asp235->Glu mutation (FH-Keuruu) with familial moderate hypercholesterolemia (Koivisto et al., 1997). A similar observation was reported in a FDB patient who has a Glu->Arg mutation in codon 3500 of the apoB gene (März et al., 1993).

(b) Hypertriglyceridemia: The calculated phenotype clearly displays both, hypertriglyceridemia and hypercholesterolemia, in the VLDL and remnant fraction as typically observed in dysbetalipoproteinemia, a combined dyslipidemia of type III (Mahley et al., 1999). Predicted increased HDL concentration coincides to observations of a terminal mutation in exon 9 of the LPL gene (Kuivenhoven et al., 1997). Predominance of small-dense LDL, as often implicated with hypertriglyceridemia (Packard, 2003), and reduced HDL cholesterol (Babirak et al., 1989) cannot be observed.

(c) Hypoalphalipoproteinemia: The simulated profile reproduces severe reduction in HDL cholesterol levels (Oram, 2000) and mild hypertriglyceridemia typically reported for patients with Familial Hypoalphalipoproteinemia and Tangier Disease (TD) (Asztalos et al., 2001). Differing behavior of

individual HDL sub-populations can be confirmed partially (Asztalos and Schaefer, 2003), and calculations agree in the decrease in 'good' LDL cholesterol. (`http://www.lipid.org/clinical/patients/1000003.php`).

It has to be mentioned, since the model refrains from any regulatory effects in the kinetic description of the processes, the pathological profiles are still a simplified picture of the overall complexity. For example, the model fails so far at discriminating between variations (polymorphisms) within one gene and of different genes playing a role in one and the same process. In fact, in all of the three simulated cases the combined action of mutations in more than one gene may cause the altered lipid phenotype. (a) the LDL receptor and/or the apoB-100 gene, (b) the LPL, apoC-II and/or apoE gene and (c) the ABCA1 and/or apoA-I gene can exhibit mutations, accordingly. Refining the kinetic description of the processes by inclusion of regulatory effects will be therefore one of the tasks in future work and might allow to address different genes to a process.

Most interesting and challenging will be also the other way around, to identify backwards, starting from a given individual lipoprotein profile of a patient, those processes that are subjected to a variation or disorder. This may give indications to underlying alterations in an enzyme, transfer protein, receptor or apolipoprotein and could subsequently give rise to suggestions for a patient-oriented therapeutic strategy.

7.5 Extensions and refinements

Based on the findings in this work, it is planned to study in a systematic manner how high-resolution lipoprotein profiles may help to explain inter-individual variability and to improve risk characterization for CVD. The approach shall further be used to evaluate the potential of a re-definition of density classes and the combination of lipoprotein component levels within these classes to define novel diagnostic parameters which sensitively and specifically indicate alterations of the lipoprotein metabolism on the molecular level and will offer answering a number of other questions. Such model-based optimization of systemic lipid diagnostics requires extensive improvements of the present core model. In view of the complex nature of the lipoprotein metabolism I make no claim to be complete, however, the most relevant extensions and refinements necessary to increase the physiological reliability of the model are:

1. Inclusion of apoA-II will allow for differentiation between LpA-I and LpA-I:A-II particles being important to discriminate, the differing

metabolic fate apoA-I exhibits in lipoprotein particles with apoA-I alone (LpA-I) and together with apoA-II (Rader et al., 1991) as well as to better satisfy the differing metabolic behavior of several HDL sub-populations in normal and pathological conditions (Asztalos and Schaefer, 2003).

2. Inclusion of apoB-48 in addition to apoB-100 to model the metabolism of intestinal synthesized chylomicrons might be important as postprandial hyperlipidemia has been discussed as a major risk factor for CVD (Dallongeville and Fruchart, 1998; Yu and Cooper, 2001). The striking advantage here is to allow for analyzing the postprandial and even individual response to various nutritional interventions (quality, content and amount of food).

3. Distinguishing between free cholesterol and cholesteryl ester by disaggregation of the model component variable C will allow for including the kinetic process of esterification of free cholesterol to cholesteryl ester mediated by LCAT, a further key enzyme of the reverse cholesterol transport (Ohashi et al., 2005). This offers the possibility to take into account the activating influence of apoA-I on LCAT (Jonas, 1998).

4. Disaggregation of the model component F into apolipoproteins E and C will allow to consider essential regulatory functions, e.g. activating effect of apoC-I on LCAT (Soutar et al., 1975), activation of LPL by apoC-II (Miller and Smith, 1973), influence on the LDL receptor binding by apoE (Barbagallo et al., 1998) and the apoE-dependent alternative path for peripheral cholesterol (Mahley et al., 2006).

5. Explicit incorporation of phospholipids as dynamic variables of the system will entail the inclusion of a new process, the phospholipid exchange mediated by the phospholipids transfer protein (PLTP). This protein plays a key role in the so-called remodeling of HDL (Huuskonen et al., 2001; van Tol, 2002) and modeling the process will be mechanistically interesting, but even more complex, as particle fusion has been reported for it (Korhonen et al., 1998).

6. Inclusion of other transporters and receptors involved either in the holoparticle uptake or in the uptake of individual lipoprotein components will allow to elucidate the role of, e.g. SR-B1, ABCG1 and ABCG4 in the uptake of peripheral cholesterol (Ji et al., 1997; Wang et al., 2004), in particular with respect to the question whether apoA-I is a causative or passive agent in this process (Marguet and Chimini, 2002; Oram, 2003).

One major advantage of the modeling approach presented here compared with the classical compartment modeling work is to address elementary processes of the lipoprotein metabolism such as the neutral lipid transfer among lipoproteins by the CETP. It has to be mentioned, that this event was modeled as a non-coupled process. Whether there is indeed a hetero-exchange of triglycerides (TG) versus cholesteryl ester (CE) is still a matter of debate. It is favored by most of the studies (Tall, 1995), but other findings demonstrate that the neutral lipid transfer among lipoproteins occur in a non-equimolar hetero-exchange and that independent pathways exist for the transfer of cholesteryl ester and triglycerides (Liu and Bagdade, 1995). However, insights gained from the crystal structure of CETP recently published will certainly help to refine the modeling of this process (Qiu et al., 2007).

Another crucial point light has to be shed on in future work is to analyze the extent of influence the values used for lipoprotein component's molecular weights and volumes have on the density calculation. Noteworthy, the molecular weights of the lipid and protein components depend on the specific fatty acid composition and, especially in case of apoB-100, on the grade of posttranslational glycosylation, respectively (Harazono et al., 2005). A number of studies have shown that differing fatty acid composition as well as glycosylation may cause differing behavior in related processes (Pufal et al., 1995; Thomas et al., 1994; Yli-Jokipii et al., 2002).

Chapter 8

Conclusion & Outlook

"Science is always wrong. It never solves a problem without creating ten more."

(George Bernard Shaw)

Noteworthy, the modeling approach takes into account major components and elementary processes of the whole lipoprotein system in blood plasma. The model simulations reproduced successfully lipoprotein composition data from common density classes of healthy subjects and enabled revealing the distribution of lipoproteins in high resolution. This may help to analyze the reasons for inter-individual variability widely observed, in particular, in the normal population, to improve risk characterization for CVD as well as to stimulate the identification of new important sub-fractions of potential clinical relevance.

The predictive capability was successfully tested in that simulations of lipid disorders by modifying one of the underlying kinetic processes have calculated abnormal lipoprotein distributions that correspond well to clinical observations. In the opposite way around, it is planned to relate lipoprotein profiles of individual subjects to a selected set of kinetic parameters and to identify those processes being possibly most responsible for alterations or disorders of the lipoprotein metabolism in that individual. This potentially offers a patient-oriented diagnosis of individual atherogenic lipid disorders.

As comprehensively outlined a number of extensions and refinements are thinkable in order to make the model even more physiologically. Either ways, adding components or processes and refining the kinetic description, e.g. by including regulatory effects, the number of parameters will automatically increase. To keep the model still useful it is indispensable to have accurate experimental data. Valuable methods for model reduction, parameter iden-

tifiability and fixation of trustworthy parameters from experimental studies have to be elucidated. Therefore, it will be most challenging to balance the physiological relevance and numerical tractability to reliably maintain a well-defined and identifiable system.

Forcing the model-based analysis of higher resolution lipoprotein profiles in normal and pathological subjects even with arbitrary density fractionation to an application useful for clinical routine will make validating the calculated profiles by detailed experimental lipid fractionation methods absolutely essential. As one vision beyond, the computer-based analysis of high resolution density sub-fractions (*hrDS*) may provide together with analytical lipid diagnostics an useful tool to improve risk characterization of patients at normal or even intermediate risk state. It might be helpful in defining prevention strategies or guiding early-stage patient-oriented therapeutic (life style and/or drug) interventions as well as monitoring treatment.

Even if it will be a long way to go, the first step is done. The model in its present state poses various questions to answer and offers a platform for many future applications. Besides simulating abnormalities in the kinetic processes, in principle, the model can even be applied to test common (e.g. statins) as well as potentially new medications designed to interfere with key players of the lipoprotein metabolism. The most promising candidate in the past, for example, has been an inhibitor of CETP named Torcetrapib.

Including regulatory effects will surely help to improve the kinetic description of the underlying processes. Even more, it might allow to address and to discriminate between different mutations in different genes involved in one and the same process which is of crucial interest as it would help to understand inter-individual variability of lipoprotein distribution patterns.

Here, a comprehensive analysis within a larger population of normolipidemic subjects is aimed at clarifying the relation between quantitative variations in the plasma lipoproteins (amount and composition) and the underlying genetic architecture in terms of number of loci involved, the frequencies and effects of their alleles, and the type of loci, i.e. structural or regulatory. Previous work on genotype-phenotype association studies, e.g. performed by (Bauerfeind et al., 2006) may provide useful help in this matter. However, most challenging will be to exactly quantify the influence of a specific genetic variation, either SNP or even haplotypes, on the appropriate parameter value.

Access to comprehensive genotype data with corresponding in-depth lipid diagnostics would be very useful. In this context, the potential of multiple data resources available from various clinical trials and prospective studies undertaken so far in the field of cardiovascular research has to be elucidated. In addition, several sources provide comprehensive data concerning genetic variations of proteins involved in the lipoprotein metabolism. As an example,

about 1000 unique allelic variants are listed in the LDL receptor database available at `www.ucl.ac.uk/ldlr/LOVDv.1.1.0/` (Varret et al., 1997).

However, since most of the clinical studies have monitored routine parameters, such as LDL-C, HDL-C and total triglycerides, the set up of a new project might be valuable and should integrate data from various profiling technologies including genome, expression and protein levels with in-depth lipoprotein fractionation data.

In this context, one further major application will aim at understanding the influence of different nutritional interventions (amount, content and composition) on the distribution of lipoproteins in the plasma.

Besides clinical applications, interesting questions regarding the mechanistic understanding of the lipoprotein metabolism under various conditions arise from the modeling approach. For example, since the stochastic approach allow to monitor the metabolic fate of each individual lipoprotein complex one may arrive at a classification of lipoproteins based on the metabolic behavior rather than on physico-chemical properties. Even more, time evolved measurements would provide sufficient information of the time-dependent behavior compared with the present snapshot of a steady state.

Finally, atherosclerosis is a systemic disorder. The long-term objective may even focus on a systemic integrative model of essential lipoprotein related paths in the human body by connecting, e.g. the synthesis and assembly of lipoprotein components in the liver and intestine, the processes involved in the lipoprotein metabolism in the blood plasma (described in the present work) and the subsequent mechanisms leading to foam cell and atherosclerotic plaque formation in the artery wall.

Bibliography

S. Acton, A. Rigotti, K. T. Landschulz, S. Xu, H. H. Hobbs, and M. Krieger. Identification of scavenger receptor sr-bi as a high density lipoprotein receptor. *Science*, 271(5248):518–520, Jan. 1996.

M. Adiels, C. Packard, M. J. Caslake, P. Stewart, A. Soro, J. Westerbacka, B. Wennberg, S.-O. Olofsson, M.-R. Taskinen, and J. Borén. A new combined multicompartmental model for apolipoprotein B-100 and triglyceride metabolism in VLDL subfractions. *J Lipid Res*, 46(1):58–67, Jan 2005.

B. F. Asztalos and E. J. Schaefer. High-density lipoprotein subpopulations in pathologic conditions. *Am J Cardiol*, 91(7A):12E–17E, Apr 2003.

B. F. Asztalos, M. E. Brousseau, J. R. McNamara, K. V. Horvath, P. S. Roheim, and E. J. Schaefer. Subpopulations of high density lipoproteins in homozygous and heterozygous Tangier disease. *Atherosclerosis*, 156(1): 217–225, May 2001.

B. F. Asztalos, D. Collins, L. A. Cupples, S. Demissie, K. V. Horvath, H. E. Bloomfield, S. J. Robins, and E. J. Schaefer. Value of high-density lipoprotein (hdl) subpopulations in predicting recurrent cardiovascular events in the Veterans Affairs HDL Intervention Trial. *Arterioscler Thromb Vasc Biol*, 25(10):2185–2191, Oct 2005a.

B. F. Asztalos, M. de la Llera-Moya, G. E. Dallal, K. V. Horvath, E. J. Schaefer, and G. H. Rothblat. Differential effects of HDL subpopulations on cellular ABCA1- and SR-BI-mediated cholesterol efflux. *J Lipid Res*, 46(10):2246–2253, Oct 2005b.

S. P. Babirak, P. H. Iverius, W. Y. Fujimoto, and J. D. Brunzell. Detection and characterization of the heterozygote state for lipoprotein lipase deficiency. *Arteriosclerosis*, 9(3):326–334, 1989.

G. D. Backer, E. Ambrosioni, K. Borch-Johnsen, C. Brotons, R. Cifkova, J. Dallongeville, S. Ebrahim, O. Faergeman, I. Graham, G. Mancia, V. M.

Cats, K. Orth-Gomér, J. Perk, K. Pyörälä, J. L. Rodicio, S. Sans, V. Sansoy, U. Sechtem, S. Silber, T. Thomsen, D. Wood, T. J. T. F. of European, and O. S. on Cardiovascular Disease Prevention in Clinical Practice. European guidelines on cardiovascular disease prevention in clinical practice. Third Joint Task Force of European and Other Societies on Cardiovascular Disease Prevention in Clinical Practice. *Eur Heart J*, 24(17):1601–1610, Sep 2003.

C. M. Barbagallo, G. A. Levine, P. J. Blanche, B. Y. Ishida, and R. M. Krauss. Influence of apoe content on receptor binding of large, bouyant ldl in subjects with different ldl subclass phenotypes. *Arterioscler Thromb Vasc Biol*, 18(3):466–472, Mar 1998.

P. Barrett, B. M. Bell, C. Cobelli, H. Golde, A. Schumitzky, P. Vicini, and D. M. Foster. SAAM II: Simulation, analysis, and modeling software for tracer and pharmacokinetic studies. *Metabolism*, 47(4):484–492, Apr. 1998.

P. H. R. Barrett, D. C. Chan, and G. F. Watts. Thematic review series: Patient-Oriented Research. Design and analysis of lipoprotein tracer kinetics studies in humans. *J Lipid Res*, 47(8):1607–1619, Aug 2006.

P. J. Barter and K. A. Rye. The rationale for using apoa-i as a clinical marker of cardiovascular risk. *Journal of Internal Medicine*, 259:447–454, 2006.

S. K. Basu, M. S. Brown, Y. K. Ho, R. J. Havel, and J. L. Goldstein. Mouse macrophages synthesize and secrete a protein resembling apolipoprotein E. *Proc Natl Acad Sci U S A*, 78(12):7545–7549, Dec 1981.

R. Batal, M. Tremblay, L. Krimbou, O. Mamer, J. Davignon, J. Genest, and J. S. Cohn. Familial HDL deficiency characterized by hypercatabolism of mature apoA-I but not proapoA-I. *Arterioscler Thromb Vasc Biol*, 18(4): 655–664, Apr 1998.

R. Batal, M. Tremblay, P. Barrett, H. Jacques, A. Fredenrich, O. Mamer, J. Davignon, and J. Cohn. Plasma kinetics of apoC-III and apoE in normolipidemic and hypertriglyceridemic subjects. *J Lipid Res*, 41:706–718, 2000.

A. Bauerfeind, H. Knoblauch, M. C. Costanza, T. Luganskaja, M. R. Toliat, P. Nürnberg, F. C. Luft, J. G. Reich, and A. Morabia. Concordant association of lipid gene variation with a combined hdl/ldl-cholesterol phenotype in two european populations. *Hum Hered*, 61(3):123–131, 2006.

M. W. Baumstark, W. Kreutz, A. Berg, I. Frey, and J. Keul. Structure of human low-density lipoprotein subfractions, determined by X-ray small-angle scattering. *Biochim Biophys Acta*, 1037(1):48–57, Jan 1990.

W. F. Beltz, Y. A. Kesäniemi, B. V. Howard, and S. M. Grundy. Development of an integrated model for analysis of the kinetics of apolipoprotein b in plasma very low density lipoproteins, intermediate density lipoproteins, and low density lipoproteins. *J Clin Invest*, 76(2):575–585, Aug 1985.

K. Berneis and M. Rizzo. LDL size: does it matter? *Swiss Med Wkly*, 134 (49-50):720–724, Dec 2004.

K. K. Berneis and R. M. Krauss. Metabolic origins and clinical significance of LDL heterogeneity. *J Lipid Res*, 43(9):1363–1379, Sept. 2002.

D. W. Bilheimer, N. J. Stone, and S. M. Grundy. Metabolic studies in familial hypercholesterolemia. evidence for a gene-dosage effect in vivo. *J Clin Invest*, 64(2):524–533, Aug 1979.

D. J. Blom, F. H. O'Neill, and A. D. Marais. Screening for dysbetalipoproteinemia by plasma cholesterol and apolipoprotein B concentrations. *Clin Chem*, 51(5):904–907, May 2005.

C. B. Blum, L. Aron, and R. Sciacca. Radioimmunoassay studies of human apolipoprotein E. *J Clin Invest*, 66(6):1240–1250, Dec 1980.

M. Bodzioch, E. Orsó, J. Klucken, T. Langmann, A. Böttcher, W. Diederich, W. Drobnik, S. Barlage, C. Büchler, M. Porsch-Ozcürümez, W. E. Kaminski, H. W. Hahmann, K. Oette, G. Rothe, C. Aslanidis, K. J. Lackner, and G. Schmitz. The gene encoding ATP-binding cassette transporter 1 is mutated in Tangier disease. *Nat Genet*, 22(4):347–351, Aug 1999.

L. Boring, J. Gosling, M. Cleary, and I. F. Charo. Decreased lesion formation in CCR2-/- mice reveals a role for chemokines in the initiation of atherosclerosis. *Nature*, 394(6696):894–897, Aug 1998.

K. Boyle, M. Phillips, and S. Lund-Katz. Kinetics and mechanism of exchange of apolipoprotein C-III molecules from very low density lipoprotein particles. *Biochim Biophys Acta*, 1430:302–312, 1999.

W. C. Breckenridge, J. A. Little, G. Steiner, A. Chow, and M. Poapst. Hypertriglyceridemia associated with deficiency of apolipoprotein C-II. *N Engl J Med*, 298(23):1265–1273, Jun 1978.

J. L. Breslow. Transgenic mouse models of lipoprotein metabolism and atherosclerosis. *Proc Natl Acad Sci U S A*, 90(18):8314–8318, Sep 1993.

J. L. Breslow. Mouse models of atherosclerosis. *Science*, 272(5262):685–688, May 1996.

E. A. Brinton, S. Eisenberg, and J. L. Breslow. Human HDL cholesterol levels are determined by apoA-I fractional catabolic rate, which correlates inversely with estimates of HDL particle size. effects of gender, hepatic and lipoprotein lipases, triglyceride and insulin levels, and body fat distribution. *Arterioscler Thromb*, 14(5):707–720, May 1994.

A. Brooks-Wilson, M. Marcil, S. Clee, L. Zhang, K. Roomp, M. van Dam, and et al. Mutations in abc1 in tangier disease and familial high-density lipoprotein deficiency. *Nature Genetics*, 22:336–345, 1999.

M. E. Brousseau, E. J. Schaefer, M. L. Wolfe, L. T. Bloedon, A. G. Digenio, R. W. Clark, J. P. Mancuso, and D. J. Rader. Effects of an inhibitor of cholesteryl ester transfer protein on HDL cholesterol. *N Engl J Med*, 350 (15):1505–1515, Apr 2004.

M. S. Brown and J. L. Goldstein. A receptor-mediated pathway for cholesterol homeostasis. *Science*, 232(4746):34–47, Apr 1986.

M. S. Brown and J. L. Goldstein. The SREBP pathway: regulation of cholesterol metabolism by proteolysis of a membrane-bound transcription factor. *Cell*, 89(3):331–340, May 1997.

J. D. Brunzell. Clinical practice. hypertriglyceridemia. *N Engl J Med*, 357 (10):1009–1017, Sep 2007.

L. A. Carlson, A. Hamsten, and A. Asplund. Pronounced lowering of serum levels of lipoprotein Lp(a) in hyperlipidaemic subjects treated with nicotinic acid. *J Intern Med*, 226(4):271–276, Oct 1989.

R. Carroll and L. Rudel. Lipoprotein separation and low density lipoprotein molecular weight determination using high performance gel-filtration chromatography. *J Lipid Res*, 24(2):200–207, Feb. 1983.

A. Chait, C. Y. Han, J. F. Oram, and J. W. Heinecke. Thematic review series: The immune system and atherogenesis. lipoprotein-associated inflammatory proteins: markers or mediators of cardiovascular disease? *J Lipid Res*, 46(3):389–403, Mar 2005.

D. C. Chan, P. H. R. Barrett, and G. F. Watts. Recent studies of lipoprotein kinetics in the metabolic syndrome and related disorders. *Curr Opin Lipidol*, 17(1):28–36, Feb 2006.

M. Chapman, S. Goldstein, D. Lagrange, and P. Laplaud. A density gradient ultracentrifugal procedure for the isolation of the major lipoprotein classes from human serum. *J Lipid Res*, 22(2):339–358, Feb. 1981.

M. Chétiveaux, K. Ouguerram, Y. Zair, P. Maugere, I. Falconi, H. Nazih, and M. Krempfra. New model for kinetic studies of HDL metabolism in humans. *Eur J Clin Invest*, 34(4):262–267, Apr 2004.

J. S. Cohn, R. Batal, M. Tremblay, H. Jacques, L. Veilleux, C. Rodriguez, O. Mamer, and J. Davignon. Plasma turnover of HDL apoC-I, apoC-III, and apoE in humans: in vivo evidence for a link between HDL apoC-III and apoA-I metabolism. *J Lipid Res*, 44(10):1976–1983, Oct. 2003.

D. T. Connolly, J. McIntyre, D. Heuvelman, E. E. Remsen, R. E. McKinnie, L. Vu, M. Melton, R. Monsell, E. S. Krul, and K. Glenn. Physical and kinetic characterization of recombinant human cholesteryl ester tranfer protein. *Biochem J*, 320:39–47, 1996.

W. C. Cromwell and J. D. Otvos. Low-density lipoprotein particle number and risk for cardiovascular disease. *Curr Atheroscler Rep*, 6(5):381–387, Sep 2004.

M. H. Cummings, G. F. Watts, M. Umpleby, T. R. Hennessy, J. R. Quiney, and P. H. Sonksen. Increased hepatic secretion of very-low-density-lipoprotein apolipoprotein B-100 in heterozygous familial hypercholesterolaemia: a stable isotope study. *Atherosclerosis*, 113(1):79–89, Feb. 1995.

M. D. Curry, W. J. McConathy, J. D. Fesmire, and P. Alaupovic. Quantitative determination of apolipoproteins C-I and C-II in human plasma by separate electroimmunoassays. *Clin Chem*, 27(4):543–548, Apr 1981.

L. K. Curtiss, D. T. Valenta, N. J. Hime, and K.-A. Rye. What is so special about apolipoprotein AI in reverse cholesterol transport? *Arterioscler Thromb Vasc Biol*, 26(1):12–19, Jan 2006.

S. D. Cushing, J. A. Berliner, A. J. Valente, M. C. Territo, M. Navab, F. Parhami, R. Gerrity, C. J. Schwartz, and A. M. Fogelman. Minimally modified low density lipoprotein induces monocyte chemotactic protein 1 in human endothelial cells and smooth muscle cells. *Proc Natl Acad Sci U S A*, 87(13):5134–5138, Jul 1990.

J. Dallongeville and J. C. Fruchart. Postprandial dyslipidemia: a risk factor for coronary heart disease. *Ann Nutr Metab*, 42(1):1–11, 1998.

R. J. Deckelbaum, R. Ramakrishnan, S. Eisenberg, T. Olivecrona, and G. Olivecrona-Bengtsson. Triacylglycerol and phospholipid hydrolysis in human plasma lipoproteins: Role of lipoprotein and hepatic lipase. *Biochemistry*, 31(36):8544–8551, 1992.

S. Dejager, E. Bruckert, and M. J. Chapman. Dense low density lipoprotein subspecies with diminished oxidative resistance predominate in combined hyperlipidemia. *J Lipid Res*, 34(2):295–308, Feb 1993.

T. Demant, C. J. Packard, H. Demmelmair, P. Stewart, A. Bedynek, D. Bedford, D. Seidel, and J. Shepherd. Sensitive methods to study human apolipoprotein B metabolism using stable isotope-labeled amino acids. *Am J Physiol*, 270(6 Pt 1):E1022–E1036, Jun 1996.

D. Duffy and D. J. Rader. Emerging therapies targeting high-density lipoprotein metabolism and reverse cholesterol transport. *Circulation*, 113(8): 1140–1150, Feb 2006.

K. P. Dwyer, P. H. R. Barrett, D. Chan, J. I. Foo, G. F. Watts, and K. D. Croft. Oxazolinone derivative of leucine for GC-MS: a sensitive and robust method for stable isotope kinetic studies of lipoproteins. *J Lipid Res*, 43 (2):344–349, Feb 2002.

S. Eisenberg. High density lipoprotein metabolism. *J Lipid Res*, 25(10): 1017–1058, Oct. 1984.

Expert Panel on Detection, Evaluation, and Treatment of High Blood Cholesterol in Adults. Executive summary of the third report of the National Cholesterol Education Program (NCEP) expert panel on detection, evaluation, and treatment of high blood cholesterol in adults (adult treatment panel III). *JAMA*, 285(19):2486–2497, May 2001.

M. L. Fernandez and J. S. Volek. Guinea pigs: A suitable animal model to study lipoprotein metabolism, atherosclerosis and inflammation. *Nutr Metab (Lond)*, 3:17, 2006.

C. J. Fielding, C. T. Lim, and A. M. Scanu. A protein component of serum high density lipoprotein with co-factor activity against purified lipoprotein lipase. *Biochem Biophys Res Commun*, 39(5):889–894, Jun 1970.

C. J. Fielding, V. G. Shore, and P. E. Fielding. A protein cofactor of lecithin:cholesterol acyltransferase. *Biochem Biophys Res Commun*, 46 (4):1493–1498, Feb 1972.

P. J. Fielding, C. J. Fielding, and R. J. Havel. Cholesterol net transport, esterification, and transfer in human hyperlipidemic plasma. *J Clin Invest*, 71(3):449–460, 1983.

R. M. Fisher, S. E. Humphries, and P. J. Talmud. Common variation in the lipoprotein lipase gene: effects on plasma lipids and risk of atherosclerosis. *Atherosclerosis*, 135(2):145–159, Dec 1997.

W. R. Fisher, L. A. Zech, and P. W. Stacpoole. Apob metabolism in familial hypercholesterolemia. inconsistencies with the LDL receptor paradigm. *Arterioscler Thromb*, 14(4):501–510, Apr 1994.

P. G. Frank and Y. L. Marcel. Apolipoprotein A-I: structure-function relationships. *J Lipid Res*, 41(6):853–872, Jun 2000.

D. S. Fredrickson. An international classification of hyperlipidemias and hyperlipoproteinemias. *Ann Intern Med*, 75(3):471–472, Sep 1971.

R. Frénais, K. Ouguerram, C. Maugeais, J. S. Marchini, P. Benlian, J. M. Bard, T. Magot, and M. Krempf. Apolipoprotein A-I kinetics in heterozygous familial hypercholesterolemia: a stable isotope study. *J Lipid Res*, 40 (8):1506–1511, Aug 1999.

C. D. Gardner, S. P. Fortmann, and R. M. Krauss. Association of small low-density lipoprotein particles with the incidence of coronary artery disease in men and women. *JAMA*, 276(11):875–881, Sep 1996.

G. S. Getz. Thematic review series: the immune system and atherogenesis. immune function in atherogenesis. *J Lipid Res*, 46(1):1–10, Jan 2005.

G. Ghiselli, E. J. Schaefer, P. Gascon, and H. B. Breser. Type III hyperlipoproteinemia associated with apolipoprotein E deficiency. *Science*, 214 (4526):1239–1241, Dec 1981.

J. C. Gibson, A. Rubinstein, P. R. Bukberg, and W. V. Brown. Apolipoprotein E-enriched lipoprotein subclasses in normolipidemic subjects. *J Lipid Res*, 24(7):886–898, Jul 1983.

D. T. Gillespie. A general method for numerically simulating the stochastic time evolution of coupled chemical reactions. *J Comput Phys*, 22:403–434, 1976.

C. K. Glass and J. L. Witztum. Atherosclerosis. the road ahead. *Cell*, 104 (4):503–516, Feb 2001.

L. Goldstein and S. Brown. The low-density lipoprotein pathway and its relation to atherosclerosis. *Ann Rev Biochem*, 46(1):897–930, 1977.

I. M. Graham. Guidelines on cardiovascular disease prevention in clinical practice: the European perspective. *Curr Opin Cardiol*, 20(5):430–439, Sep 2005.

S. R. Green and R. C. Pittman. Selective uptake of cholesteryl esters from low density lipoproteins in vitro and in vivo. *J Lipid Res*, 32(4):667–678, Apr 1991.

B. A. Griffin, M. J. Caslake, B. Yip, G. W. Tait, C. J. Packard, and J. Shepherd. Rapid isolation of low density lipoprotein (ldl) subfractions from plasma by density gradient ultracentrifugation. *Atherosclerosis*, 83(1):59–67, Jul 1990.

B. A. Griffin, D. J. Freeman, G. W. Tait, J. Thomson, M. J. Caslake, C. J. Packard, and J. Shepherd. Role of plasma triglyceride in the regulation of plasma low density lipoprotein (LDL) subfractions: relative contribution of small, dense LDL to coronary heart disease risk. *Atherosclerosis*, 106 (2):241–253, Apr 1994.

V. Gudnason, I. N. Day, and S. E. Humphries. Effect on plasma lipid levels of different classes of mutations in the low-density lipoprotein receptor gene in patients with familial hypercholesterolemia. *Arterioscler Thromb*, 14 (11):1717–1722, Nov 1994.

A. Harazono, N. Kawasaki, T. Kawanishi, and T. Hayakawa. Site-specific glycosylation analysis of human apolipoprotein B100 using LC/ESI MS/MS. *Glycobiology*, 15(5):447–462, May 2005.

K. E. Harchaoui, W. A. van der Steeg, E. S. G. Stroes, J. A. Kuivenhoven, J. D. Otvos, N. J. Wareham, B. A. Hutten, J. J. P. Kastelein, K.-T. Khaw, and S. M. Boekholdt. Value of low-density lipoprotein particle number and size as predictors of coronary artery disease in apparently healthy men and women: the EPIC-Norfolk Prospective Population Study. *J Am Coll Cardiol*, 49(5):547–553, Feb 2007.

R. J. Havel, H. A. Eder, and J. H. Bragdon. The distribution and chemical composition of ultracentrifugally separated lipoproteins in human serum. *J Clin Invest*, 34(9):1345–1353, Sep 1955.

N. J. Hime, P. J. Barter, and K. A. Rye. The influence of apolipoproteins on the hepatic lipase-mediated hydrolysis of high density lipoprotein phospholipid and triacylglycerol. *J Biol Chem*, 273(42):27191–27198, Oct. 1998.

T. Hirano, Y. Ito, H. Saegusa, and G. Yoshino. A novel and simple method for quantification of small, dense LDL. *J Lipid Res*, 44(11):2193–2201, Nov 2003.

J. D. Horton, J. C. Cohen, and H. H. Hobbs. Molecular biology of PCSK9: its role in LDL metabolism. *Trends Biochem Sci*, 32(2):71–77, Feb 2007.

K. Hübner. Mathematical modeling of the lipoprotein metabolism: Characterization of the metabolic fate of individual lipoprotein components and their phase distribution within the lipoprotein particle. (german). Diploma Thesis, 2000.

J. Huuskonen, V. Olkkonen, M. Jauhiainen, and C. Ehnholm. The impact of phospholipid transfer protein (PLTP) on hdl metabolism. *Atherosclerosis*, 155:269–281, 2001.

K. Ikewaki, D. J. Rader, T. Sakamoto, M. Nishiwaki, N. Wakimoto, J. R. Schaefer, T. Ishikawa, T. Fairwell, L. A. Zech, and H. Nakamura. Delayed catabolism of high density lipoprotein apolipoproteins A-I and A-II in human cholesteryl ester transfer protein deficiency. *J Clin Invest*, 92(4): 1650–1658, Oct 1993.

K. Ikewaki, M. Nishiwaki, T. Sakamoto, T. Ishikawa, T. Fairwell, L. A. Zech, M. Nagano, H. Nakamura, H. B. Brewer, and D. J. Rader. Increased catabolic rate of low density lipoproteins in humans with cholesteryl ester transfer protein deficiency. *J Clin Invest*, 96(3):1573–1581, Sep 1995.

T. L. Innerarity, T. P. Bersot, K. S. Arnold, K. H. Weisgraber, P. A. Davis, T. M. Forte, and R. W. Mahley. Receptor binding activity of high-density lipoproteins containing apoprotein E from abetalipoproteinemic and normal neonate plasma. *Metabolism*, 33(2):186–195, Feb 1984.

A. S. Jarnagin, W. Kohr, and C. Fielding. Isolation and specificity of a Mr 74,000 cholesteryl ester transfer protein from human plasma. *Proc Natl Acad Sci*, 84(7):1854–1857, Apr 1987.

J. Ji, G. F. Watts, A. G. Johnson, D. C. Chan, E. M. M. Ooi, K.-A. Rye, A. P. Serone, and P. H. R. Barrett. High-density lipoprotein (HDL) transport in the metabolic syndrome: application of a new model for HDL particle kinetics. *J Clin Endocrinol Metab*, 91(3):973–979, Mar 2006.

Y. Ji, B. Jian, N. Wang, Y. Sun, M. L. Moya, M. C. Phillips, G. H. Rothblat, J. B. Swaney, and A. R. Tall. Scavenger receptor BI promotes high density lipoprotein-mediated cellular cholesterol efflux. *J Biol Chem*, 272 (34):20982–20985, Aug 1997.

A. Jonas. Regulation of lecithin cholesterol acyltransferase activity. *Progress in Lipid Research*, 37(4):209–234, Sept. 1998.

J. P. Kane. Apolipoprotein B: structural and metabolic heterogeneity. *Annu Rev Physiol*, 45:637–650, 1983.

F. Karpe and K. N. Frayn. The nicotinic acid receptor–a new mechanism for an old drug. *Lancet*, 363(9424):1892–1894, Jun 2004.

E. Kim and S. G. Young. Genetically modified mice for the study of apolipoprotein B. *J Lipid Res*, 39(4):703–723, Apr 1998.

J. Y. King, R. Ferrara, R. Tabibiazar, J. M. Spin, M. M. Chen, A. Kuchinsky, A. Vailaya, R. Kincaid, A. Tsalenko, D. X.-F. Deng, A. Connolly, P. Zhang, E. Yang, C. Watt, Z. Yakhini, A. Ben Dor, A. Adler, L. Bruhn, P. Tsao, T. Quertermous, and E. A. Ashley. Pathway analysis of coronary atherosclerosis. *Physiol.Genomics*, 23(1):103–118, Sept. 2005.

S. Kirkpatrick, C. D. Gelatt, and M. P. Vecchi. Optimization by simulated annealing. *Science*, 220:671–680, 1983.

H. Knoblauch, H. Schuster, F. C. Luft, and J. Reich. A pathway model of lipid metabolism to predict the effect of genetic variability on lipid levels. *J Mol Med*, 78(9):507–515, 2000.

H. Knoblauch, A. Bauerfeind, C. Krahenbuhl, A. Daury, K. Rohde, S. Bejanin, L. Essioux, H. Schuster, F. C. Luft, and J. Georg Reich. Common haplotypes in five genes influence genetic variance of LDL and HDL cholesterol in the general population. *Hum.Mol.Genet.*, 11(12):1477–1485, June 2002.

H. Knoblauch, A. Bauerfeind, M. R. Toliat, C. Becker, T. Luganskaja, U. P. Gunther, K. Rohde, H. Schuster, C. Junghans, F. C. Luft, P. Nurnberg, and J. G. Reich. Haplotypes and SNPs in 13 lipid-relevant genes explain most of the genetic variance in high-density lipoprotein and low-density lipoprotein cholesterol. *Hum Mol Genet*, 13(10):993–1004, May 2004.

R. H. Knopp. Drug treatment of lipid disorders. *N Engl J Med*, 341(7): 498–511, Aug 1999.

U. M. Koivisto, H. Gylling, T. A. Miettinen, and K. Kontula. Familial moderate hypercholesterolemia caused by Asp235–>Glu mutation of the LDL receptor gene and co-occurrence of a de novo deletion of the LDL receptor gene in the same family. *Arterioscler Thromb Vasc Biol*, 17(7): 1392–1399, Jul 1997.

A. Korhonen, M. Jauhiainen, C. Ehnholm, P. T. Kovanen, and M. Ala-Korpela. Remodeling of HDL by phospholipid transfer protein: demonstration of particle fusion by 1H NMR spectroscopy. *Biochem Biophys Res Commun*, 249(3):910–916, Aug 1998.

G. Kostner and W. März. Zusammensetzung und stoffwechsel der lipoproteine (german). In P. Schwandt and W. O. Richter, editors, *Handbuch der Stoffwechselstoerungen*, volume 1. korr. Nachdruck, pages 3–47. Schattauer Verlag, Stuttgart, 1996.

G. M. Kostner, P. Avogaro, G. Cazzolato, E. Marth, G. Bittolo-Bon, and G. B. Qunici. Lipoprotein Lp(a) and the risk for myocardial infarction. *Atherosclerosis*, 38(1-2):51–61, 1981.

R. M. Krauss and D. J. Burke. Identification of multiple subclasses of plasma low density lipoproteins in normal humans. *J Lipid Res*, 23(1):97–104, Jan. 1982.

R. M. Krauss and P. W. Siri. Metabolic abnormalities: triglyceride and low-density lipoprotein. *Endocrinol Metab Clin North Am*, 33(2):405–415, Jun 2004.

R. M. Krauss, P. N. Herbert, R. I. Levy, and D. S. Fredrickson. Further observations on the activation and inhibition of lipoprotein lipase by apolipoproteins. *Circ Res*, 33(4):403–411, Oct 1973.

J. A. Kuivenhoven, B. E. Groenemeyer, J. M. Boer, P. W. Reymer, R. Berghuis, T. Bruin, H. Jansen, J. C. Seidell, and J. J. Kastelein. Ser447stop mutation in lipoprotein lipase is associated with elevated HDL cholesterol levels in normolipidemic males. *Arterioscler Thromb Vasc Biol*, 17(3):595–599, Mar 1997.

B. Lamarche, S. Moorjani, P. J. Lupien, B. Cantin, P. M. Bernard, G. R. Dagenais, and J. P. DesprÃ©s. Apolipoprotein A-I and B levels and the risk of ischemic heart disease during a five-year follow-up of men in the Québec cardiovascular study. *Circulation*, 94(3):273–278, Aug 1996.

B. Lamarche, A. Tchernof, S. Moorjani, B. Cantin, G. R. Dagenais, P. J. Lupien, and J. P. DesprÃ©s. Small, dense low-density lipoprotein particles as a predictor of the risk of ischemic heart disease in men. prospective results from the Québec cardiovascular study. *Circulation*, 95(1):69–75, Jan 1997.

J. C. LaRosa, R. I. Levy, P. Herbert, S. E. Lux, and D. S. Fredrickson. A specific apoprotein activator for lipoprotein lipase. *Biochem Biophys Res Commun*, 41(1):57–62, Oct 1970.

G. F. Lewis and G. Steiner. Hypertriglyceridemia and its metabolic consequences as a risk factor for atherosclerotic cardiovascular disease in non-insulin-dependent diabetes mellitus. *Diabetes Metab Rev*, 12(1):37–56, Apr 1996.

P. Libby. Inflammation in atherosclerosis. *Nature*, 420(6917):868–874, 2002.

F. T. Lindgren, H. A. Elliott, and J. W. Gofman. The ultracentrifugal characterization and isolation of human blood lipids and lipoproteins, with applications to the study of atherosclerosis. *J Phys Colloid Chem*, 55(1): 80–93, Jan 1951.

X. Q. Liu and J. D. Bagdade. Neutral lipid mass transfer among lipoproteins in plasma from normolipidemic subjects is not an equimolar heteroexchange. *J Lipid Res*, 36(12):2574–2579, Dec 1995.

J. M. Lopez, M. K. Bennett, H. B. Sanchez, J. M. Rosenfeld, and T. E. Osborne. Sterol regulation of acetyl coenzyme A carboxylase: a mechanism for coordinate control of cellular lipid. *Proc Natl Acad Sci U S A*, 93(3): 1049–1053, Feb 1996.

M. M. Magana and T. F. Osborne. Two tandem binding sites for sterol regulatory element binding proteins are required for sterol regulation of fatty-acid synthase promoter. *J Biol Chem*, 271(51):32689–32694, Dec 1996.

V. M. Maher and B. G. Brown. Lipoprotein (a) and coronary heart disease. *Curr Opin Lipidol*, 6(4):229–235, Aug 1995.

R. W. Mahley. Apolipoprotein E: cholesterol transport protein with expanding role in cell biology. *Science*, 240(4852):622–630, Apr 1988.

R. W. Mahley, T. L. Innerarity, S. C. Rall, and K. H. Weisgraber. Plasma lipoproteins: apolipoprotein structure and function. *J Lipid Res*, 25(12): 1277–1294, Dec 1984.

R. W. Mahley, Y. Huang, and S. C. Rall. Pathogenesis of type III hyperlipoproteinemia (dysbetalipoproteinemia). questions, quandaries, and paradoxes. *J Lipid Res*, 40(11):1933–1949, Nov 1999.

R. W. Mahley, Y. Huang, and K. H. Weisgraber. Putting cholesterol in its place: apoE and reverse cholesterol transport. *J Clin Invest*, 116(5): 1226–1229, May 2006.

D. Marguet and G. Chimini. The ABCA1 transporter and ApoA-I: obligate or facultative partners? *Trends Cardiovasc Med*, 12(7):294–298, Oct 2002.

J. Marsh, F. Welty, A. Lichtenstein, S. Lamon-Fava, and E. J. Schaefer. Apolipoprotein B metabolism in humans: studies with stable isotope-labeled amino acid precursors. *Atheroscerlosis*, 162:227–244, 2002.

W. März, M. W. Baumstark, H. Scharnagl, V. Ruzicka, S. Buxbaum, J. Herwig, T. Pohl, A. Russ, L. Schaaf, and A. Berg. Accumulation of "small dense" low density lipoproteins (ldl) in a homozygous patients with familial defective apolipoprotein B-100 results from heterogenous interaction of LDL subfractions with the LDL receptor. *J Clin Invest*, 92(6):2922–2933, Dec 1993.

C. Maugeais, S. Braschi, K. Ouguerram, P. Maugeais, P. Mahot, B. Jacotot, D. Darmaun, T. Magot, and M. Krempf. Lipoprotein kinetics in patients with analbuminemia : Evidence for the role of serum albumin in controlling lipoprotein metabolism. *Arterioscler Thromb Vasc Biol*, 17(7):1369–1375, July 1997.

J. R. Mead, S. A. Irvine, and D. P. Ramji. Lipoprotein lipase: structure, function, regulation, and role in disease. *Journal of Molecular Medicine*, 80(12):753–769, Dec. 2002.

M. Merkel, R. H. Eckel, and I. J. Goldberg. Lipoprotein lipase: genetics, lipid uptake, and regulation. *J Lipid Res*, 43(12):1997–2006, Dec 2002.

J. S. Millar, A. H. Lichtenstein, G. G. Dolnikowski, J. M. Ordovas, and E. J. Schaefer. Proposal of a multicompartmental model for use in the study of apolipoprotein E metabolism. *Metabolism*, 47(8):922–928, Aug 1998.

A. L. Miller and L. C. Smith. Activation of lipoprotein lipase by apolipoprotein glutamic acid. Formation of a stable surface film. *J Biol Chem*, 248 (9):3359–3362, May 1973.

M. Miller, J. Rhyne, S. Hamlette, J. Birnbaum, and A. Rodriguez. Genetics of HDL regulation in humans. *Curr Opin Lipidol*, 14(3):273–279, Jun 2003.

C. G. Moles, P. Mendes, and J. R. Banga. Parameter estimation in biochemical pathways: A comparison of global optimization methods. *Genome Res*, 13(11):2467–2474, Nov. 2003.

R. E. Morton and D. J. Greene. Partial suppression of CETP activity beneficially modifies the lipid transfer profile of plasma. *Atherosclerosis*, 192 (1):100–107, May 2007.

C. Murray and A. Lopez. Global mortality, disability, and the contribution of risk factors: Global burden of disease study. *Lancet*, 349:1436–1442, 1997.

P. J. Nestel and N. H. Fidge. Apoprotein c metabolism in man. *Adv Lipid Res*, 19:55–83, 1982.

A. V. Nichols, R. M. Krauss, and T. A. Musliner. Nondenaturing polyacrylamide gradient gel electrophoresis. *Methods Enzymol*, 128:417–431, 1986.

F. Nigon, P. Lesnik, M. Rouis, and M. Chapman. Discrete subspecies of human low density lipoproteins are heterogeneous in their interaction with the cellular LDL receptor. *J Lipid Res*, 32(11):1741–1753, Nov. 1991.

S. E. Nissen, J.-C. Tardif, S. J. Nicholls, J. H. Revkin, C. L. Shear, W. T. Duggan, W. Ruzyllo, W. B. Bachinsky, G. P. Lasala, E. M. Tuzcu, and I. L. L. U. S. T. R. A. T. E. Investigators. Effect of torcetrapib on the progression of coronary atherosclerosis. *N Engl J Med*, 356(13):1304–1316, Mar 2007.

R. Ohashi, H. Mu, X. Wang, Q. Yao, and C. Chen. Reverse cholesterol transport and cholesterol efflux in atherosclerosis. *QJM*, 98(12):845–856, Dec 2005.

J. F. Oram. Tangier disease and ABCA1. *Biochim Biophys Acta*, 1529(1-3): 321–330, Dec 2000.

J. F. Oram. HDL apolipoproteins and ABCA1: partners in the removal of excess cellular cholesterol. *Arterioscler Thromb Vasc Biol*, 23(5):720–727, May 2003.

J. D. Otvos. Measurement of lipoprotein subclass profiles by nuclear magnetic resonance spectroscopy. *Clin Lab*, 48(3-4):171–180, 2002.

J. D. Otvos, E. J. Jeyarajah, D. W. Bennett, and R. M. Krauss. Development of a proton nuclear magnetic resonance spectroscopic method for determining plasma lipoprotein concentrations and subspecies distributions from a single, rapid measurement. *Clin Chem*, 38(9):1632–1638, Sep 1992.

K. Ouguerram, M. Krempf, C. Maugeais, P. Maugére, D. Darmaun, and T. Magot. A new labeling approach using stable isotopes to study in vivo plasma cholesterol metabolism in humans. *Metabolism*, 51(1):5–11, Jan 2002.

C. J. Packard. Triacylglycerol-rich lipoproteins and the generation of small, dense low-density lipoprotein. *Biochem Soc Trans*, 31(Pt 5):1066–1069, Oct 2003.

C. J. Packard, A. Gaw, T. Demant, and J. Shepherd. Development and application of a multicompartmental model to study very low density lipoprotein subfraction metabolism. *J Lipid Res*, 36(1):172–187, Jan 1995.

C. J. Packard, T. Demant, J. P. Stewart, D. Bedford, M. J. Caslake, G. Schwertfeger, A. Bedynek, J. Shepherd, and D. Seidel. Apolipoprotein B metabolism and the distribution of VLDL and LDL subfractions. *J Lipid Res*, 41(2):305–318, Feb 2000.

K. Parhofer, P. Barrett, D. Bier, and G. Schonfeld. Lipoproteins containing the truncated apolipoprotein, apoB-89, are cleared from human plasma more rapidly than apoB-100-containing lipoproteins in vivo. *J Clin Invest*, 89:1931–1937, 1991.

K. G. Parhofer and P. H. R. Barrett. Thematic review series: Patient-Oriented Research. What we have learned about VLDL and LDL metabolism from human kinetics studies. *J Lipid Res*, 47(8):1620–1630, Aug 2006.

K. G. Parhofer, P. H. Barrett, C. A. Aguilar-Salinas, and G. Schonfeld. Positive linear correlation between the length of truncated apolipoprotein B and its secretion rate: in vivo studies in human apoB-89, apoB-75, apoB-54.8, and apoB-31 heterozygotes. *J Lipid Res*, 37(4):844–852, Apr 1996.

B. W. Patterson, G. Zhao, and S. Klein. Improved accuracy and precision of gas chromatography/mass spectrometry measurements for metabolic tracers. *Metabolism*, 47(6):706–712, Jun 1998.

B. W. Patterson, B. Mittendorfer, N. Elias, R. Satyanarayana, and S. Klein. Use of stable isotopically labeled tracers to measure very low density lipoprotein-triglyceride turnover. *J Lipid Res*, 43(2):223–233, Feb 2002.

J. Pietzsch, U. Julius, S. Nitzsche, and M. Hanefeld. In vivo evidence for increased apolipoprotein A-I catabolism in subjects with impaired glucose tolerance. *Diabetes*, 47(12):1928–1934, Dec 1998.

A. S. Plump and J. L. Breslow. Apolipoprotein E and the apolipoprotein E-deficient mouse. *Annu Rev Nutr*, 15:495–518, 1995.

G. Ponsin and H. J. Pownall. Equilibrium of apoproteins between high density lipoprotein and the aqueous phase: Modelling of in vivo metabolism. *Journal of Theoretical Biology*, 112:183–192, 1985.

L. Powell-Braxton, M. Véniant, R. D. Latvala, K. I. Hirano, W. B. Won, J. Ross, N. Dybdal, C. H. Zlot, S. G. Young, and N. O. Davidson. A mouse model of human familial hypercholesterolemia: markedly elevated low density lipoprotein cholesterol levels and severe atherosclerosis on a low-fat chow diet. *Nat Med*, 4(8):934–938, Aug 1998.

H. J. Pownall and C. Ehnholm. The unique role of apolipoprotein A-i in HDL remodeling and metabolism. *Curr Opin Lipidol*, 17(3):209–213, Jun 2006.

D. A. Pufal, P. T. Quinlan, and A. M. Salter. Effect of dietary triacylglycerol structure on lipoprotein metabolism: a comparison of the effects of dioleoylpalmitoylglycerol in which palmitate is esterified to the 2- or 1(3)-position of the glycerol. *Biochim Biophys Acta*, 1258(1):41–48, Aug 1995.

D. A. Purcell-Huynh, R. V. Farese, D. F. Johnson, L. M. Flynn, V. Pierotti, D. L. Newland, M. F. Linton, D. A. Sanan, and S. G. Young. Transgenic mice expressing high levels of human apolipoprotein B develop severe atherosclerotic lesions in response to a high-fat diet. *J Clin Invest*, 95(5): 2246–2257, May 1995.

X. Qiu, A. Mistry, M. J. Ammirati, B. A. Chrunyk, R. W. Clark, Y. Cong, J. S. Culp, D. E. Danley, T. B. Freeman, K. F. Geoghegan, M. C. Griffor, S. J. Hawrylik, C. M. Hayward, P. Hensley, L. R. Hoth, G. A. Karam, M. E. Lira, D. B. Lloyd, K. M. McGrath, K. J. Stutzman-Engwall, A. K. Subashi, T. A. Subashi, J. F. Thompson, I.-K. Wang, H. Zhao, and A. P. Seddon. Crystal structure of cholesteryl ester transfer protein reveals a

long tunnel and four bound lipid molecules. *Nat Struct Mol Biol*, 14(2): 106–113, Feb 2007.

D. J. Rader, G. Castro, L. Zech, J. Fruchart, and J. H. B. Brewer. In vivo metabolism of apolipoprotein A-I on high density lipoprotein particles LpA-I and LpA-I,A-II. *J Lipid Res*, 32:1849–1859, 1991.

S. Rashid, B. W. Patterson, and G. F. Lewis. Thematic review series: Patient-Oriented Research. What have we learned about HDL metabolism from kinetics studies in humans? *J Lipid Res*, 47(8):1631–1642, Aug 2006.

A. Ratushny, V. Likhoshvai, E. Ignatieva, I. Goryanin, and N. Kolchanov. Resilience of cholesterol concentration to a wide range of mutations in the cell. *Complexus*, 1(3):142–148, 2003. ISSN 1424-8492.

P. W. Reymer, E. Gagné, B. E. Groenemeyer, H. Zhang, I. Forsyth, H. Jansen, J. C. Seidell, D. Kromhout, K. E. Lie, and J. Kastelein. A lipoprotein lipase mutation (Asn291Ser) is associated with reduced HDL cholesterol levels in premature atherosclerosis. *Nat Genet*, 10(1):28–34, May 1995.

D. Rhainds and L. Brissette. Low density lipoprotein uptake: holoparticle and cholesteryl ester selective uptake. *Int J Biochem Cell Biol*, 31(9): 915–931, Sep 1999.

P. M. Ridker, N. Rifai, L. Rose, J. E. Buring, and N. R. Cook. Comparison of C-reactive protein and low-density lipoprotein cholesterol levels in the prediction of first cardiovascular events. *N Engl J Med*, 347(20):1557–1565, Nov 2002.

P. Roma, R. E. Gregg, M. S. Meng, R. Ronan, L. A. Zech, G. Franceschini, C. R. Sirtori, and H. B. Brewer. In vivo metabolism of a mutant form of apolipoprotein A-I, apo A-IMilano, associated with familial hypoalphalipoproteinemia. *J Clin Invest*, 91(4):1445–1452, Apr 1993.

R. Ross. Atherosclerosis–an inflammatory disease. *N Engl J Med*, 340(2): 115–126, Jan 1999.

J. Rouleau. Improved outcome after acute coronary syndromes with an intensive versus standard lipid-lowering regimen: Results from the pravastatin or atorvastatin evaluation and infection therapy-thrombolysis in myocardial infarction 22 (PROVE IT-TIMI 22) trial. *Am J Med*, 118 Suppl 12A: 28–35, 2005.

I. L. Ruel, P. Couture, J. S. Cohn, A. Bensadoun, M. Marcil, and B. Lamarche. Evidence that hepatic lipase deficiency in humans is not associated with proatherogenic changes in HDL composition and metabolism. *J Lipid Res*, 45(8):1528–1537, Aug 2004.

S. Rust, M. Rosier, H. Funke, J. Real, Z. Amoura, J. C. Piette, J. F. Deleuze, H. B. Brewer, N. Duverger, P. DenÃ¨fle, and G. Assmann. Tangier disease is caused by mutations in the gene encoding ATP-binding cassette transporter 1. *Nat Genet*, 22(4):352–355, Aug 1999.

K. A. Rye and P. J. Barter. Formation and metabolism of prebeta-migrating, lipid-poor apolipoprotein A-I. *Arterioscleros Thromb Vasc Biol*, 24(3):421–428, Mar. 2004.

E. J. Schaefer, S. Lamon-Fava, S. D. Cohn, M. M. Schaefer, J. M. Ordovas, W. P. Castelli, and P. W. Wilson. Effects of age, gender, and menopausal status on plasma low density lipoprotein cholesterol and apolipoprotein B levels in the Framingham Offspring Study. *J Lipid Res*, 35(5):779–792, May 1994a.

E. J. Schaefer, S. Lamon-Fava, J. M. Ordovas, S. D. Cohn, M. M. Schaefer, W. P. Castelli, and P. W. Wilson. Factors associated with low and elevated plasma high density lipoprotein cholesterol and apolipoprotein A-I levels in the Framingham Offspring Study. *J Lipid Res*, 35(5):871–882, May 1994b.

J. R. Schaefer, K. Winkler, H. Schweer, M. M. Hoffmann, M. Soufi, H. Scharnagl, B. Maisch, H. Wieland, A. Steinmetz, and W. März. Increased production of HDL ApoA-I in homozygous familial defective ApoB-100. *Arterioscler Thromb Vasc Biol*, 20(7):1796–1799, Jul 2000.

C. C. Schwartz, M. Berman, Z. R. Vlahcevic, and L. Swell. Multicompartmental analysis of cholesterol metabolism in man. Quantitative kinetic evaluation of precursor sources and turnover of high density lipoprotein cholesterol esters. *J Clin Invest*, 70(4):863–876, Oct 1982.

P. Shorten and G. Upreti. A mathematical model of fatty acid metabolism and vldl assembly in human liver. *Biochimica et Biophysica Acta (BBA) - Molecular and Cell Biology of Lipids*, 1736(2):94–108, Sept. 2005.

A. D. Sniderman, A. C. St-Pierre, B. Cantin, G. R. Dagenais, J.-P. Després, and B. Lamarche. Concordance/discordance between plasma apolipoprotein B levels and the cholesterol indexes of atherosclerotic risk. *Am J Cardiol*, 91(10):1173–1177, May 2003.

A. K. Soutar, C. W. Garner, H. N. Baker, J. T. Sparrow, R. L. Jackson, A. M. Gotto, and L. C. Smith. Effect of the human plasma apolipoproteins and phosphatidylcholine acyl donor on the activity of lecithin: cholesterol acyltransferase. *Biochemistry*, 14(14):3057–3064, Jul 1975.

B. Staels and J. Auwerx. Regulation of apo A-I gene expression by fibrates. *Atherosclerosis*, 137 Suppl:S19–S23, Apr 1998.

D. Steinberg. Atherogenesis in perspective: hypercholesterolemia and inflammation as partners in crime. *Nat Med*, 8(11):1211–1217, Nov 2002.

D. Steinberg, S. Parthasarathy, T. E. Carew, J. C. Khoo, and J. L. Witztum. Beyond cholesterol. modifications of low-density lipoprotein that increase its atherogenicity. *N Engl J Med*, 320(14):915–924, Apr 1989.

W. J. Strittmatter and C. B. Hill. Molecular biology of apolipoprotein E. *Curr Opin Lipidol*, 13(2):119–123, Apr 2002.

A. Tall. Plasma lipid transfer proteins. *Annu Rev Biochem*, 64:235–257, 1995.

A. R. Tall. CETP inhibitors to increase HDL cholesterol levels. *N Engl J Med*, 356(13):1364–1366, Mar 2007.

T. Teerlink, P. G. Scheffer, S. J. Bakker, and R. J. Heine. Combined data from LDL composition and size measurement are compatible with a discoid particle shape. *J Lipid Res*, 45(5):954–966, May 2004.

M. J. Thomas, T. Thornburg, J. Manning, K. Hooper, and L. L. Rudel. Fatty acid composition of low-density lipoprotein influences its susceptibility to autoxidation. *Biochemistry*, 33(7):1828–1834, Feb 1994.

S. T. Thuahnai, S. Lund-Katz, D. L. Williams, and M. C. Phillips. Scavenger receptor class B, type I-mediated uptake of various lipids into cells. influence of the nature of the donor particle interaction with the receptor. *J Biol Chem*, 276(47):43801–43808, Nov. 2001.

A. J. Tremblay, B. Lamarche, I. L. Ruel, J.-C. Hogue, J. Bergeron, C. Gagné, and P. Couture. Increased production of VLDL apoB-100 in subjects with familial hypercholesterolemia carrying the same null LDL receptor gene mutation. *J Lipid Res*, 45(5):866–872, May 2004.

B. Trigatti, H. Rayburn, M. Vinals, A. Braun, H. Miettinen, M. Penman, M. Hertz, M. Schrenzel, L. Amigo, A. Rigotti, and M. Krieger. Influence

of the high density lipoprotein receptor SR-BI on reproductive and cardiovascular pathophysiology. *Proc Natl Acad Sci U S A*, 96(16):9322–9327, Aug 1999.

B. Trigatti, A. Rigotti, and M. Krieger. The role of the high-density lipoprotein receptor SR-BI in cholesterol metabolism. *Curr Opin Lipidol*, 11(2): 123–131, Apr 2000a.

B. L. Trigatti, A. Rigotti, and A. Braun. Cellular and physiological roles of SR-BI, a lipoprotein receptor which mediates selective lipid uptake. *Biochim Biophys Acta*, 1529(1-3):276–286, Dec 2000b.

G. Utermann, M. Hees, and A. Steinmetz. Polymorphism of apolipoprotein E and occurrence of dysbetalipoproteinaemia in man. *Nature*, 269(5629): 604–607, Oct 1977.

A. van Tol. Phospholipid transfer protein. *Curr Opin Lipidol*, 13(2):135–139, Apr 2002.

J. E. Vance and D. E. Vance. Lipoprotein assembly and secretion by hepatocytes. *Annu Rev Nutr*, 10:337–356, 1990.

M. Varret, J. P. Rabes, G. Collod-Béroud, C. Junien, C. Boileau, and C. Béroud. Software and database for the analysis of mutations in the human LDL receptor gene. *Nucleic Acids Res*, 25(1):172–180, Jan 1997.

W. Vélez-Carrasco, A. H. Lichtenstein, P. H. Barrett, Z. Sun, G. G. Dolnikowski, F. K. Welty, and E. J. Schaefer. Human apolipoprotein A-I kinetics within triglyceride-rich lipoproteins and high density lipoproteins. *J Lipid Res*, 40(9):1695–1700, Sep 1999.

G. Walldius and I. Jungner. The apoB/apoA-I ratio: a strong, new risk factor for cardiovascular disease and a target for lipid-lowering therapy–a review of the evidence. *J Intern Med*, 259(5):493–519, May 2006.

G. Walldius, I. Jungner, I. Holme, A. H. Aastveit, W. Kolar, and E. Steiner. High apolipoprotein B, low apolipoprotein A-I, and improvement in the prediction of fatal myocardial infarction (AMORIS study): a prospective study. *Lancet*, 358(9298):2026–2033, Dec 2001.

N. Wang, D. Lan, W. Chen, F. Matsuura, and A. R. Tall. ATP-binding cassette transporters G1 and G4 mediate cellular cholesterol efflux to high-density lipoproteins. *Proc Natl Acad Sci U S A*, 101(26):9774–9779, Jun 2004.

G. F. Watts, P. Moroz, and P. H. Barrett. Kinetics of very-low-density lipoprotein apolipoprotein B-100 in normolipidemic subjects: pooled analysis of stable-isotope studies. *Metabolism*, 49(9):1204–1210, Sep 2000.

K. L. West and M. L. Fernandez. Guinea pigs as models to study the hypocholesterolemic effects of drugs. *Cardiovasc Drug Rev*, 22(1):55–70, 2004.

K. J. Williams and I. Tabas. The response-to-retention hypothesis of atherogenesis reinforced. *Curr Opin Lipidol*, 9(5):471–474, Oct 1998.

K. Winkler. Low density lipoprotein-heterogenität als prognostischer marker kardiovaskulärer erkrankungen / low density lipoprotein heterogeneity for risk evaluation of cardiovascular disease. *J Lab Med*, 28(5):447–452, 2004.

K. Winkler, J. Schaefer, B. Klima, C. Nuber, A. Sattler, I. Friedrich, W. Köster, A. Steinmetz, H. Wieland, and W. März. Lifibrol enhances the low density lipoprotein apolipoprotein B-100 turnover in patients with hypercholesterolemia and mixed hyperlipidemia. *Atherosclerosis*, 144(1): 167–175, May 1999.

K. Winkler, J. R. Schaefer, B. Klima, C. Nuber, I. Friedrich, W. Köster, H. Gierens, H. Scharnagl, M. Soufi, H. Wieland, and W. März. HDL steady state levels are not affected, but HDL apoA-I turnover is enhanced by Lifibrol in patients with hypercholesterolemia and mixed hyperlipidemia. *Atherosclerosis*, 150(1):113–120, May 2000.

A. L. Wu and H. G. Windmueller. Relative contributions by liver and intestine to individual plasma apolipoproteins in the rat. *J Biol Chem*, 254 (15):7316–7322, Aug 1979.

K. M. Yli-Jokipii, U. S. Schwab, R. L. Tahvonen, J.-P. Kurvinen, H. M. Mykkänen, and H. P. T. Kallio. Triacylglycerol molecular weight and to a lesser extent, fatty acid positional distribution, affect chylomicron triacylglycerol composition in women. *J Nutr*, 132(5):924–929, May 2002.

K. C. Yu and A. D. Cooper. Postprandial lipoproteins and atherosclerosis. *Front Biosci*, 6:D332–D354, Mar 2001.

S. Yusuf, S. Hawken, S. Ounpuu, T. Dans, A. Avezum, F. Lanas, M. McQueen, A. Budaj, P. Pais, J. Varigos, L. Lisheng, and I. N. T. E. R. H. E. A. R. T. S. Investigators. Effect of potentially modifiable risk factors associated with myocardial infarction in 52 countries (the INTERHEART study): case-control study. *Lancet*, 364(9438):937–952, 2004.

A. Zambon, S. Bertocco, N. Vitturi, V. Polentarutti, D. Vianello, and G. Crepaldi. Relevance of hepatic lipase to the metabolism of triacylglycerol-rich lipoproteins. *Biochemical Society Transactions*, 31(5): 1070–1074, 2003.

L. A. Zech, S. M. Grundy, D. Steinberg, and M. Berman. Kinetic model for production and metabolism of very low density lipoprotein triglycerides. Evidence for a slow production pathway and results for normolipidemic subjects. *J Clin Invest*, 63(6):1262–1273, Jun 1979.

Appendix A

Calculating the Number of Phospholipids

The core volume V_c of a lipoprotein particle results from the number of neutral lipids n_i ($i = C, T$) and their molecular volume mv_i (in ml/mol) divided by the Avogadro constant L ($6.022 \cdot 10^{23} mol^{-1}$) and is given as nm^3 per particle.

$$V_c = \sum_{i=\{C,T\}} n_i mv_i \cdot \frac{10^{21}}{L} \tag{A.1}$$

From the core volume the core radius r_c (in nm) can be calculated as follows. The surface radius r_s is assumed to have a fixed volume of $2nm$ (Miller and Smith, 1973)

$$r_c = \sqrt[3]{\frac{3}{4} \cdot \frac{V_c}{\pi}} \tag{A.2}$$

The surface volume V_s (in ml/mol) is then determined as:

$$V_s = 4 \cdot \pi \cdot r_c^2 \cdot r_s \cdot \frac{L}{10^{21}} \tag{A.3}$$

The surface of a lipoprotein is predominantly occupied by apolipoproteins and phospholipids. Thus, the surface volume captured by phospholipids V_P is estimated as the difference of the total surface volume V_s and the surface volume already filled with apolipoproteins V_{AP}.

$$V_{AP} = \sum_{i=\{A,B,F\}} n_i mv_i \tag{A.4}$$

$$V_P = V_s - V_{AP} \tag{A.5}$$

Subsequently, the number of phospholipid molecules n_P is calculated.

$$n_P = \frac{V_P}{mv_P} \tag{A.6}$$

In the end, the density is recalculated by adding the weight and the volume for the phospholipid content.

$$d = \frac{\sum n_i mw_i + n_p mw_p}{\sum n_i mv_i + n_p mv_p} \tag{A.7}$$

Appendix B

Model Parameter Values

However, the comparison of calculated and measured rate constants for elevated processes such as the exchange of apolipoproteins, cholesteryl ester and triglycerides is difficult. In the model, the rate constants concern to elementary processes while kinetic measurements settle on compartment analyses. Furthermore, the underlying reaction mechanism can either be monomolecular (e.g. *EffluxA*) or bimolecular (e.g. $ExchangeC_A$) which is important to know while comparing the stochastic rate constant with parameters obtained from, e.g. tracer kinetic studies. In case of a monomolecular reaction both constants are equal. Since bimolecular reactions depend on the collision probability of both reaction partners the rate constant even depends on the volume in that the reaction takes place (Eq. B.1).

$$c_\mu = \frac{k_\mu}{N_A \cdot V} \tag{B.1}$$

where c_μ and k_μ are the stochastic and kinetic rate constants of reaction μ, respectively. N_A is the Avogadro constant and V denotes the small sample volume used in the stochastic simulation. Most of the transfer and exchange processes in plasma are bimolecular.

An attempt to relate measured kinetic data to the estimated model parameters is proposed in the following for some examples. Each of them is marked in Table 6.1 with the appropriate index.

a) *Transfer of cholesteryl ester from HDL to apoB-100 carrying lipoproteins, e.g. VLDL, by the CETP.* This process is comparable to the bimolecular reaction we modeled in $ExchangeC_A$ which follows the rate law

$$v_{exchangeC_A} = c_{exchangeC_A} \cdot C \cdot CETP(0) \tag{B.2}$$

Jarnagin et al. characterized the specifity of a cholesteryl ester transfer protein from human plasma with a molecular weight of 74,000 Dalton Jarnagin et al. (1987). The total transfer activity $v_{exchangeC_A}$ was assayed with 110.52 mg/dl $\cdot$ day^{-1} as the rate of loss of H^3-labeled cholesteryl ester in HDL (50 μg/ml in 0.5 ml incubation volume). The CETP mass is given with 0.049 mg/dl (= $6.6{\cdot}10^{-6}$ mmol/l). The kinetic rate constant $k_{exchangeC_A}$ equals according Eq. B.2 the total transfer activity divided by the concentration of cholesteryl ester in HDL and by that CETP mass being in its non-lipid bound form $CETP(0)$ (in our calculations approximately 25.3 % of total CETP mass). Most of the CETP is loaded with C while the T-loaded form of CETP is very rarely with approximately 73.3 % and 1.4 %, respectively.

$$\begin{aligned} k_{exchangeCA} &= \frac{v_{exchangeCA}}{[CE] \cdot [CETP(0)]} \\ &= \frac{110.52(\text{mg/dl}) \cdot \text{day}^{-1}}{10\text{mg/dl} \cdot 1.67 \cdot 10^{-6}\text{mmol/l}} \\ &= 6.63 \cdot 10^6 \text{ l/(mmol} \cdot \text{day)} \end{aligned}$$

According to Eq. B.1 the kinetic rate constant is scaled to the volume (factor 60,220 l/mmol) in that the simulation takes place and agrees in the order of magnitude to the calculated stochastic rate constant $c_{exchangeC_A}$ in our model (110.6 vs. 397.1 day^{-1}). However, the reference HDL-CE concentration is approximately one third of that in our simulation and the CETP mass is much less even. Thus, comparing the fluxes (total transfer activities) instead being 110.52 vs. 72.13 mg/dl $\cdot$ day^{-1} might be more useful.

b) *Transfer of triglycerides (TG) from VLDL to, e.g. HDL by the CETP.* Similarily, Jarnagin et al. provide the rate value of this process relative to the CE transfer (0.11 nmol TG relative to 1 nmol CE per ml per h). We modeled this bimolecular process in $ExchangeT_{B1}$ which follows the rate law

$$v_{exchangeT_{B1}} = c_{exchangeT_{B1}} \cdot T \cdot CETP(0) \tag{B.3}$$

The total transfer activity $v_{exchangeT_{B1}}$ is 15.87 mg/dl $\cdot$ d^{-1}, accordingly. From the given CE (100 μg in 0.5 ml incubation volume) to TG ratio for VLDL (0.15) follows the VLDL-TG concentration of 133.3 mg/dl. By taking the CETP(0) mass given above the (volume scaled) kinetic rate constant is more than two magnitudes less than the estimated

model parameter (1.2 vs. 887.75 day^{-1}). However, in this case the reference VLDL-TG concentration is approximately double of that in our simulation and even the CETP mass is less. Thus again, comparing the fluxes (total transfer activity) instead being 15.87 vs. 297.45 mg/dl $\cdot$ day^{-1} might be more useful.

In general, one major reason for discrepancies in these processes might be due to the fact that we modeled the exchange of CE and TG uncoupled. That means that e.g. triglycerides (component T) of B-particles can be transfered as long as triglycerides and an appropriate acceptor (non-lipid bound CETP) are available independent on the amount of CE (component C) in A-particles.

The parameters for the transfer and uptake processes of component F are only slightly interpretable with the current state of our model because we do not specify a particular apolipoprotein. However, Batal et al. investigated the plasma kinetics of VLDL and HDL apoC-III and apoE, both are potential candidates for component F Batal et al. (2000).

c) *Transfer of apolipoproteinF (apoC+apoE) from HDL.* We modeled this process in $TransferF_A$ which follows the rate law

$$v_{transferF_A} = c_{transferF_A} \cdot F \cdot poolF(0) \tag{B.4}$$

Batal et al. have proposed fractional catabolic rates (FCR) of both apolipoprotein (apo) CIII and E in HDL with 0.285 and 1.1 day $^{-1}$, respectively. The sum of concentration of apoCIII (5.34 mg/dl) and apoE (2.99 mg/dl) is 8.33 mg/dl. Subsequently, the total transfer rate of component F is the sum of the transfer rates of apoCIII (1.52 mg/dl per day) and apoE (3.29 mg/dl per day) = 4.81 mg/dl per day. This value includes two elementary processes by which the apolipoproteins can disappear: i) by the receptor-mediated uptake of HDL and ii) by the selective transfer out of HDL. The uptake rate of F can be calculated from the FCR (0.2 day^{-1}) and concentration of HDL apoA-I (118 mg/dl). By taking the proportion of F relative to apoA-I in a HDL particle we get a HDL apoF uptake rate of 0.22 mg/dl per day. Accordingly, the transfer rate out of HDL (difference between the total and the uptake rate) and the appropriate FCR are 4.59 mg/dl $\cdot$ day^{-1} and 0.551 day^{-1}, respectively. In the model, the process is formulated in that the monomolecular transfer reaction also depends on the capacity of the plasma to accept a further free apolipoprotein of type F ($poolF(0)$). The literature reference value, however, does not consider this factor but can taken from our calculations (1.2e-3

mmol/l). Thus, the kinetic constant is divided by that factor yiedling an experimental value that agree in one order of magnitude less with the simulated parameter value (459.2 vs. 56.9 l/mmol per day). The volume scaled (factor of 60220 l/mmol) values are 7.6e-3 and 9.4e-4 day^{-1}, accordingly. Since this process is monomolecular we scale both constants equally.

d) *Uptake of apolipoprotein F (apoC+apoE) by HDL.* Apolipoproteins can also newly enter a lipoprotein complex, e.g. an A-particle. In our model, this bimolecular process is called $UptakeF_A$ and follows the rate law

$$v_{uptakeF_A} = c_{uptakeF_A} \cdot poolF \tag{B.5}$$

Batal et al. (Batal et al., 2000) provide a transfer rate (TR) for HDL apoC-III and apoF of 0.8 mg/kg·day^{-1} and 1.56 mg/kg·day^{-1}, respectively. Thus, for both apolipoproteins the total transfer activity being 5.24 mg/dl·day^{-1} (0.45 dl/kg body weight). This value again comprises two processes by which apolipoproteins can enter a lipoprotein complex: i) as components of newly synthesized A-particles and ii) by the selective uptake from a free plasma pool. Since in our model nascent A-particles are free of apoC and apoE the total transfer activity equals the uptake activity from a free plasma pool. Thus, the kinetic rate constant yields the value of 4.77 day^{-1} by dividing the uptake activity by the concentration of the free plasma pool (approximately 1.1 mg/dl). However, this experimental rate constant does not taking int account the amount of lipoprotein complexes being available as acceptor molecules in the plasma. In the simulation approximately 0.02 mmol/l of A-particles are present by which the kinetic rate constant is divided. According to Eq. B.1 the kinetic rate constant is scaled to the volume (factor 60220 l/mmol) in that the simulation takes place and agrees in the order of magnitude with the estimated stochastic rate constant (3.9e-3 vs. 1.9e-3 day^{-1}).

e) *Transfer of apolipoproteinF (apoC+apoE) from VLDL.* We modeled this process in $TransferF_B$ which follows the rate law

$$v_{transferF_B} = c_{transferF_B} \cdot F \cdot poolF(0) \tag{B.6}$$

FCR of apoCIII and VLDL apoE in VLDL proposed by Batal et al. (Batal et al., 2000) are 0.85 and 4.76 day^{-1}, respectively. Concentrations are 3.59 mg/dl VLDL apoCIII and 0.72 mg/dl VLDL apoE - in sum 4.31 mg/dl. The total transfer activity for both apolipoproteins

is 6.48 mg/dl per day. Assuming that the selective transfer of the apolipoproteins takes a minor part the rate was set to 0.5 mg/dl per day. The kinetic rate constant is then divided by the factor $poolF(0)$ (see c)) and agrees well to the model parameter value (96.67 vs. 120.54 l/mmol per day). The volume scaled (factor of 60220 l/mmol) values are 1.6e-3 and 2.0e-3 day^{-1}, accordingly. Since this process is monomolecular we scale both constants equally.

f) *Uptake of apolipoprotein F (apoC+apoE) by VLDL.* In our model, this bimolecular process is called $UptakeF_B$ and follows the rate law

$$v_{uptakeF_B} = c_{uptakeF_B} \cdot poolF \tag{B.7}$$

Batal et al. (Batal et al., 2000) provide a transfer rate (TR) for VLDL apoC-III and apoF of 1.35 mg/kg $\cdot day^{-1}$ and 1.59 mg/kg $\cdot day^{-1}$, respectively, yielding a total transfer activity of 6.53 mg/dl $\cdot day^{-1}$ (0.45 dl/kg body weight). The rate of selective uptake of component F from the plasma pool (difference of total transfer activity and fractional synthesis) is assumed to be approximately half of the total synthesis rate (=3.25 mg/dl per day). According to d) the kinetic rate constant is obtained by: i) dividing the selective uptake activity by the concentration of the free 'apoF' in plasma ($poolF$ approximately 1.1 mg/dl), ii) dividing the amount of lipoprotein complexes being available as acceptor molecules in the plasma (in the simulation 8.04e-4 mmol/l) and iii) scaling to the volume (factor 60220 l/mmol) in that the simulation takes place. Finally, the experimental value agrees in one order of magnitude less to the simulated parameter value (0.061 vs. 3.5e-3 day^{-1})

g) *Transfer of apolipoproteinA from HDL.* We modeled this process in $TransferA$ which follows the rate law

$$v_{transferA} = c_{transferA} \cdot A \cdot poolA(0) \tag{B.8}$$

Cohn et al. (Cohn et al., 2003) provide FCR and total transfer activity of HDL apoA-I of 0.196 day^{-1} and 24.44 mg/dl per day. The concentration of HDL apoA-I is given with 118.4 mg /dl. According to c) the transfer activity includes two elementary processes by which apoA-I can disappear: i) by the receptor-mediated uptake of HDL and ii) by the selective transfer out of HDL. The receptor-mediated uptake rate is 23.13 mg/dl per day (FCR times concentration) yielding the selective transfer rate of 1.31 mg/dl per day (difference of total transfer

rate and receptor-mediated uptake rate). According to Eq. B.8, the kinetic rate constant is obtained by: i) dividing the concentration of HDL apoA-I, ii) dividing by the factor $poolA(0)$ being the capacity of the plasma to accept a further free apolipoprotein A-I (in our simulation 0.002 mmol/l). Finally, the experimental value agrees in the order of magnitude to the model parameter value (5.53 vs. 12.62 l/mmol per day). The volume scaled (factor of 60220 l/mmol) values are 9.2e-5 and 2.0e-4 day^{-1}, accordingly. Since this process is monomolecular we scale both constants equally.

h) *Uptake of apolipoprotein A by HDL.* In our model, this bimolecular process is called $UptakeA$ and follows the rate law

$$v_{uptakeA} = c_{uptakeA} \cdot poolA \tag{B.9}$$

HDL apoA-I total transfer activity of 24.44 mg/dl per day is taken from (Cohn et al., 2003). This value includes i) apoA-I as component of newly synthesized A-particles and ii) the selective uptake of apoA-I from a free plasma pool. In the model, newly synthesized particles contain two apoA-I molecules. Together with the synthesis rate of 4e-3 mmol/l per day and the molecular weight of 28500 g/mol we get a selective synthesis rate of 22.8 mg/dl per day. Thus, the selective uptake rate from the plasma is 1.64 mg/dl per day (difference of total transfer activity and selective synthesis rate). The kinetic rate constant is obtained by: i) dividing the selective uptake rate by the concentration of the free 'apoA' in plasma (in the model $poolA$ approximately 0.01 mg/dl), ii) dividing the amount of lipoprotein complexes being available as acceptor molecules in the plasma (in the simulation 0.02 mmol/l) and iii) scaling to the volume (factor 60220 l/mmol) in that the simulation takes place. Finally, the experimental value agrees in one order of magnitude less to the simulated parameter value (0.136 vs. 0.02 day^{-1}).

For processes such as *EffluxB*, $ExchangeT_A$, $ExchangeC_B$ and $ExchangeT_{B2}$ no suitable reference values could be found.

Abbreviations

Abbreviation	Explanation
Apo	apolipoprotein
CM	Chylomicrons
VLDL	Very low density lipoproteins
IDL	Intermediate density lipoproteins
LDL	Low density lipoproteins
HDL	High density lipoproteins
LDL-C	LDL cholesterol
HDL-C	HDL cholesterol
RCT	Reverse cholesterol transport
PR	Production rate
FCR	Fractional catabolic rate
LDLR	LDL receptor
LRP	LDL receptor related protein
SR	Scavenger receptor
LPL	Lipoprotein lipase
HL	Hepatic lipase
LCAT	Lecithin cholesterol acyl transferase
CETP	Cholesterol ester transfer protein
ABCA1	ATP-binding cassette class A type 1
CVD	Cardiovascular disease
FH	Familial hypercholesterolemia
FDB	Familial defective apoB-100
HA	Hypoalphalipoproteinemia
TD	Tangier disease
FHA	Familial hypoalphalipoproteinemia
IGT	Impaired glucose tolerance

Contributions

The present work has been prepared myself and without the use of illegitimate aids. Nevertheless, I would like to specify work from selected partners involved in the project. The stochastic model was developed with grateful support and supervision by Thomas Schwager. Prof. Holzhütter provided extensive aid in the formulation of the deterministic model. All clinical measurements have been performed by our collaborators from the Department of Clinical Chemistry at the University Hospital of Freiburg.

Acknowledgement

The thesis arose in part out of research that has been done in the group of Prof. Jens-Georg Reich before I came to Prof. Hermann-Georg Holzhütter's group.

In the first place, I would like to record my gratitude to Prof. Hermann-Georg Holzhütter who has taken the major part of supervision in the last three years, but likewise to Prof. Jens-Georg Reich both for their mentoring, advice, and guidance throughout the work. They provided me continuous encouragement in various ways and enriched my path with the picture about true values of science. I am grateful for the patience and faith in success, for the impatience and critical comments, for the right words at the right time.

Special thanks go to my colleagues who enabled a very fruitful, enjoyable and creative atmosphere. In particular, I want to thank Thomas Schwager for his help, crucial support and supervision regarding the stochastic model, for manifold discussions, for very helpful corrections of the manuscript and for his specialty in thinking from a typical physicist's point of view. To Sascha Bulik I express my gratitude for taking often and spontaneously time to discuss crucial points of modeling work and results interpretation, for the ability to very quickly transfer general matters to the special subject of my thesis and for continuously asking for a badminton match. I would like to thank Sabrina Hoffmann for the very creative work together across the desk and for establishing an own 'art design department'.

I gratefully acknowledge Prof. Karl Winkler and his team from the Department of Clinical Chemistry at the University hospital in Freiburg for their excellent support by measuring detailed clinical lipoprotein profiles, in particular Nülüfer Ödünc for time-consuming additional ultracentrifugation runs in order to provide a comprehensive composition picture in all selected lipoprotein sub-fractions.

Many thanks to Jana Mehlhase for reading the manuscript in a quite short time period, for the helpful corrections and discussions even late after midnight as well as for inspiring me with her particular passion in science. I am fortunate about the close, warm and familiar friendship over years and

even over long distances which render it possible to be called a 'nut' without getting angry.

In a very special way, I would like to thank Jürgen Pahle who is delighting my life from the time on we met each other. You marvelously make me laugh even when clouds darken the sky. Many thanks for inspiring me with great ideas, for continuously motivating and for providing all the patience and encouragement I needed to finish this work. Thank you!

It is close to my heart to thank my family, my parents for being grown up in a harmonic and loving environment, for providing me persistent encouragement, trust and to have believed in me through out the entire time of my life. I am very grateful to my sister who established the 'always think positive' rule in our family and to the little princess Silvia Elena who delights my life as aunt. With pleasure I gratefully acknowledge the efforts of my family to empathize with the work of a scientist and to understand what the hell I am actually doing.

Finally, I would like to thank everybody who has confronted me again and again with the question 'And? How is your work going on?' which substantially helped to accelerate the progress of my work.

For financial support of this work I am grateful for the grants from the research initiative "HepatoSys" and "MEDSEQ2" by the German Ministry of Education and Research (BMBF) as well as from the Investitionsbank Berlin within the ProFIT initiative.

Publications

Original paper

Hübner K, Schwager T, Winkler K, Reich JG, Holzhütter HG (2007). Computational Lipidology: Predicting lipoprotein density profiles in human blood plasma. *PLoS Computational Biology*, May 23; 4(5): e1000079

Invited talks

Hübner K (2006). In silico analysis and prediction of lipoprotein density profiles in high resolution. University Hospital Freiburg, Department of Clinical Chemistry, Oct 17, Freiburg, Germany

Conference contributions (talks)

Hübner K, Schwager T, Winkler K, Reich JG, Holzhütter HG (2006). A novel approach towards analysis and prediction of lipoprotein density profiles. *36^{th} Annual conference of the study group 'Clinical Lipid Metabolism'*, Nov 30-Dec 2, Maikammer, Germany

Hafez K (now Hübner), Schwager T, Reich JG, Holzhütter HG (2005). Kinetic modeling of the lipoprotein metabolism. *Platform Meeting 'Modeling&Bioinformatics'* of the BMBF HepatoSys Research Initiative, Jan 27-28, 2005, Berlin, Germany

Conference contributions (poster)

Hübner K, Schwager T, Winkler K, Reich JG, Holzhütter HG (2007). The distribution of blood lipid values in high resolution: A computer-based approach. *XV Lipid Meeting Leipzig*, Dec 6-8, Leipzig, Germany

Conference contributions (poster) - continuation

Hübner K, Schwager T, Winkler K, Reich JG, Holzhütter HG (2006). Computational approaches towards prediction of lipoprotein composition. *XIV International Symposium on Atherosclerosis*, June 18-22, Rome, Italy

Hafez K (now Hübner) (2005). Modeling the human plasma lipoprotein metabolism and its regulation by the liver. *Status Seminar of the BMBF HepatoSys Research Initiative*, April 28-29, Heidelberg, Germany

Hafez K (now Hübner), Reich JG (2004). Modeling Approaches in Lipid Metabolism. *4^{th} International Workshop on Bioinformatics and Systems Biology*, June 1-3, Kyoto, Japan

Hafez K (now Hübner), Reich JG (2003). Metabolites containing "Flags" and "Cargo" - a More Detailed Model of the Human Lipoprotein Network in Blood Plasma. *European Conference on Computational Biology (ECCB)*, Sep 27-30, Paris, France

Declaration

Herewith, I declare that I prepared the present dissertation myself and without the use of illegitimate aids. I used no other but the indicated sources and accessories. Further, I insure that this dissertation has not before been submitted to any other faculty for examination.

Berlin, Katrin Hübner